Scanning Electron Microscopy of Shell and Mantle in the Order Arcoida (Mollusca: Bivalvia)

THOMAS R. WALLER

SMITHSONIAN CONTRIBUTIONS TO ZOOLOGY • NUMBER 313

SERIES PUBLICATIONS OF THE SMITHSONIAN INSTITUTION

Emphasis upon publication as a means of "diffusing knowledge" was expressed by the first Secretary of the Smithsonian. In his formal plan for the Institution, Joseph Henry outlined a program that included the following statement: "It is proposed to publish a series of reports, giving an account of the new discoveries in science, and of the changes made from year to year in all branches of knowledge." This theme of basic research has been adhered to through the years by thousands of titles issued in series publications under the Smithsonian imprint, commencing with *Smithsonian Contributions to Knowledge* in 1848 and continuing with the following active series:

Smithsonian Contributions to Anthropology
Smithsonian Contributions to Astrophysics
Smithsonian Contributions to Botany
Smithsonian Contributions to the Earth Sciences
Smithsonian Contributions to Paleobiology
Smithsonian Contributions to Zoology
Smithsonian Studies in Air and Space
Smithsonian Studies in History and Technology

In these series, the Institution publishes small papers and full-scale monographs that report the research and collections of its various museums and bureaux or of professional colleagues in the world of science and scholarship. The publications are distributed by mailing lists to libraries, universities, and similar institutions throughout the world.

Papers or monographs submitted for series publication are received by the Smithsonian Institution Press, subject to its own review for format and style, only through departments of the various Smithsonian museums or bureaux, where the manuscripts are given substantive review. Press requirements for manuscript and art preparation are outlined on the inside back cover.

S. Dillon Ripley
Secretary
Smithsonian Institution

SMITHSONIAN CONTRIBUTIONS TO ZOOLOGY • NUMBER 313

Scanning Electron Microscopy of Shell and Mantle in the Order Arcoida (Mollusca: Bivalvia)

Thomas R. Waller

SMITHSONIAN INSTITUTION PRESS
City of Washington
1980

Contents

ABSTRACT

Waller, Thomas R. Scanning Electron Microscopy of Shell and Mantle in the Order Arcoida (Mollusca: Bivalvia). *Smithsonian Contributions to Zoology*, number 313, 58 pages, 46 figures, 1 table, 1980.—Field investigations of living bivalves of the order Arcoida led to the rediscovery of a contradiction to the longstanding three-fold, three-function concept of bivalve mantle edges. In contrast to the simple secretory role usually ascribed to the outer fold, it was found that this fold is also photoreceptive, having both simple and compound eyes beneath the newly generated periostracum, and that it also may serve as a mantle curtain, controlling the flow of water into and out of the mantle cavity. Preserved specimens of *Arca zebra*, *Arca imbricata*, *Barbatia cancellaria*, and *Glycymeris glycymeris* were subsequently examined by scanning electron microscopy, with particular emphasis on mantle-shell relationships in specimens prepared by critical-point drying.

These methods suggest two different modes of calcification: one inside the pallial line and characterized by high calcium mobility, the other outside the pallial line and closely controlled by a fibrous organic film that overlies the growth surface of the marginal shell band and is distinct from the periostracum. The pallial line in the Arcoida is primarily the result of morphological changes in the mantle epithelium and does not represent a continuous line of pallial-retractor insertions. Shell tubules, abundantly present in all arcoids examined, are formed by greatly elongated processes extending into the shell from the apical surfaces of epithelial cells inside the pallial line. These may chemically deter borers. The presence of two marginal mantle folds lateral to the periostracal groove as well as the presence of photoreceptors on one of these suggest that growth of the mantle is not by means of simple conveyor-belt-like proliferation of cells from a single zone. Rather, cell generation in the epithelia outside the pallial line is probably widely distributed, with many cells tending to maintain both their position and function during ontogeny.

The peculiar arrangement of marginal mantle folds and the structure of compound eyes both probably result from very early divergence from a primitive bivalve and represent independently derived characters unique to the order Arcoida.

OFFICIAL PUBLICATION DATE is handstamped in a limited number of initial copies and is recorded in the Institution's annual report, *Smithsonian Year*. SERIES COVER DESIGN: The coral *Montastrea cavernosa* (Linnaeus).

Library of Congress Cataloging in Publication Data
Waller, Thomas R.
Scanning electron microscopy of shell and mantle in the order Arcoida (Mollusca: Bivalvia)
(Smithsonian contributions to zoology ; no. 313)
Bibliography: p.
1. Arcoida—Anatomy. 2. Arcoida—Evolution. 3. Calcification. 4. Mollusks—Anatomy. 5. Mollusks—Evolution. I. Title. II. Series: Smithsonian Institution. Smithsonian contributions to zoology; no. 313.
QL1.S54 no. 313 [QL430.6] 591'.08s [594'.11] 79-607786.

Scanning Electron Microscopy of Shell and Mantle in the Order Arcoida (Mollusca: Bivalvia)

Thomas R. Waller

Introduction

The present study grew out of an examination of living bivalves at Carrie Bow Cay, Belize, in April 1976. I observed there that the compound eyes of arcoid bivalves, such as *Arca*, *Barbatia*, and *Glycymeris*, are not positioned on a middle mantle fold as in other bivalves, but rather on an outer fold beneath the newly generated periostracum. Furthermore, in the case of *Arca* and *Glycymeris* it is this photoreceptive outer fold that also serves as a mantle curtain, there being no other fold medial to the periostracal groove other than a small one that merely buttresses one side of the groove and has no other apparent function. This contradicts the three-fold, three-function concept of the mantle margin that has pervaded the study of bivalve anatomy and general works on Mollusca since the nineteenth century. According to the latter concept, there are three marginal folds along the free margins of the mantle: (1) an outer fold, which is concerned with secretion of shell distal to the pallial line; (2) a middle fold, separated from the outer by the periostracal groove and concerned with sensory perception; and (3) an inner fold, which, although also sensory, is concerned primarily with the control of water flow into and out of the mantle cavity (Yonge, 1957).

The presence, however, in the Arcoida of a photoreceptive mantle curtain lateral to the periostracal groove is not the only contradiction to current concepts of bivalve anatomy. A second outer fold is also present, with its crest abutting the pallial line and set off from the first outer fold by a small infolding of mantle tissue. It is generally thought that the pallial line of bivalves represents a line of attachment of pallial muscles that retract the mantle margin, but here the second outer fold is not retractable, and there is a possibility that the pallial line of arcoids is not homologous with that of other bivalves.

In view of the magnitude of these differences between the arcoid mantle edge and that of "typical" bivalves, specimens were prepared for scanning electron microscopy by critical-point drying. This technique allows both soft and hard tissues to be examined in relation to each other with a far greater depth of field than is obtainable by conventional techniques of optical and transmission electron microscopy. The following report describes the shell and mantle surfaces and discusses the significance of the findings relative to the following problems: (1) the formation and function of shell tubules; (2) the relationships between the mantle and the calcified fabrics of the shell, and the bearing of these relationships

Thomas R. Waller, Department of Paleobiology, National Museum of Natural History, Smithsonian Institution, Washington, D.C. 20560.

on processes of calcification; (3) modes of cell generation leading to growth of the mantle edge and shell; and (4) the functional and evolutionary significance of the peculiar arrangement of mantle folds and eyes in the Arcoida.

ACKNOWLEDGMENTS.—I am grateful to many individuals in the Smithsonian Institution: Dr. Klaus Ruetzler, Mr. Barry Spracklin, and colleagues in Project IMSWE for help in the field at Carrie Bow Cay; Drs. W. Duane Hope and John C. Harshbarger for instruction in critical-point drying and the use of laboratory facilities; Mr. Kjell B. Sandved for photography of living arcoids; Mr. Walter R. Brown and Mss. Mary-Jaque Mann and Susann Braden for their expert operation of scanning electron microscopes; Mr. Warren C. Blow, my research assistant, for help in the laboratory, library, and darkroom; Dr. Peter W. Skelton, visiting Smithsonian fellow, for enduring many hours of discussion and critically reading the manuscript; and Dr. Kenneth M. Towe, for review of the manuscript and many helpful suggestions. The artwork is by Larry B. Isham, illustrator for the Department of Paleobiology. Drs. Annie Dhondt and Jackie van Goethem of the Royal Institute of Natural Sciences of Belgium kindly provided specimens of *Glycymeris glycymeris*. Dr. Joseph G. Carter, Department of Geology, University of North Carolina, provided another critical review. Drs. Karl M. Wilbur and Richard M. Dillaman, Department of Zoology, Duke University, gave helpful suggestions and encouragement.

This is Contribution No. 48, Investigations of Marine Shallow Water Ecosystems (IMSWE) Project, partially supported by the Exxon Corporation.

Background

Extant arcoid bivalves comprise two superfamilies, the Arcacea and Limopsacea, which, with the extinct Cyrtodontacea, are included in the order Arcoida (Newell *in* Moore, 1969). Most authors agree that the order is primitive and that it has a long geological history stemming from the early Paleozoic era (Pojeta, 1971; Waller, 1978).

Taylor, Kennedy, and Hall (1969) have reviewed the literature on shell microstructure of the major bivalve groups and have determined that shells of extant species in the arcoid superfamilies Arcacea and Limopsacea are completely aragonitic in composition. The inner surface of the shell in every case consists of three regions: an inner region delimited peripherally on all sides by a continuous pallial line from a marginal shell band, which itself is bordered along its free, outer margins by a periostracal fringe. As described by these authors, the inner shell region consists of complex crossed lamellar fabric except in areas of muscle attachment, where an irregular prismatic fabric is secreted. The latter, termed myostracum by Oberling (1964), is generally assumed to indicate the presence of muscle insertions on the shell surface. The fabric secreted in the marginal shell band is said to be concentric crossed lamellar, although Kobayashi (1976) showed the intermittent presence of an outermost composite prismatic fabric in some species of *Anadara*. This must be secreted along the periphery of the marginal shell band.

The entire inner surface of the shell inside the pallial line and outside myostraca is marked by minute pores, which are the openings of tubules. Mutvei (1964), Taylor et al. (1969), and Wise (1971) have reviewed the literature on these structures in the Mollusca. Studies dealing specifically with arcoid tubules are by Omori, Kobayashi, and Shibata (1962), Omori and Kobayashi (1963), Kobayashi (1964), Oberling (1964), and Wise (1971).

From these studies it is known that tubules are formed inside the pallial line and perforate the outer, crossed lamellar shell layer along remarkably straight paths inclined to the inner shell surface. They remain open as complex crossed lamellar shell is deposited around them, but during this latter process their orientation abruptly changes, becoming normal to the growth surface of the inner shell layer. Taylor et al. (1969) remarked that tubules penetrate entirely through

the shell including the periostracum; Wise (1971) indicated that they penetrate through the shell but did not specify whether this included the periostracum. Schröder (1907), in a contribution now frequently overlooked, determined that in the bivalve family Sphaeriidae the tubules penetrate through the shell up to, but not through, the periostracum. Schröder was also able to determine that tubules are formed by extended cells of the mantle epithelium.

Only Rawitz (1890) has given a reasonably detailed description of the mantle edge of arcoid bivalves. In *Arca* and *Glycymeris* he found three marginal mantle folds, two of which are lateral to the periostracal groove. He also found that compound and simple photoreceptors, described earlier by Patten (1886) as occurring on the "middle fold," actually are lateral to the periostracal groove and hence lie beneath newly generated periostracum. Rawitz said little about the relationship between mantle and shell, nor did he describe the function of the various mantle folds in living specimens.

Subsequent attention to arcoid mantle edges focused on the detailed anatomy of the photoreceptors (Jacob, 1926; Nowikoff, 1926; Schulz, 1932; Levi and Levi, 1971) and analysis of their sensitivity (Braun, 1954). Modern general descriptions of bivalve mantle edges overlook Rawitz's discovery and place the eyes of arcoids in the same position as those of other bivalves—on the "middle fold" medial to the periostracal groove and hence unshielded by periostracum (e.g., Yonge, 1953; Charles, 1966).

Little attention has been paid to mantle differentiation across the boundaries that separate different shell fabrics, although Beedham (1958) demonstrated such changes in mantle tissue outside of the pallial line. Modern ultrastructural studies on bivalve mantle-shell relationships have instead concentrated on a particular location within a specimen, either outside the pallial line (Bevelander and Nakahara, 1967; Wada, 1968; Nakahara and Bevelander, 1971; Neff, 1972b; Bubel, 1973a, 1973b; Saleuddin, 1974) or inside it (Neff, 1972a; Tsujii, 1976). Other ultrastructural studies have dealt with the nature of muscle attachments or areas of adhesion between mantle and shell (Hubendick, 1958; Nakahara and Bevelander, 1970; Tompa and Watabe, 1976; Petit, Davis, and Jones, 1978). As pointed out by Taylor et al. (1969), the irregular prismatic shell fabric commonly associated with muscle-attachment areas is found in a variety of distributions in bivalve shells, not all of which are the result of muscle attachment. It seems that this fabric may also form adjacent to specialized mantle epithelium unassociated with muscle. In either case the same function—the anchoring of tissue to shell—may be served.

Terms

Figures 1 through 3 show the application of anatomical terms. The usual three-fold terminology of "inner, middle, and outer" with reference to marginal folds of the mantle is abandoned in favor of a system that numbers functionally distinct mantle folds consecutively inward and outward from the periostracal groove. I have argued elsewhere that, in view of the complexity of mantle margins in the Bivalvia and their primary two-fold condition, such a system avoids connotations of homology except for the periostracal groove itself, which indeed appears to be homologous throughout the class (Waller, 1978).

Terms referring to shell fabrics are adapted from Taylor, Kennedy, and Hall (1969). The terms "distal" and "proximal" refer, respectively, to directions toward and away from the margin of the shell or mantle. "Lateral" and "medial" are used in the customary anatomical sense, meaning away from or toward the median plane of the animal. "Commarginal" means parallel to the shell margin and is used in preference to "concentric." "Radial" is used in the special sense commonly found in descriptions of bivalve shell sculpture: it means perpendicular to the shell margin. A "ray" is thus any structure or group of structures having a radial orientation with respect to the shell margin. "Pallial line," as used herein, is the distal edge of the inner shell layer and

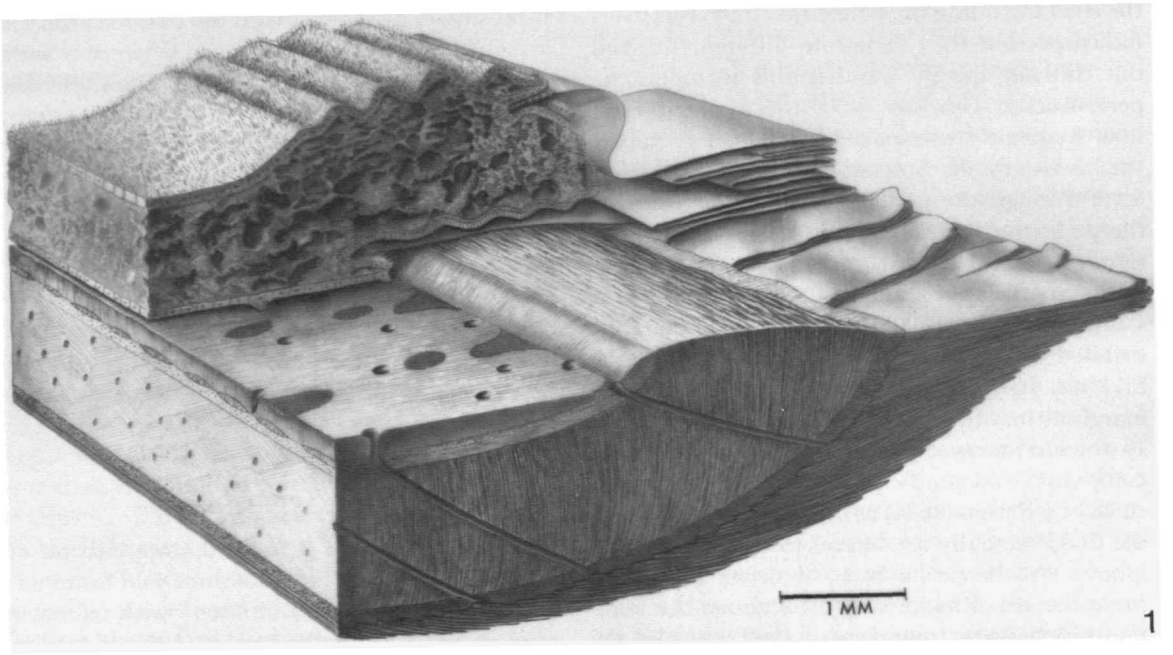

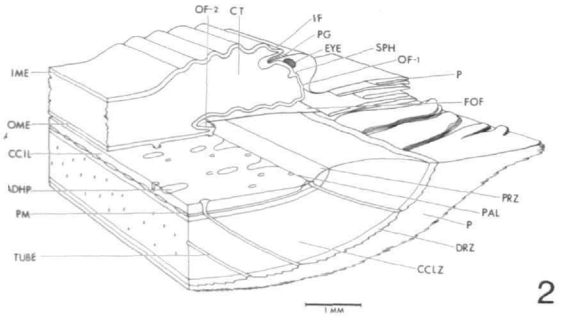

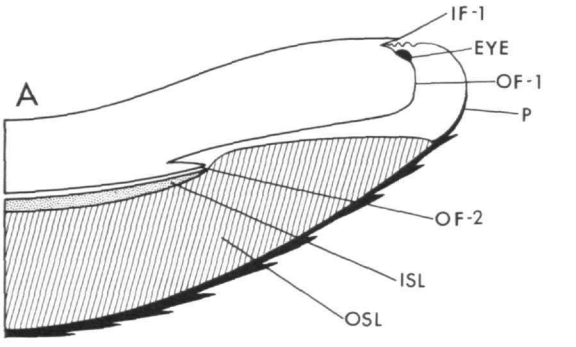

FIGURES 1, 2.—Schematic block diagram and anatomical key showing relationship between mantle and shell in ventral region of mature *Arca zebra*. (Nerves and muscles not shown; smaller parts not to scale; bar for overall size only; ADHP = adhesive patch on inner shell layer, CCIL = complex crossed lamellar inner shell layer, CCLZ = commarginal crossed lamellar zone of outer shell layer, CT = connective tissue with blood sinuses, DRZ = distal radial zone of outer shell layer, EYE = compound eye, FOF = fibrous organic film overlying marginal band of shell, IF = inner fold of mantle, IME = inner mantle epithelium, OF-1 = first outer fold of mantle, OF-2 = second outer fold of mantle, OME = outer mantle epithelium, P = periostracum, PAL = pallial line, PG = periostracal groove, PM = pallial myostracum, PRZ = proximal radial zone of outer shell layer, SPH = simple invaginated photoreceptor, TUBE = tubule.)

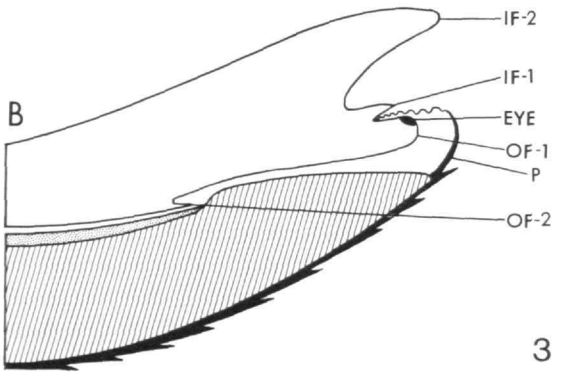

marks the distal end of close, constant apposition of mantle to shell. It is generally but not necessarily a line or zone of attachment of pallial muscles. The growth surface of the shell distal to the pallial line is referred to as the "marginal band." The term "myostracum" is used in its original sense (Oberling, 1964), meaning a shell layer that is secreted in an area of muscle attachment. So far as known, myostracal fabric consists of irregular prisms composed of aragonite.

Material and Methods

Specimens of *Arca zebra* (Swainson, 1833), *Arca imbricata* Bruguière, 1789, *Barbatia cancellaria* (Lamarck, 1819), *Arcopsis adamsi* (Dall, 1886), and *Glycymeris pectinata* (Gmelin, 1791) were collected in the vicinity of Carrie Bow Cay, Belize, in late April 1976. These were placed with ventral margins upward in shallow bowls and covered with seawater. After the specimens had opened their valves and were actively circulating water, they were anesthetized by adding a few drops of 2-Phenoxyethanol (Eastman Kodak Co.) to the surface of the water in each bowl. The drops diffused slowly, so that several hours were required before anesthetization was complete for small animals. Large specimens were allowed to stand overnight, and an additional drop or two of anesthetic was added the following morning. Anesthetized specimens gaped widely and responded very slowly, if at all, to touch and to changes in light intensity, but ciliary activity and circulation of water through the gills continued to be vigorous.

The anesthetized specimens were studied at Carrie Bow Cay with a Wild M-5 binocular microscope at magnifications up to × 50 under incandescent reflected light. Some of the specimens were then fixed in 10% formalin in seawater buffered with carbonate sand and, after about one month, were transferred to 70% ethanol buffered with borax.

Samples of the mantle edge including compound eyes of a large *Arca zebra* were prepared for scanning electron microscopy in June 1976, using the method of critical-point drying developed by Anderson (1951, 1956) and now widely employed in biology and medicine (Becker and Johari, 1978). Briefly, the tissue was dehydrated from the original 70% ethanol in which it was preserved by bathing in 90% and 100% ethanol, then in 30% amyl acetate in ethanol, 50% amyl acetate in ethanol, and 100% amyl acetate. Critical-point drying was by means of a Denton DCP-1 unit using liquid carbon dioxide as the drying medium. The tissue was then sputter-coated, first with carbon and then with gold palladium, and viewed with Cambridge Mark-IIA, Cambridge S4-10, and Coates and Welter 106B scanning electron microscopes.

No further work on the preserved specimens was done until April 1978. At that time, a piece of the mantle like that originally studied with the scanning electron microscope was removed from the same specimen of *Arca zebra* and prepared in the same way. Because no appreciable deterioration could be detected in the scanning electron micrographs, other specimens brought back from Carrie Bow Cay—*Arca imbricata* and *Barbatia cancellaria*—were prepared at this time.

Specimens of *Glycymeris glycymeris* from Europe were anesthetized in a 4% solution of $MgSO_4$ in seawater and after 24 hours were preserved in 4% neutral formalin. Subsequent preparation for scanning electron microscopy was the same as above.

It should be noted that some shrinkage of tissue occurs during dehydration and critical-point drying (estimated to be up to 25% linear by Boyde, 1978), but this does not seem to be a serious problem at the levels of magnification and interpretation of the present study. In fact, shrinkage-induced fracture along cell boundaries proved to be useful for revealing the outlines of cells and the relationship between cell surfaces and adjacent structures.

FIGURE 3.—Two basic configurations of the mantle edge in the Arcoida shown diagramatically: A, the three-fold condition, as in *Arca* and *Glycymeris*; B, the four-fold condition, as in *Barbatia*. (EYE = compound eye, IF-1 = first inner fold, IF-2 = second inner fold, ISL = inner shell layer, OF-1 = first outer fold, OF-2 = second outer fold, OSL = outer shell layer, P = periostracum.)

Pieces of shell were prepared by stripping off the mantle tissue with forceps and drying in air before coating for scanning electron microscopy. Other specimens were treated with dilute sodium hypochlorite for various periods, then washed in neutral distilled water in an ultrasonic cleaner.

The specimens that provided the materials for illustration in the following report are preserved in the collections of the National Museum of Natural History, Smithsonian Institution, Washington, D.C., under the collection numbers of the former United States Museum (USNM). Their museum numbers, sizes, and localities are as follows:

USNM 707292. *Arca zebra*, length 47 mm, beach drift at Atwood Harbor, Acklin Island, Bahamas, 16 April 1971

USNM 794957. *Arca zebra*, length 77 mm, lagoon side of Carrie Bow Cay, Belize, depth 3 m, 22 April 1976

USNM 794958. *Arca imbricata*, length 17 mm, reef front off Carrie Bow Cay, Belize, depth 30 m, 26 April 1976

USNM 794959. *Barbatia cancellaria*, length 35 mm, among mangrove roots, Twin Cay, Belize, depth 1 m, 22 April 1976

USNM 794960. *Glycymeris glycymeris*, length 55 mm, purchased live in a French restaurant in Brussels, Belgium, and probably from the Atlantic coast of France, south of Normandy, March 1978

The total number of micrographs examined is 1014.

Observations

Shell

This section describes features of the shells of *Arca zebra*, *Arca imbricata*, *Barbatia cancellaria*, and *Glycymeris glycymeris* exclusive of the periostracum. The latter, although an integral part of the shell, will be discussed below in connection with the mantle edge and periostracal groove.

Marginal Band

The marginal band on the inner surface of a shell of *Arca zebra* 77 mm long varies in width from 1.8 to 2.5 mm, being broadest posteriorly and narrowest midventrally. The surface of this band differs from that found inside the pallial line in a number of features observable with the naked eye or under low magnification: (1) it is dark reddish brown in color and thus contrasts with the inner shell surface, which is unpigmented; (2) it has a porcelaneous luster, whereas the inner surface is dull or chalky; (3) it is completely devoid of tubule openings, whereas these are abundant inside the pallial line (Figure 4*a*); and (4) it is higher in elevation, the pallial line coinciding with an abrupt downward step from the marginal band to the shell surface inside the line (Figures 4*a*, 5*a*).

Examination of the marginal band of *Arca zebra* by low-power optical microscopy under reflected light (Figure 6) reveals that it is not entirely composed of the commarginal crossed lamellar fabric described in detail by Taylor et al. (1969) and Wise (1971). Rather, a zone along the distal edge of the band and another along its proximal edge, each approaching 150 μm in width, display radial fabrics that appear to merge with the centrally located commarginal crossed lamellar zone.

Examination of the growth surface of these marginal zones by scanning electron microscope requires the removal of a tenacious organic film that is present over the entire marginal band but absent, or at least not so well developed, on the shell surface inside the pallial line (Figures 7*a*, 9*a*). Distally this film contacts and possibly merges with the periostracal fringe (Figure 7*b*).

Except for its radial orientation the fabric of the proximal radial zone of *Arca zebra* (Figure 2) is similar to that of the commarginal crossed lamellar zone. First-order lamels reaching 10 μm in width contain uniformly inclined third-order elements (laths) of highly variable width (0.2 to 1.0 μm), the laths of adjacent first-order lamels being inclined in opposite directions (Figure 8). Second-order lamels, which in the commarginal crossed lamellar fabric are formed by the side-by-side alignment of third-order laths, are poorly developed. Radial fractures through this zone (Figure 5*b*) show a crossed structure similar to that which appears in commarginal fractures through the central zone.

The microstructure of the distal radial zone is

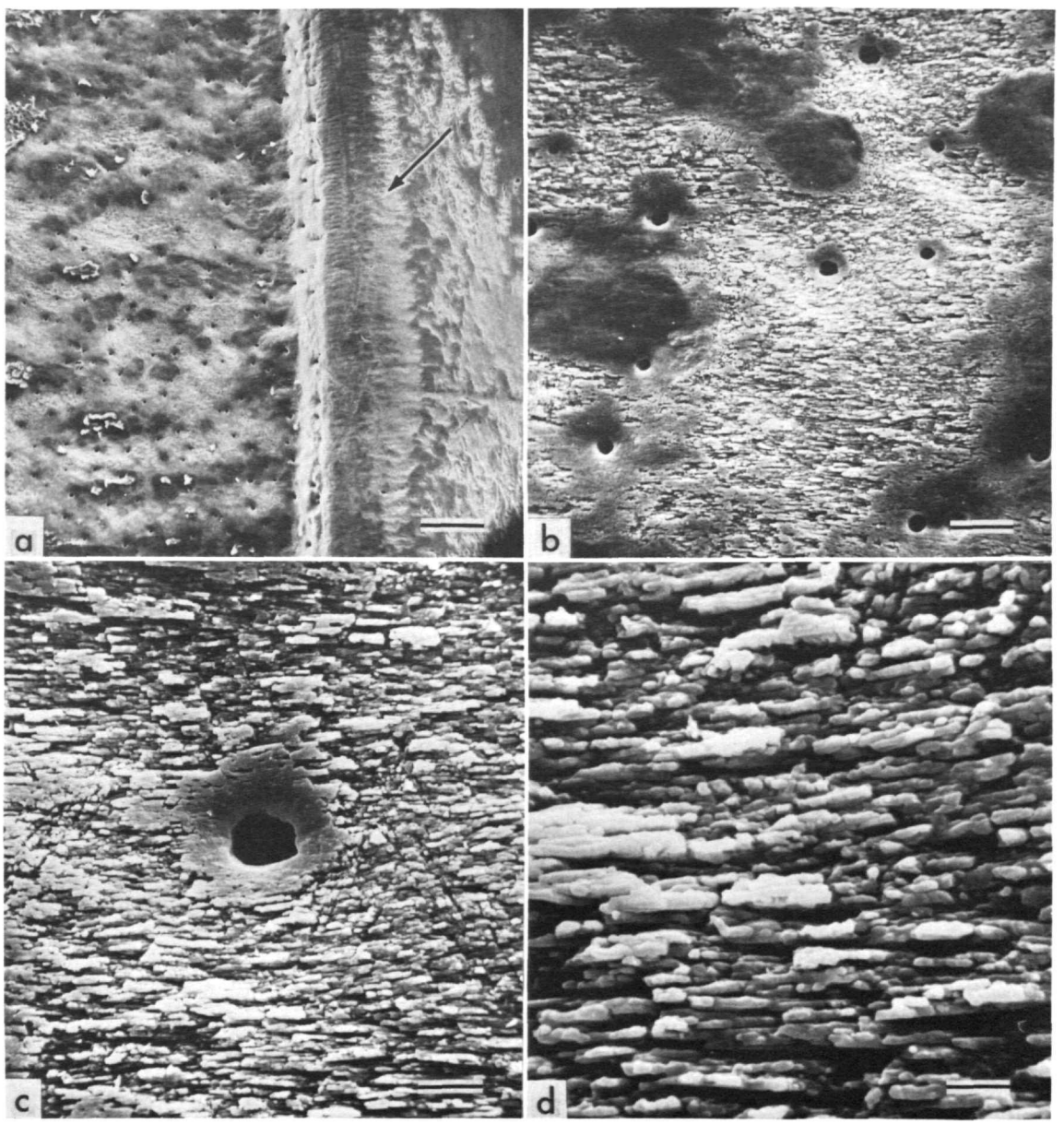

FIGURE 4.—*Arca zebra*, USNM 794957 (planar views of growth surface of shell near posteroventral edge of left valve; tissue mechanically stripped, direction of shell margin to right): *a*, boundary between tabulate inner shell layer (left) and marginal band with proximal radial zone (arrow) and part of commarginal crossed lamellar zone (right) (× 100, bar = 100 μm); *b*, detail of *a*, surface of inner shell layer (× 500, bar = 20 μm); *c*, detail of *b*, tubule opening (× 2000, bar = 5 μm); *d*, detail of *c*, complex crossed lamellar fabric (× 5000, bar = 2 μm).

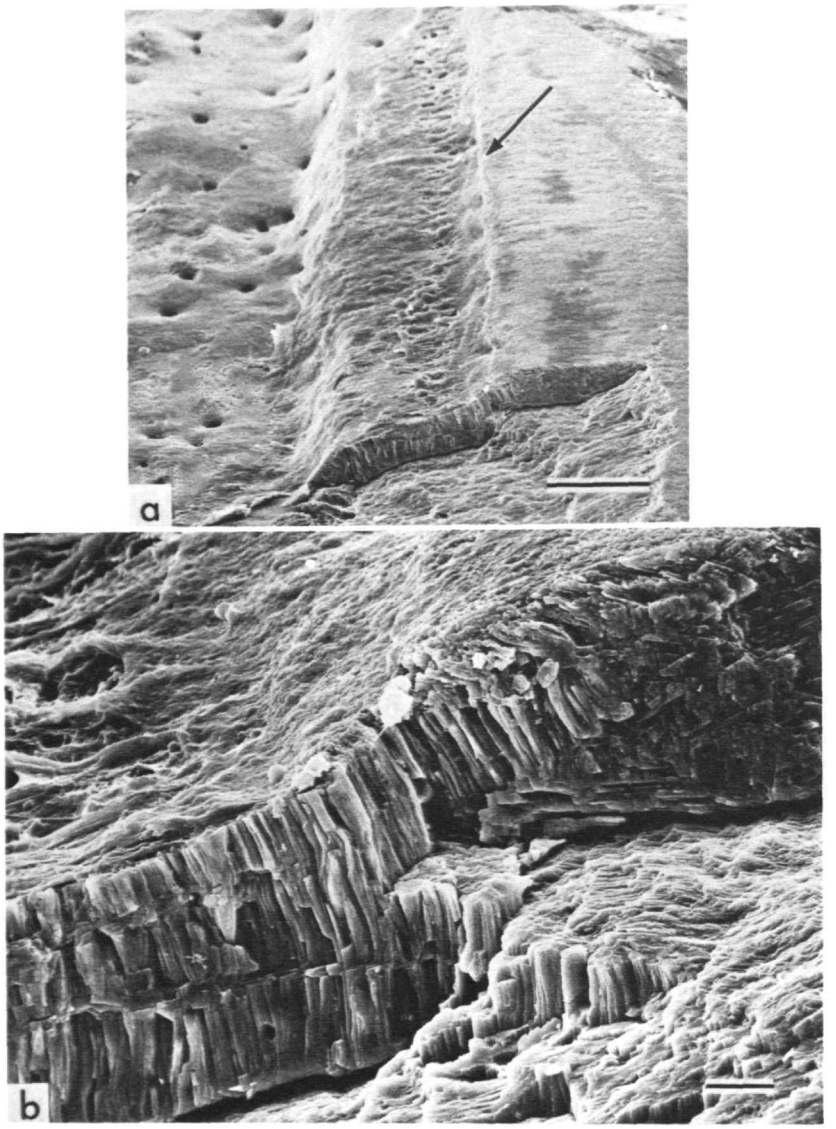

FIGURE 5.—*Arca zebra*, USNM 794957 (oblique (70°) views of stepped pallial line in posteroventral region of left valve, most of tissue mechanically removed, direction of shell margin to right): *a*, pallial line (arrow) separating tubulate growth surface of inner shell layer on left from growth surface of proximal radial zone of marginal band on right (× 300, bar = 50 μm); *b*, detail of *a*, radial fracture across pallial line, pallial myostracum (lower left) and radial crossed lamellar fabric (upper right) (× 2000, bar = 5 μm).

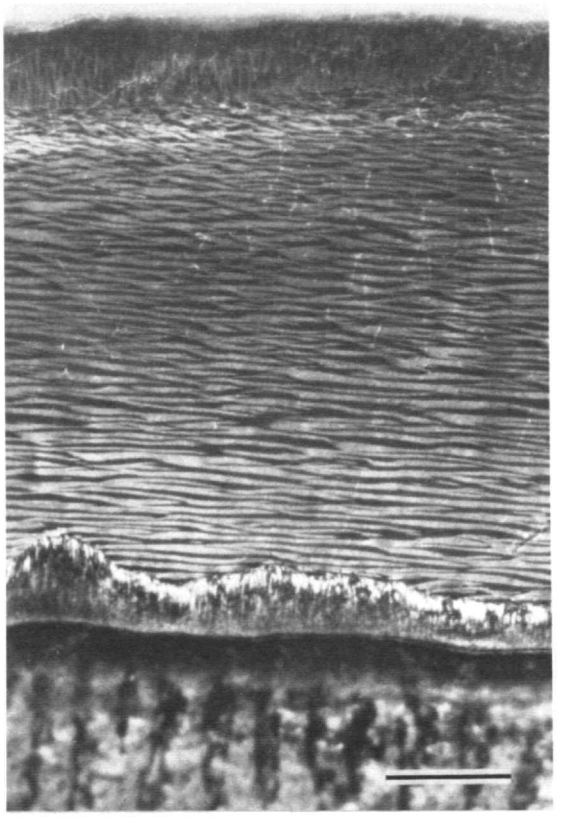

FIGURE 6.—*Arca zebra*, USNM 794957: Planar view of growth surface of marginal shell band photographed under reflected light through alcohol, shell margin at top, inner shell layer at bottom, tubules appearing as radial white streaks beneath surface of commarginal crossed lamellar zone (× 36, bar = 0.5 mm).

more difficult to discern due to the presence of the organic film and the thinness of the shell at its distal edge. There seems to be no ordered structure along the leading edge adjacent to the inner surface of the periostracum, but proximally the radial fabric becomes more evident, particularly in reflected light (Figure 6). Radial fractures through the proximal part of this zone show a crossed arrangement of laths, indicating that the fabric in this area is at least in part radial crossed lamellar as in the proximal radial zone.

The marginal band of the shell of a young *Arca imbricata* 17 mm long has a distribution of shell fabrics similar to that in the marginal band of *Arca zebra*. Here, however, the nature of the organic film covering the marginal band was re-

FIGURE 7.—*Arca zebra*, USNM 794957 (planar view of posteroventral growth surface of left valve, washed in distilled water and air dried; direction of shell margin to right): *a*, boundary between periostracal fringe (right) and marginal shell band (left) (× 300, bar = 50 μm); *b*, detail of *a*, proximal edge of periostracal fringe (× 5000, bar = 2 μm).

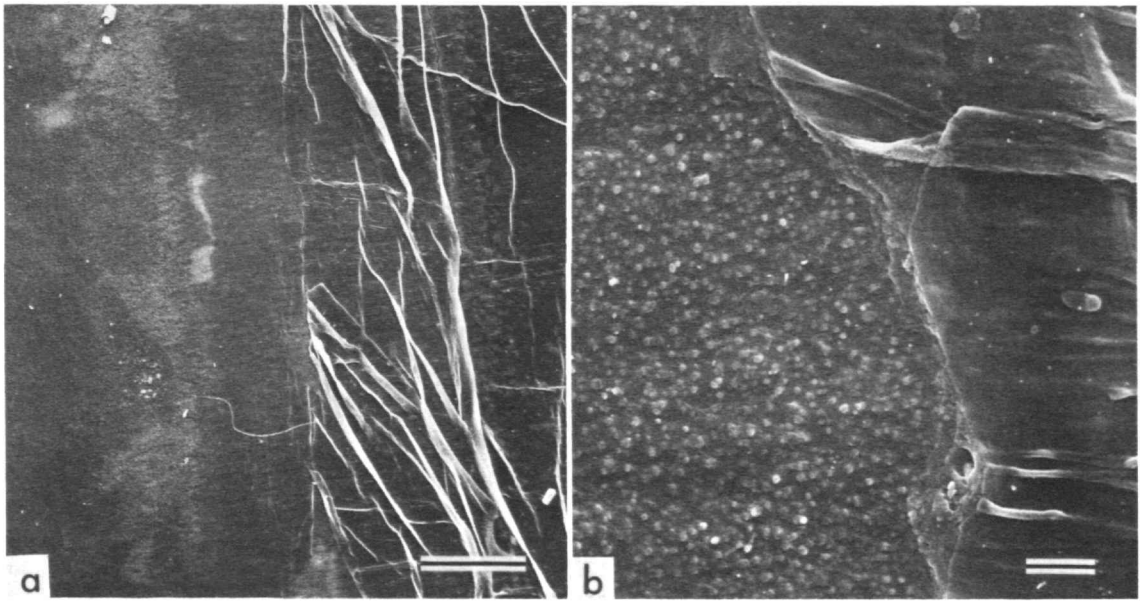

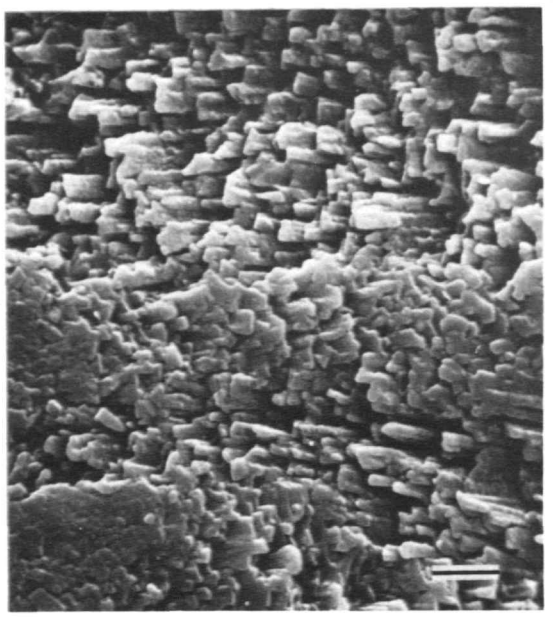

FIGURE 8.—*Arca zebra*, USNM 794957: planar view of growth surface of proximal radial zone of marginal shell band at posteroventral edge of left valve, direction of shell margin to right (× 5000, bar = 2 μm).

vealed in greater detail on a critical-point dried specimen. Where the film has cracked and curled back from the surface of the marginal band, the inner and outer surfaces of the film as well as the stripped surface of the underlying shell fabric can all be examined in detail (Figure 9). In the center of the marginal band, where the fabric is commarginal crossed lamellar, the film is 0.1 μm thick. Its medial surface is smooth, except for an exceedingly fine radial texture suggesting a fibrous composition and the presence of numerous surficial blebs of various sizes (Figure 9*b*). The outer surface of the film is an organic framework reflecting the growing surface of the underlying aragonitic shell. Traces of first-order lamels are clearly present (Figure 9*d*), as well as much finer radially aligned organic ridges that represent the outlines of second and third-order elements. Some crystals of aragonite adhere to the outer surface of the film, and it can be seen in Figure 9*c* that these crystals are alternately inclined in adjacent traces of first-order lamels. The organic film can be followed distally to the edge of the shell, where it meets the periostracal fringe, and proximally onto the inner surface of the second outer fold of the mantle.

In *Barbatia cancellaria* the marginal band lacks the proximal radial zone seen in *Arca*, the commarginal crossed lamellar fabric extending proximally to the pallial line. Distally, the commarginal crossed lamellar fabric grades into an irregular crossed structure consisting of clusters of third-order laths 0.1 to 0.3 μm in width (Figure 10). Within each cluster the laths are of uniform inclination relative to the growth surface, but the angles of inclination differ between clusters. There is little tendency for the laths to group into second-order lamels; the clusters themselves represent the first-order elements of the fabric.

Critical-point dried specimens of *Barbatia cancellaria* show an organic film (Figure 11*a*) completely covering the surface of the marginal band and similar to the film previously described in *Arca imbricata*. The structure of the film is radially fibrous (Figure 11*b*,*c*), the diameters of the fibers being on the order of 0.05 μm. As in *A. imbricata*, surface blebs are present, grading in size up to a maximum diameter of 0.3 μm. These are not present on adjacent surfaces outside of the marginal band in the same specimen and thus are either integral components of the organic film or artifacts produced by the interaction of preparation procedures with the film itself. Also as in the previous species discussed, the outer surface of the film has an organic framework reflecting the elements of the underlying shell fabric (Figure 12*a*). The organic sheaths of adhering third-order elements of the shell fabric appear to be continuous with the outer surface of the film (Figure 12*b*).

The marginal band of *Glycymeris glycymeris* has a distribution of shell fabrics resembling that of *Barbatia cancellaria*. There is no proximal radial zone; distally the first-order lamels of the commarginal crossed lamellar fabric become shorter and more irregular and are highly irregular at the distal edge. Once again, the entire growth surface of the marginal band is covered by an organic film.

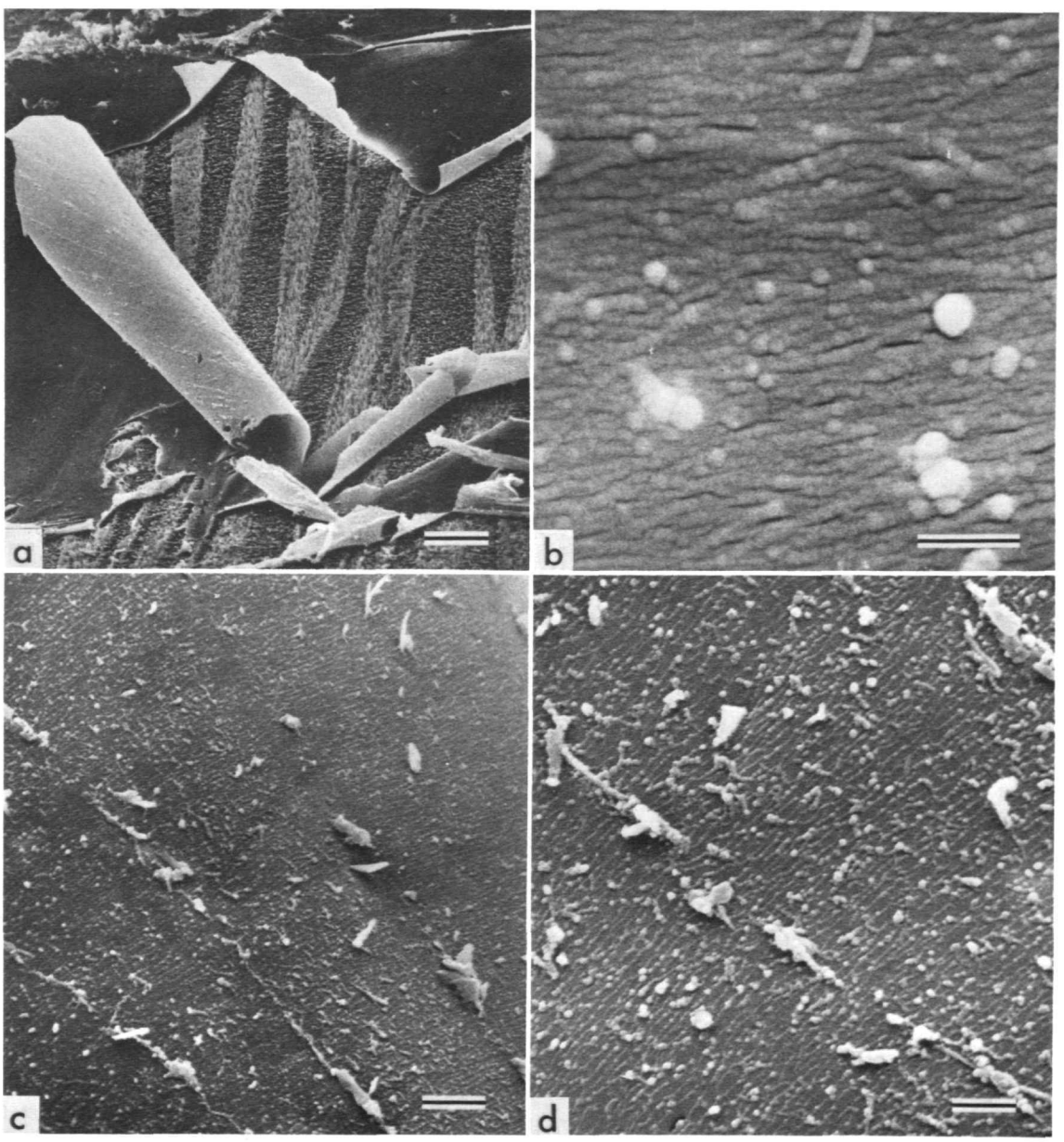

FIGURE 9.—*Arca imbricata*, USNM 794958 (organic film overlying growth surface of marginal shell band in anterior region, critical-point dried): *a*, oblique (74°) view of film curled back to reveal underlying commarginal crossed lamellar fabric, direction of shell margin to right (× 500, bar = 2 μm); *b*, oblique (30°) view of growth surface of film, direction of shell margin to right (× 40,000, bar = 0.4 μm); *c*, surface of film originally facing shell surface, on curled-back portion to left of center in *a* (× 5000, bar = 2 μm); *d*, detail of *c* (× 10,000, bar = 1 μm).

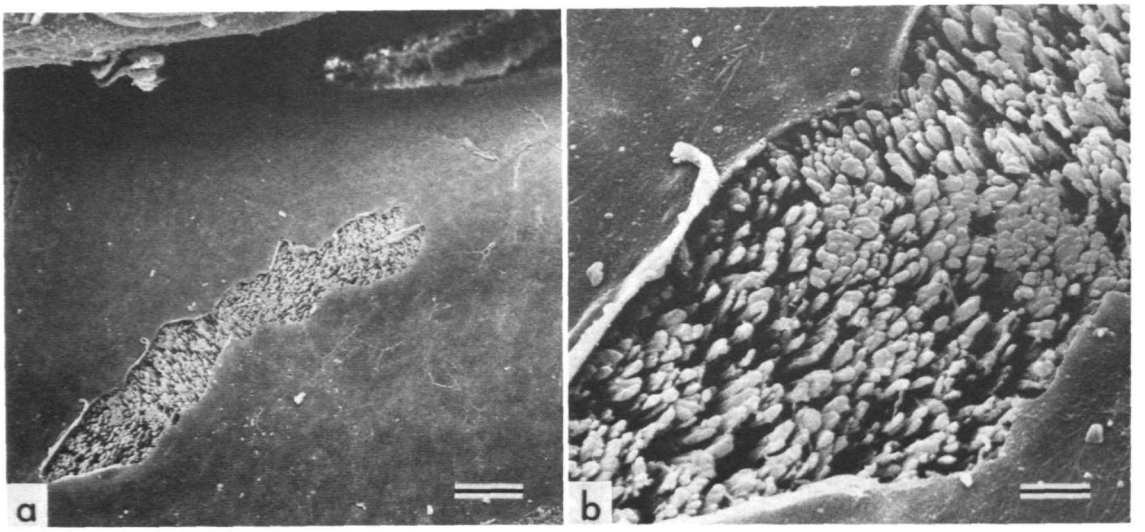

FIGURE 10.—*Barbatia cancellaria*, USNM 794959 (planar views of growth surface of marginal shell band of left valve, critical-point dried, direction of shell margin toward top): *a*, distal edge of marginal band, with periostracal fringe along top edge and tear in organic film extending diagonally across center (× 1000, bar = 10 μm); *b*, detail of *a*, aragonite crystals in irregular crossed pattern beneath organic film (× 5000, bar = 2 μm).

Shell Surface inside Pallial Line

Wise (1971) described the shell margins of *Anadara notabilis* with particular emphasis on the pallial line. He found that in this arcoid species the distal portion of the inner shell surface inside the pallial line is marked by distinct, tubulate, radial grooves separated by low, nontubulate ridges, both terminating distally at the pallial line. The ridges are underlain by irregular prismatic fabric and presumably represent the tracks of distally migrating attachment scars of pallial muscles; the grooves are underlain by complex crossed lamellar fabric secreted by the surface of the mantle outside muscle insertions. At their proximal ends, the myostracal ridges are gradually covered by the advancing zone of secretion of complex crossed lamellar fabric, which assumes a "cross-matted" appearance where it covers the proximal ends of the ridges.

The species examined in the present study have other patterns of pallial attachment and fabrics in the region inside the pallial line. These can best be discussed separately for each genus. Detailed observations on tubules follow in a separate section.

Arca.—In both *Arca zebra* and *Arca imbricata* the pallial line coincides with a distinct commarginal step on the inner surface of the shell, which raises the marginal band above the level of the surface inside the pallial line (Figures 1, 4*a*, 5*a*). The precise position of the pallial line on the sloping surface of the step is variable. Generally it lies at about midlevel, so that the upper portion of the step is underlain by the proximal radial zone of the marginal band and the lower portion by the leading edge of the inner shell layer. However, in some mature or gerontic *A. imbricata* (e.g., USNM 734738, Limón Bay, Panama) the step is exaggerated, with the leading edge of the inner shell layer actually protruding beneath the overhanging proximal edge of the marginal band.

On the basis of binocular, reflected-light microscopy, the entire pallial line ventral to the adductors seems to be underlain by thin, clear myostracum, which transmits the dark color of the underlying outer shell layer (Figure 6). The line is generally straight on its distal side but

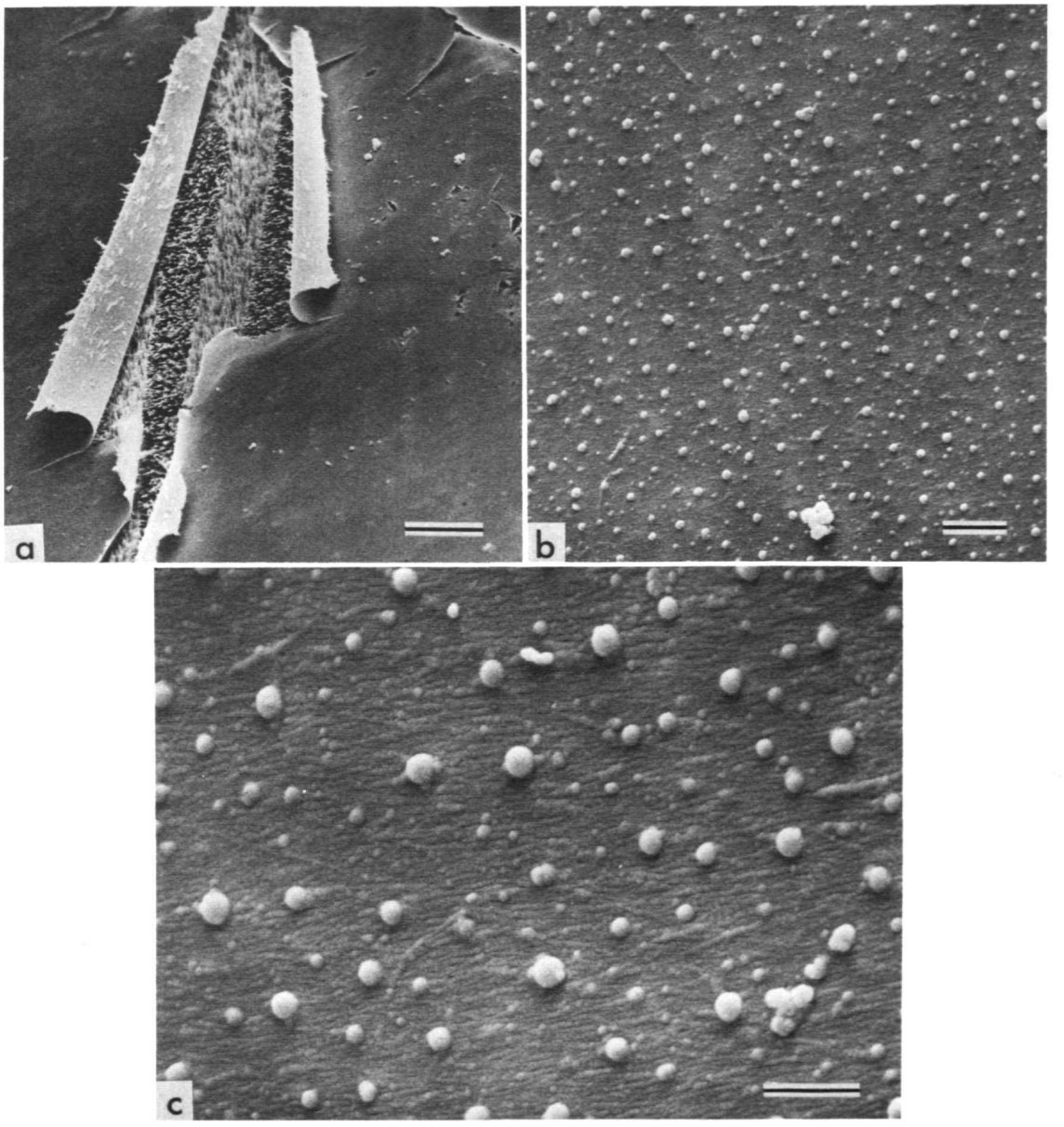

FIGURE 11.—*Barbatia cancellaria*, USNM 794959 (growth surface of marginal shell band of left valve, critical-point dried): *a*, oblique (45°) view of organic film over growth surface of marginal band, cracked and curled back to reveal underlying commarginal crossed lamellar fabric, direction of shell margin toward upper right (× 600, bar = 20 μm); *b*, planar view of growth surface of organic film, direction of shell margin to right (× 5000, bar = 2 μm); *c*, detail of *b*, radially fibrous fabric of organic film and surface blebs (× 15,000, bar = 1 μm).

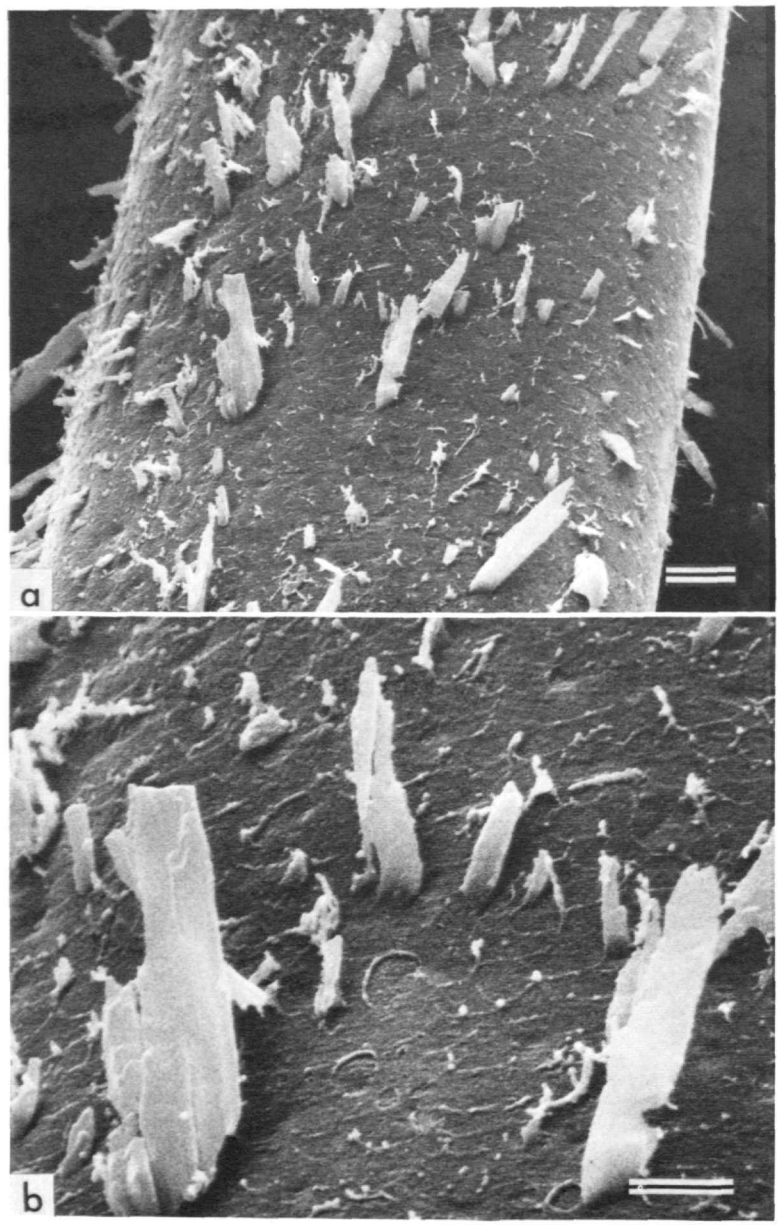

FIGURE 12.—*Barbatia cancellaria*, USNM 794959: *a*, detail of Figure 11*a*, surface of organic film peeled back from underlying crossed lamellar fabric (× 5000, bar = 2 μm); *b*, detail of *a*, third-order laths of aragonite adhering to and encased by film (× 15,000, bar = 1 μm).

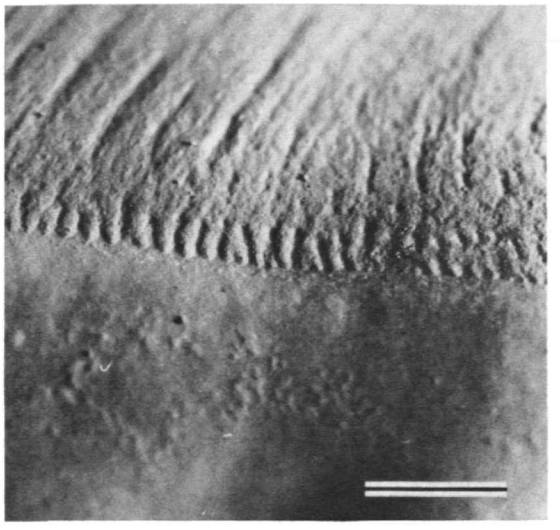

FIGURE 13.—*Arca zebra*, USNM 707292: planar view of pallial line in posterior region, direction of shell margin toward bottom (× 21, bar = 1 mm; optical photograph).

digitate on its proximal side, particularly in the posterior region (Figure 13). Radial rows of tiny dark spots, which range in diameter from 5 to 200 μm and presumably represent either muscle attachments or zones of adhesion between mantle and shell, lead proximally from the digitations, and so also do low radial undulations, the troughs of which align with the digitations on the pallial line. Tubule openings are distributed in a random pattern over the entire inner shell surface inside the pallial line but tend to be absent from the central portions of the growth surfaces of the adductor myostraca (Figure 4*a*).

This pattern is unlike that of *Anadara notabilis* described by Wise (1971). In that species the radial undulations next to the pallial line are far coarser (9 ridges per 5-mm distance along the pallial line of a 40-mm-long *A. notabilis* but over 30 in a specimen of *Arca zebra* of similar size). Furthermore, in *Anadara notabilis* the tubule openings are restricted to ridges, which Wise showed to be underlain by "myostracum" (irregular prismatic fabric). In *Arca zebra* and *A. imbricata* tubule distribution is unrelated to the ridges, and the troughs rather than the ridges align with pallial muscle scars.

Myostracal fabric in *Arca* conforms to the general pattern in bivalves described by Taylor et al. (1969), but scanning electron micrographs of the growth surface reveal additional features not previously described. Three orders of structure appear to be present on the growth surface of the anterior adductor scar of the 17-mm-long *Arca imbricata*: (1) first-order polygons, highly variable in shape and size but generally with diameters on the order of 10 to 25 μm (Figure 14*a,b*); (2) second-order patches of highly irregular shape and size (1 to 8 μm), commonly with very irregular wavy borders (Figure 14*c*); and (3) third-order needle-like elements, about 0.1 or 0.2 μm in diameter and of unknown length, inclined uniformly to the growth surface within each second-order patch but differing greatly in direction and degree of inclination between patches (Figure 14*c*).

Fractures through adductor myostracum reveal the typical irregular prismatic fabric described by Taylor et al. (1969) and Wise (1971). The irregular prisms seen in fractures through the myostracum (Figure 14*a,b*) range in diameter from less than 1 μm to over 5 μm and appear to correspond in scale and cross-sectional shape to the second-order patches present on the growth surface. Neither the first-order polygons nor the third-order, needle-like elements of the growth surface are expressed in cross-sectional views. However, the third-order units resemble the lineations on etched nacre tablets described by Mutvei (1978) and considered by him to be indicative of polysynthetic twinning of crystals. This resemblance suggests that individual prisms may be crystallographically uniform but that crystal orientation differs between adjacent prisms.

In both species of *Arca* the three-dimensional fabric of the inner shell layer near the pallial line differs markedly from the complex crossed fabric described by Wise (1971) in *Anadara notabilis*. Only the distal portion of the region inside the pallial line was examined in the present study, but in this area the expression of the fabric at the growth surface is radial, as shown in Figures 4*b,d* and

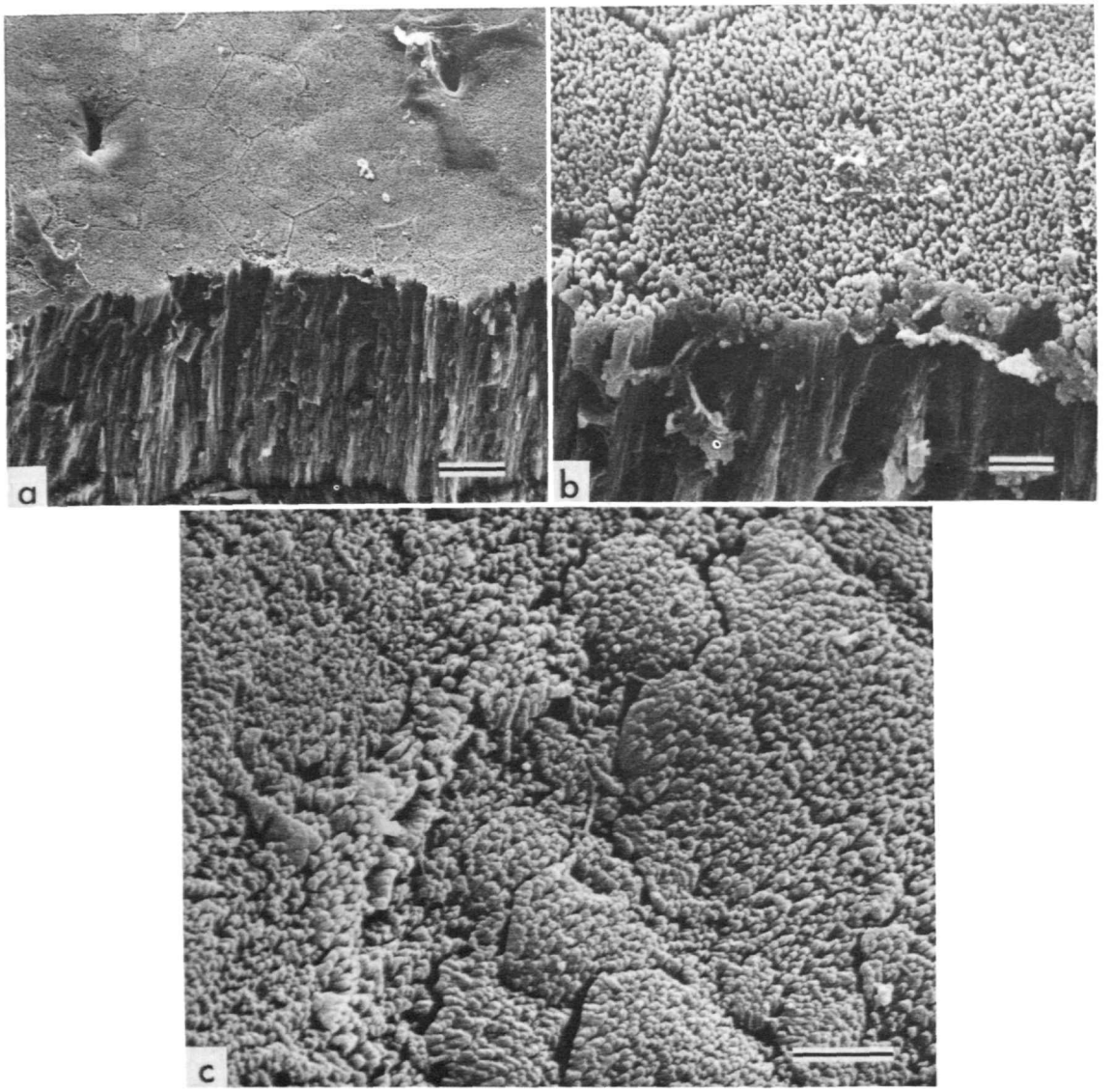

FIGURE 14.—*Arca imbricata*, USNM 794958 (oblique (45°) views of growth surface of anterior adductor scar of left valve, tissues mechanically removed before critical-point drying): *a*, two tubule openings and first-order polygonal pattern on growth surface (× 1000, bar = 10 μm); *b*, detail of *a*, growth surface at edge of fracture, second-order patches not visible (× 5000, bar = 2 μm); *c*, growth surface in another region of same adductor scar, irregular second-order patches and inclined third-order elements within each patch (× 7500, bar = 2 μm).

15*a*. The principal elements are vertical plates of aragonite 0.3 to 0.5 μm in thickness and of highly variable length in the plane of the shell surface. It can be seen in Figures 4*d* and 15*b* that these plates are in turn composed of finer elements, which appear to be blocky laths of a cross-sectional diameter comparable to the thickness of the plates. A comparison of radial and commarginal fractures through this fabric (Figure 15), demonstrates that the first-order vertical plates taper in a radial plane and do not exceed 2 μm in depth between their inner and outer surfaces. This same dimension is the maximum length of the second-order laths comprising the plates.

Barbatia.—In *Barbatia cancellaria* the inner shell region is only very slightly depressed below the surface of the marginal band. A shallow commarginal step is barely discernible by reflected-light microscopy but appears clearly in oblique views with the scanning electron microscope (Figure 16*a*). As in *Anadara notabilis* described by Wise (1971), broadly spaced nontubulate rays of myostracum (numbering 15 in a 5-mm distance along the inner side of the pallial line of a 40-mm-long specimen) are separated by tubulate rays along the inner side of the pallial line. Here, however, the nontubulate myostracal rays are not raised but instead are depressed below the level of the intervening tubulate rays. The myostracal rays broaden distally and merge along the pallial line, thereby preventing the majority of the intervening tubulate rays from reaching this point. However, the fact that some tubulate rays also reach the pallial line suggests that the pallial myostracum is laterally discontinuous.

The fabric of the myostracal surface within nontubulate rays (Figure 16*c*) resembles that found in adductor myostracum except that first-order structures are not polygonal but rather are highly irregular in form. The fabric of the tubulate rays (Figure 16*b*) resembles the cross-matted fabric found in tubulate rays of *Anadara* (Wise, 1971); there is no predominantly radial fabric inside the pallial line as in *Arca*.

Glycymeris.—The inner surface of the shell of *Glycymeris glycymeris* gradually changes in curva-

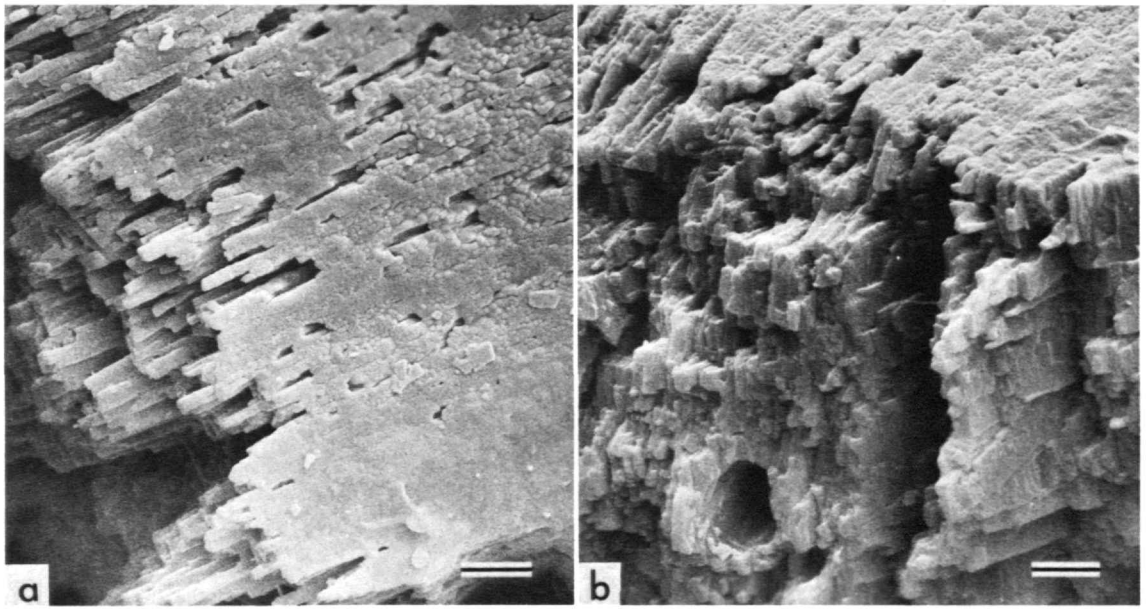

FIGURE 15.—*Arca zebra*, USNM 794957 (inner shell layer from which tissue has been mechanically stripped): *a*, planar view of growth surface, direction of shell margin toward upper right; *b*, oblique view of commarginal fracture at left side of *a* (both × 5000, bar = 2 μm).

ture from the concave region inside the pallial line to the nearly flat marginal band (Figures 17, 18*a*). As in *Anadara* and *Barbatia*, distinct pallial attachment scars are present, and these leave nontubulate myostracal tracks separated by tubulate rays, the two kinds of surfaces being at essentially the same level (Figure 17). Here, however, the myostracal rays all merge along the pallial line, so that the entire leading edge of the region inside the pallial line is irregularly prismatic in fabric (Figure 18*b*). The shell fabric between myostracal rays is a complex crossed structure differing from fabrics occupying comparable regions in *Arca*, *Barbatia*, and *Anadara*. This fabric was not studied in detail.

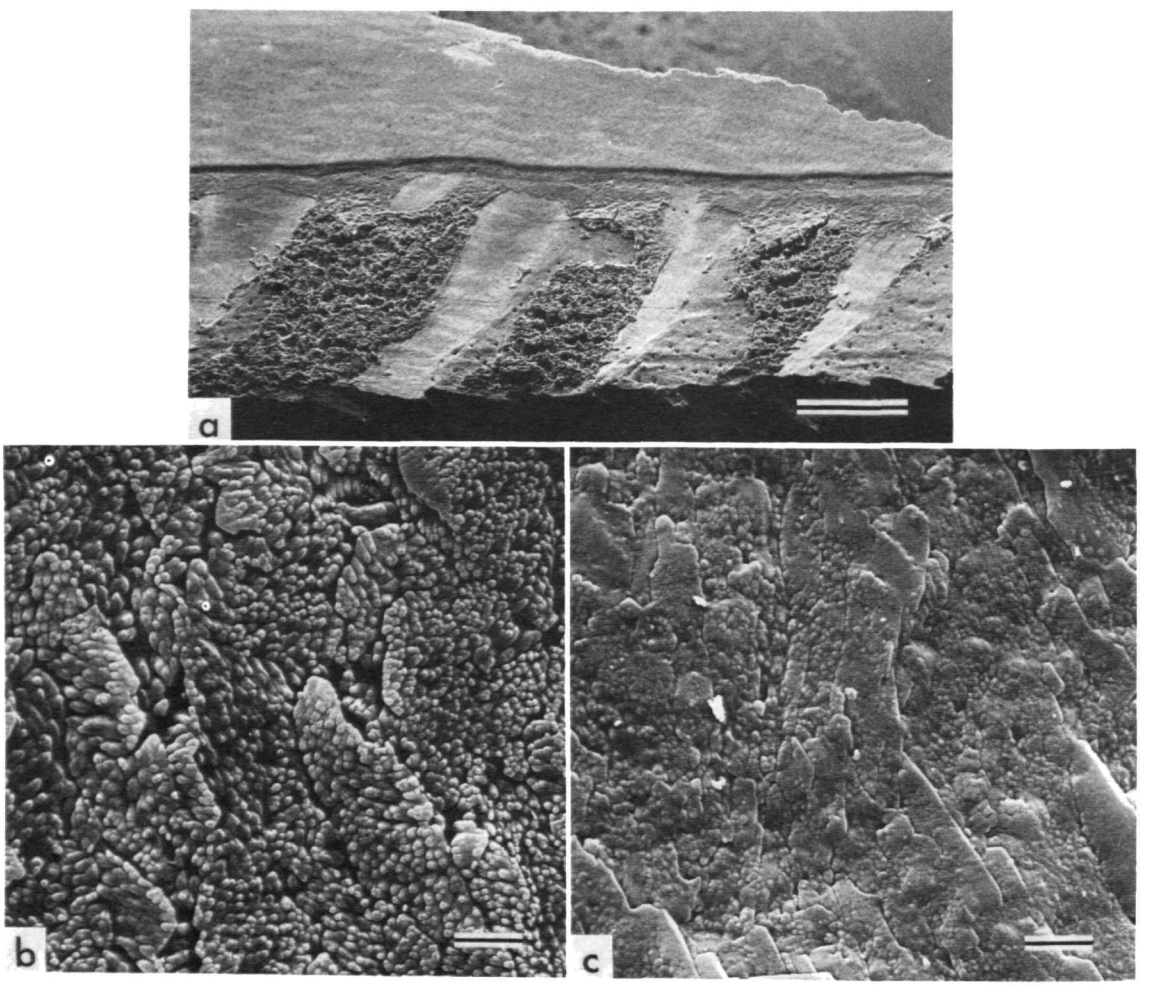

FIGURE 16.—*Barbatia cancellaria*, USNM 794959 (ventral edge of left valve bleached 200 hours and ultrasonically cleaned): *a*, oblique (45°) view across pallial line, tubulate rays with adhering tissue separated by nontubulate myostracal rays along bottom, pallial line across center, and marginal band ending along fracture at top (× 80, bar = 200 μm); *b*, planar view of growth surface of complex crossed fabric in a tubulate ray (× 1000, bar = 10 μm); *c*, planar view of growth surface of "crossed-matted" fabric in a myostracal ray (× 1000, bar = 10 μm).

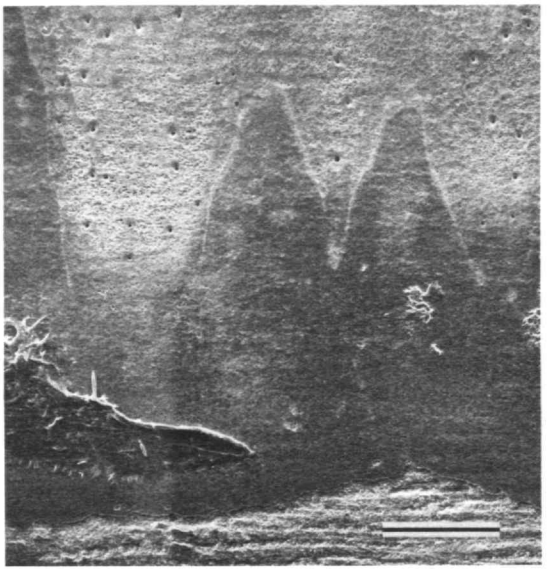

FIGURE 17.—*Glycymeris glycymeris*, USNM 794960: planar view of growth surface at pallial line, air dried, tissues mechanically removed, myostracum dark gray, tubulate rays at top, myostracum stripped off surface of commarginal crossed lamellar zone at bottom, direction of shell margin toward bottom (× 85, bar = 200 μm).

Tubules

In each of the four species studied by scanning electron microscopy, tubules in the shell conform to the basic pattern outlined by Omori et al. (1962), Oberling (1964), Taylor et al. (1969), and Wise (1971). They are remarkably straight or very gently curved tunnels 2 to 10 μm in diameter, which in the outer shell layer are inclined to the inner surface of the shell at a high angle (Figures 19, 21) but in the inner shell layer are generally perpendicular to the growth surface (Figure 20). In spite of the fact that not all tubules are parallel, no intersections between them have yet been observed in areas examined stereoscopically.

The sides of tubules are parallel and without noticeable tapering, although in some cases small annular expansions may occur. Near the outer surface of the shell, the tubules become difficult to trace because of the presence of numerous borings. In a young individual of *Arca imbricata*, however, some of the tubules could be followed to the outer surface of the shell beneath the periostracum. As shown in Figure 21*b*, a tubule having a diameter of less than 2 μm in the outer shell layer begins to broaden within 58 μm of the outer surface of this layer and finally expands to nearly 7 μm at the surface. Elliptical areas on the inner surface of the critical-point dried periostracum peeled from this area have about the same diameter as the flared distal ends of tubules (Figure 21*c*). These areas show disruption of the compact fibrous fabric of the inner surface of the periostracum and presumably overlie the outer ends of tubules. It thus seems that although the mantle projections that form tubules are able to dissolve calcium carbonate, they cannot completely penetrate the organic material comprising the periostracum. Neither can they destroy the loose network of organic fibers that is present in the outermost layer of shell (secreted in the distal radial zone), because such a network remains in the distal ends of tubules (Figure 21*b*).

The secondary nature of tubules in the outer shell layer surmised by Oberling (1964) and Wise (1971) is evident in scanning electron micrographs. All three orders of structure in the commarginal crossed lamellar fabric are neatly transected (Figure 19*a*, *b*). There is no evidence of organic linings on the walls of tubules, although some secondary calcification is present, as shown by the fact that tiny crystals grow inward into the tubule from third-order elements of the adjacent crossed lamellar structure (Figure 19*b*). It is not known whether these secondary deposits are postmortem artifacts or whether they may have formed during life.

As shown by Omori et al. (1962) and Wise (1971), the angle of inclination of tubules changes at the interface between the outer and inner shell layers, so that within the latter they are generally perpendicular to the inner shell surface. The complex fabric of the inner shell layer is secreted around the mantle projection forming the tubule and is not transected, indicating that in this area the tubules are primary rather than secondary. This is shown in *Glycymeris glycymeris* in Figure 20

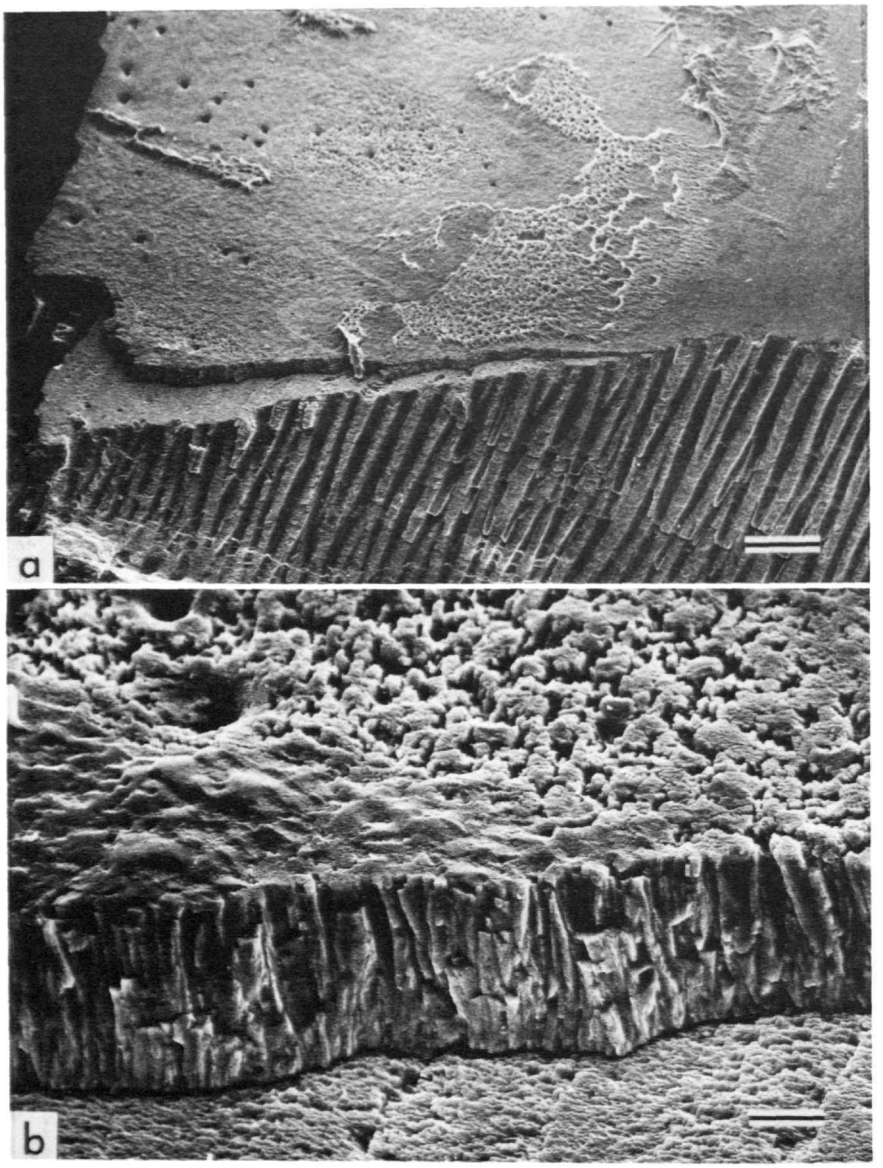

FIGURE 18.—*Glycymeris glycymeris*, USNM 794960 (oblique (45°) views of pallial line prepared as in Figure 17, direction of shell margin toward lower right): *a*, oblique radial fracture through outer shell layer on bottom, inner shell layer attenuating toward pallial line on top (× 110, bar = 100 μm); *b*, detail of *a*, fracture through inner shell layer (× 1100, bar = 10 μm).

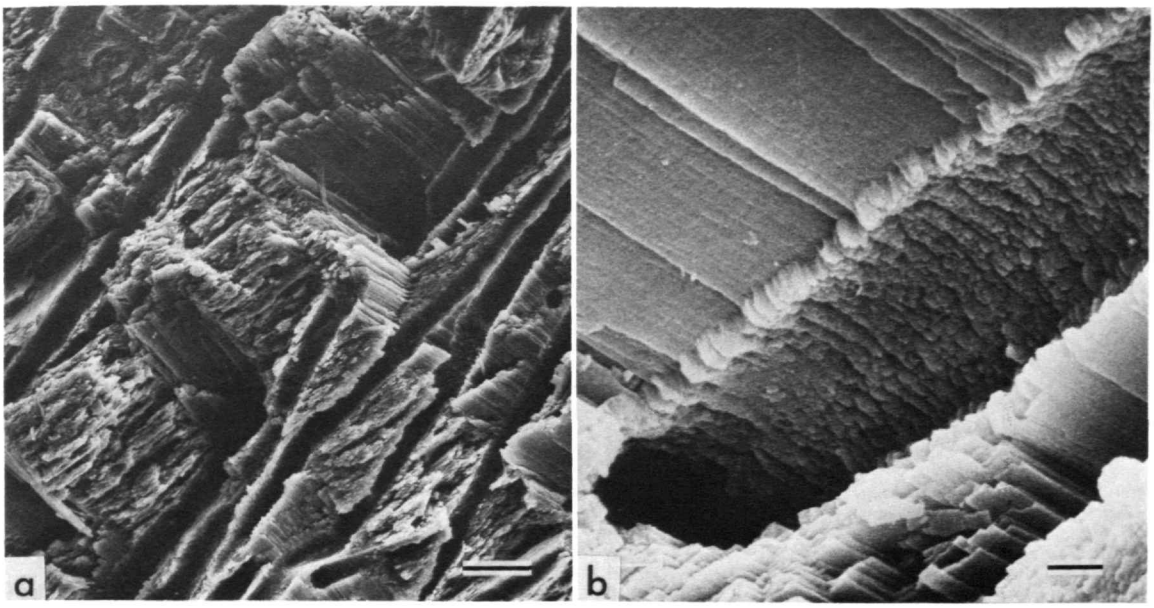

FIGURE 19.—*Arca zebra*, USNM 794957 (radial fracture through outer shell layer near poster-oventral edge of shell, ultrasonically cleaned and air dried): *a*, tubules crossing commarginal crossed lamellar fabric, direction of shell margin toward left, inner surface of shell toward top (× 1000, bar = 10 μm); *b*, detail of a fractured tubule crossing second- and third-order elements of crossed lamellar fabric and having secondary crystal growth on its wall (× 8000, bar = 1 μm).

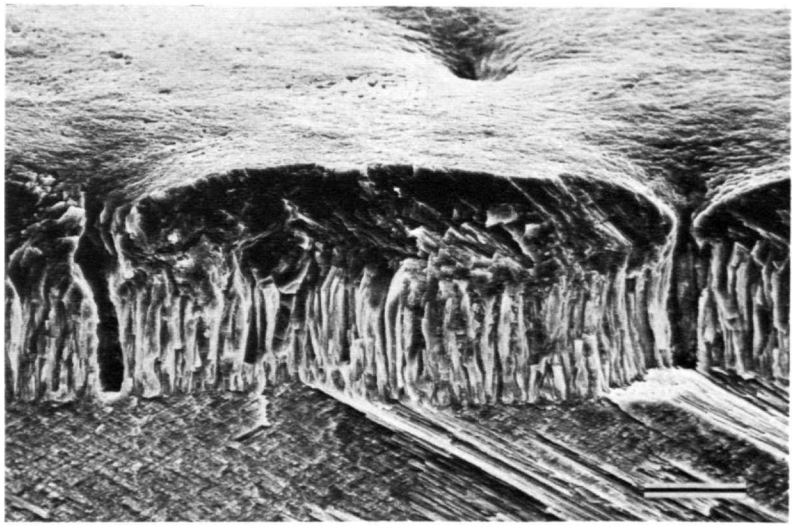

FIGURE 20.—*Glycymeris glycymeris*, USNM 794960: oblique view of commarginal fracture across growth surface of a tubulate ray proximal to pallial line (× 750, bar = 20 μm).

and in *Arca imbricata* in Figure 22. In the latter case, which is a commarginal section through the anterior adductor scar, a loose network of fibers is present in the tubule below its conical opening on the inner shell surface. These fibers appear to be part of the organic matrix, which is integrated in the myostracal fabric elsewhere.

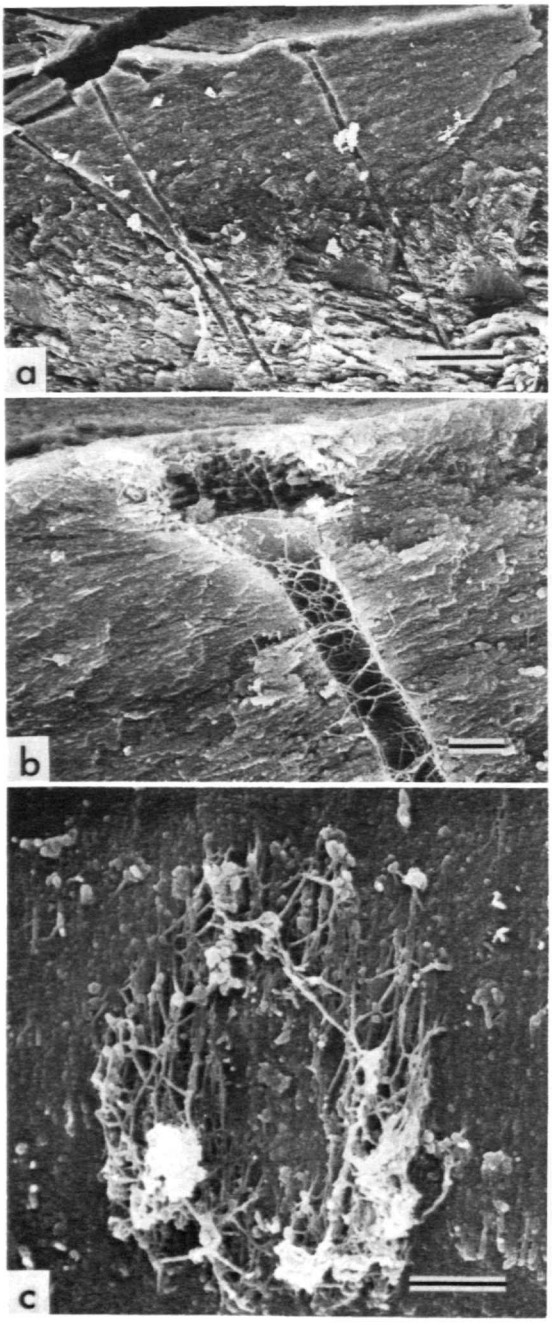

FIGURE 21.—*Arca imbricata*, USNM 794958 (fragments of outer shell layer near ventral margin, critical-point dried): *a*, radial fracture through outer shell layer, tubules reaching outer surface of shell (top) from which periostracum has been removed, direction of shell margin to left (× 630, bar = 20 μm); *b*, detail of *a*, distal end of tubule, penetrating outermost shell layer and flaring at its distal opening (× 4000, bar = 2 μm); *c*, planar view of inner surface of periostracum stripped from same area of shell shown in *a* and *b*, disturbed area was adjacent to a tubule opening (× 7000, bar = 2 μm).

MANTLE

General Configuration

The mantle margins of *Arca* and *Glycymeris* have the basic configurations shown in Figures 1, 3*a*, and 23*a*. Those of *Barbatia* are as shown in Figures 3*b* and 23*b*. The outer surface of the mantle adheres closely to the inner surface of the shell inside the pallial line. At the pallial line, the epithelium turns sharply back to form a tiny second outer fold. As seen in radial section, the base of this fold is marked by the point at which the epithelium comprising its inner surface bends sharply once again to extend distally as the outer surface of the first outer fold. The depth of the second outer fold, as measured from its crest to its base, is in all cases shallow (about 1 mm in a 77-mm-long *Arca zebra*).

The first outer fold is prominent in all of the specimens. It is highly asymmetrical in radial cross section, its outer surface emerging from the groove separating it from the second outer fold and passing around a broad, poorly defined crest. The surface of the fold then turns proximally and plunges into a shallow periostracal groove, from which the newly generated periostracum emerges. Compound eyes occur along the crest of this fold adjacent to the distal side of the periostracal groove beneath the new, transparent periostracum (Figures 1, 24*b*, 37*b*, 39*a*). Simple photoreceptors are also present, occurring in arcuate

rows lateral to the compound eyes (Figure 37*a*, *b*).

Both the number and degree of development of eyes, as well as the density of pigment in the epithelium of the marginal mantle folds, tend to be related to the degree of exposure of the mantle margin to light. Thus in *Arca zebra*, which lives attached by a strong midventral byssus with its anterior end slightly inclined toward the substrate and its posterior end more exposed (Stanley, 1970; Waller, 1973), variably developed compound eyes are present along the entire free margin. In a specimen 77 mm long, these number approximately 300 and range from 30 to 140 μm in diameter. Spacing is variable, but in general the photoreceptors are largest and most closely spaced posteriorly, smallest midventrally adjacent to the massive byssus, and intermediate in size anteriorly. In *Barbatia cancellaria*, which lives byssally attached in crevices so that only its posterior end is exposed (Stanley, 1970), eyes on the posterior margin are almost all of the compound type, large in size (reaching a diameter of nearly 200 μm in a specimen 35 mm long), and so closely spaced that they impinge on one another. At the point where the posterior curvature of the mantle margin merges with the relatively straight ventral margin, the size of compound photoreceptors abruptly diminishes, and the entire ventral margin has only very small, simple eyes. At the anterior end, more compound eyes appear, but these do not approach those of the posterior region in size and closeness of spacing. Pigmentation follows a similar pattern, being dense anteriorly and posteriorly but sparse midventrally. In *Glycymeris glycymeris*, known to be a shallow burrower and probably positioned in living position with its posterior margin exposed at the sediment surface (Stanley, 1970), both pigment and compound eyes are limited to the posterior region. Compound eyes in this species are small and sparse, numbering no more than a dozen in a specimen 55 mm long. *Arcopsis adamsi*, which was observed alive at Carrie Bow Cay but was not studied in detail, lives byssally attached deep underneath rocks, with little exposure to light. It lacks both pigment and eyes along its entire mantle margin.

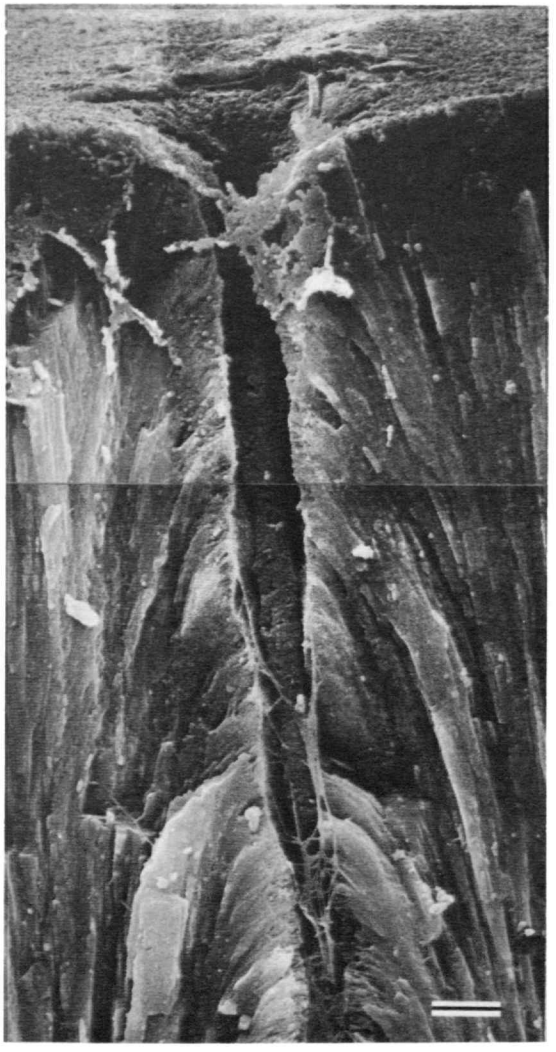

FIGURE 22.—*Arca imbricata*, USNM 794958: commarginal fracture through anterior adductor scar, fractured before critical-point drying, growth surface of myostracal prisms extending along wall of tubule, shrunken epithelial projection and strands of organic matrix present within tubule (× 5000, bar = 2 μm).

The first inner fold in all species examined is small, lacks obvious sensory structures on its leading edge, and seems to serve little purpose other than to form the inner side of the periostracal groove (Figures 1, 3). Its inner surface is confluent with either the inner surface of the mantle or, in the case of *Barbatia cancellaria*, with the outer

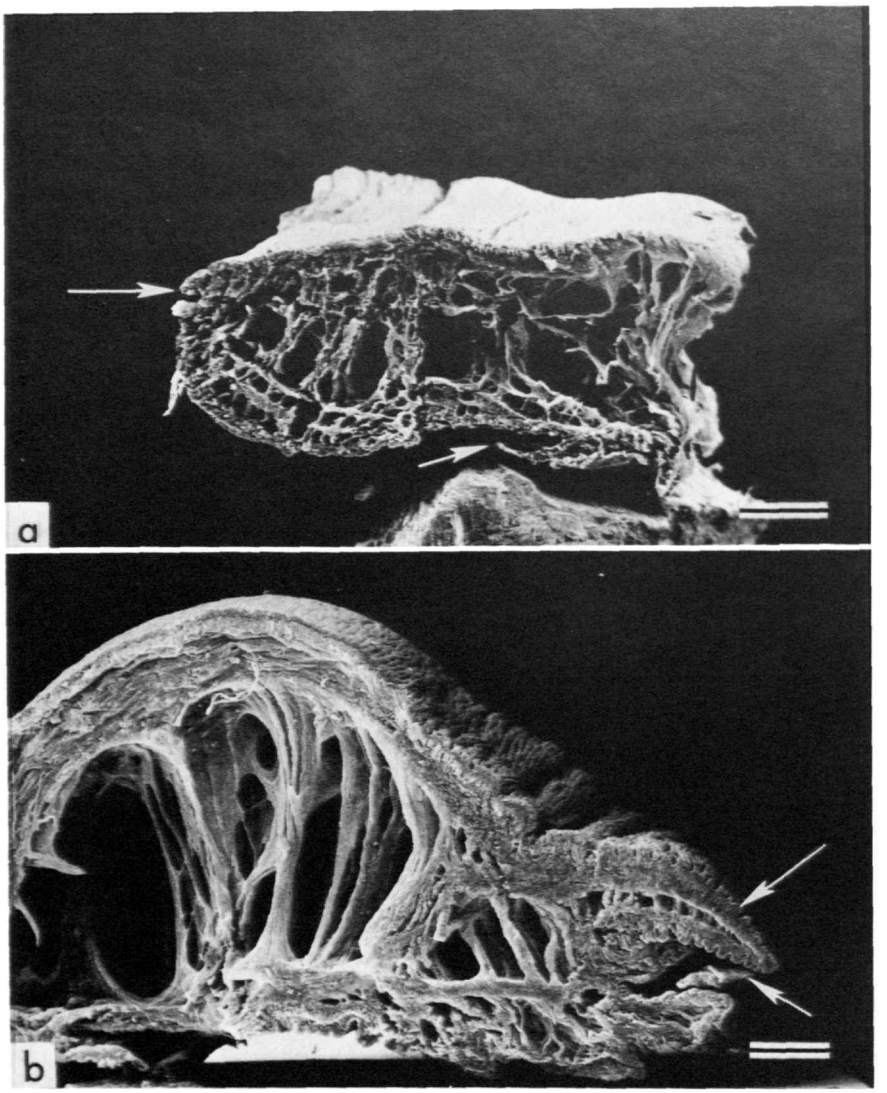

FIGURE 23.—Mantle edges cut from preserved specimens and critical-point dried: *a*, *Arca zebra*, USNM 794957, distal edge at left, outer side with adhering shell fragment at bottom, second outer fold (small arrow), periostracal groove (large arrow), and connective tissue with blood sinuses filling space between inner epithelium of mantle (top) and outer surfaces of outer folds (bottom) (about × 25, bar = 0.5 mm); *b*, *Barbatia cancellaria*, USNM 794959, distal edge at right, outer side at bottom second inner fold (long arrow) lying above first inner fold, periostracal groove with fragment of periostracum (short arrow), and first outer fold; torn second outer fold is in lower left corner (× 116, bar = 100 μm).

surface of the second inner fold. In *B. cancellaria*, the inner surface of the first inner fold bears opaque, white, variably tumescent papillae in the posterior region. These stand out in marked contrast to the surrounding tissue, which in this region is very darkly pigmented.

The second inner fold of *Barbatia cancellaria* is similar in size to the first outer fold in the anterior region but gradually becomes greater in size posteriorly. Its maximum development is along the sharply rounded posterior margin. Pigmentation also gradually increases toward the posterior, where both surfaces of the second inner fold are dark brown in color. Along the posterior margin, particularly in the dorsal half, both surfaces of this fold as well as its crest bear opaque white tumescent spots or papillae. These grade in size from about 20 μm in diameter to nearly 200 μm, and some of the largest merge with one another, the mergers in some cases consisting of up to five papillae. At higher magnifications under reflected light, each papilla appears to consist of a mass of opaque white granules underlying a transparent zone in the epithelium.

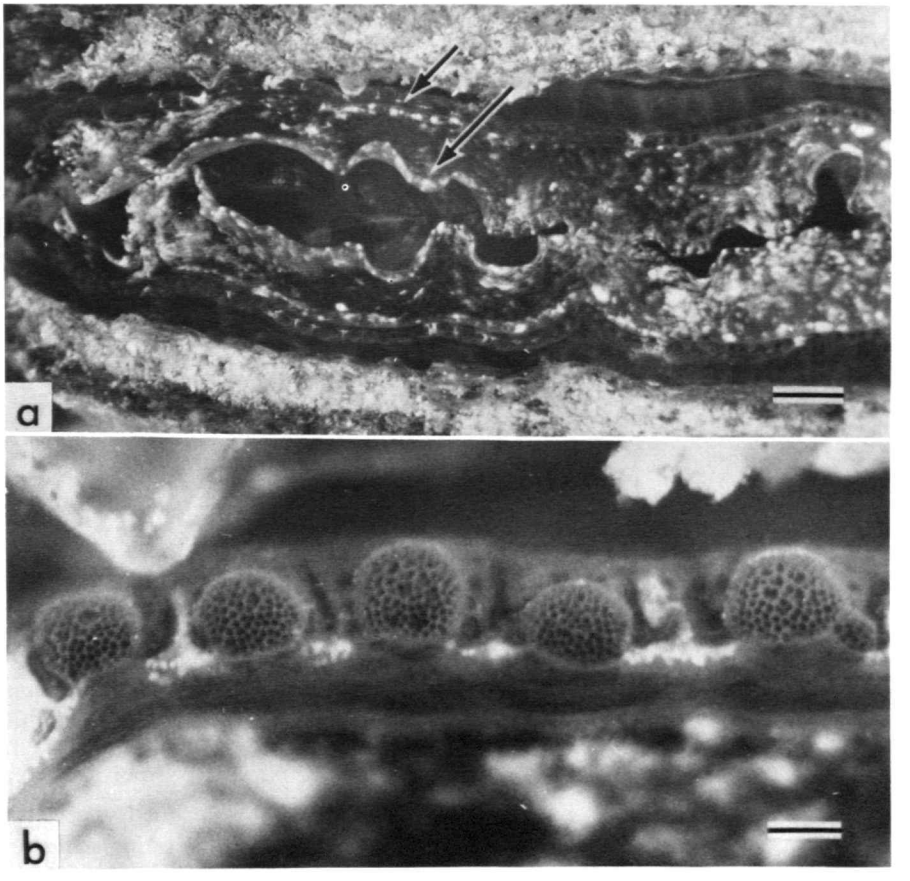

FIGURE 24.—*Barbatia cancellaria*, USNM 794959 (living, anesthesized): *a*, gaping ventral side showing photoreceptors on first outer fold (short arrow) and convoluted second inner fold (long arrow), anterior to right (about × 5, bar = 2 mm); *b*, detail of compound photoreceptors on mantle margin (about × 50, bar = 200 μm; optical photographs).

Behavior

The behavior of mantle margins was observed in living, anesthetized specimens of *Arca zebra*, *Arca imbricata*, *Barbatia cancellaria*, *Arcopsis adamsi*, and *Glycymeris pectinata*. In all of these specimens, the first outer fold is capable of extension to the edge of the shell, retraction toward the pallial line, and strong inward flexure to a position perpendicular to the inner shell surface. In contrast, the first inner fold does not seem to be extendible and merely follows the movement of the first outer fold when the latter flexes. In the anesthetized state, the outer surface of the first outer fold is separated from the inner surface of the shell while the valves are broadly gaping (Figure 24*a*); in the natural state the valves open less widely and the separation between the tissue surface and the shell is less.

During both inward flexure and retraction of the first outer fold, the periostracum remains unbroken as a continuous transparent sheet extending from the periostracal groove to the periostracal fringe bordering the edge of the calcified shell (Figure 1). Clearly, the periostracum can be stretched and is slightly elastic, but inward flexure and retraction of the first outer fold also appear to pull out excess, convoluted periostracum, which is normally present in the periostracal groove. It is inferred that subsequent extension of this fold then pushes the excess periostracum outward to the edge of the shell, where it folds upon itself during the next retraction or flexure. In this manner the thick multilayered periostracum of the outer shell surface is formed.

In species lacking a second inner fold, the massive first outer fold is capable of assuming the function of a mantle curtain in its inwardly flexed position and indeed does so in *Arca*, *Arcopsis*, and *Glycymeris*. In its outwardly extended position along the inner surface of the shell margin, eyes, if present, lie at the edge of the shell and perceive light through the transparent periostracum. Because the eyes are in this position, light perception is still possible when the valves are closed to the point that the periostraca of opposite valves are in contact but the calcified valve margins are not. It is probably this situation that has caused some investigators to remark on the ability of arcoids to perceive changes in light intensity even though the valves are closed (Braun, 1954).

The second inner fold of *Barbatia cancellaria*, which is absent in the other species examined, is thick, highly muscular, and scalloped along its crest, so that the scallops of opposing folds interlock to form an effective mantle curtain (Figure 24*a*). The first outer fold is still highly mobile, however, and may serve as a subsidiary mantle curtain, particularly in the midventral and anterior regions, where the second inner fold is less developed than in the posterior region.

Scanning Electron Microscopy

Outer Epithelium and Second Outer Fold.—In each of the species examined by scanning electron microscopy, the outer surface of the outer epithelium of the mantle presents two contrasting textures: one corresponds to areas of adhesion of mantle to shell; the other lies between these areas. For present purposes these two types of epithelium will be referred to as "adhesive" and "regular," respectively.

The configuration of adhesive zones along the pallial line differs between species. In both *Arca zebra* and *Arca imbricata*, radially aligned, nearly circular, adhesive patches extend proximally from the distal edge of the second outer fold (Figure 25*a*); in *Barbatia cancellaria* the adhesive surfaces are in the form of broad, distally widening rays (Figure 27); and in *Glycymeris glycymeris* they are narrow rays (Figure 28*a*). Where sufficiently broad so that their width is greater than that of a single cell, these surfaces consist of polygonal plates of a dense organic secretion having a granular rather than a fibrous texture (Figure 28*b*). The shapes and sizes of the plates are somewhat variable. On the surface of the adhesive epithelium overlying the anterior adductor of *Arca imbricata*, the plates are more or less equidimensional, measuring from 10 to 20 μm in diameter (Figure 30*a*). On the pallial adhesive rays of *Barbatia* and *Glycymeris* (Figure 28*a*), the plates are

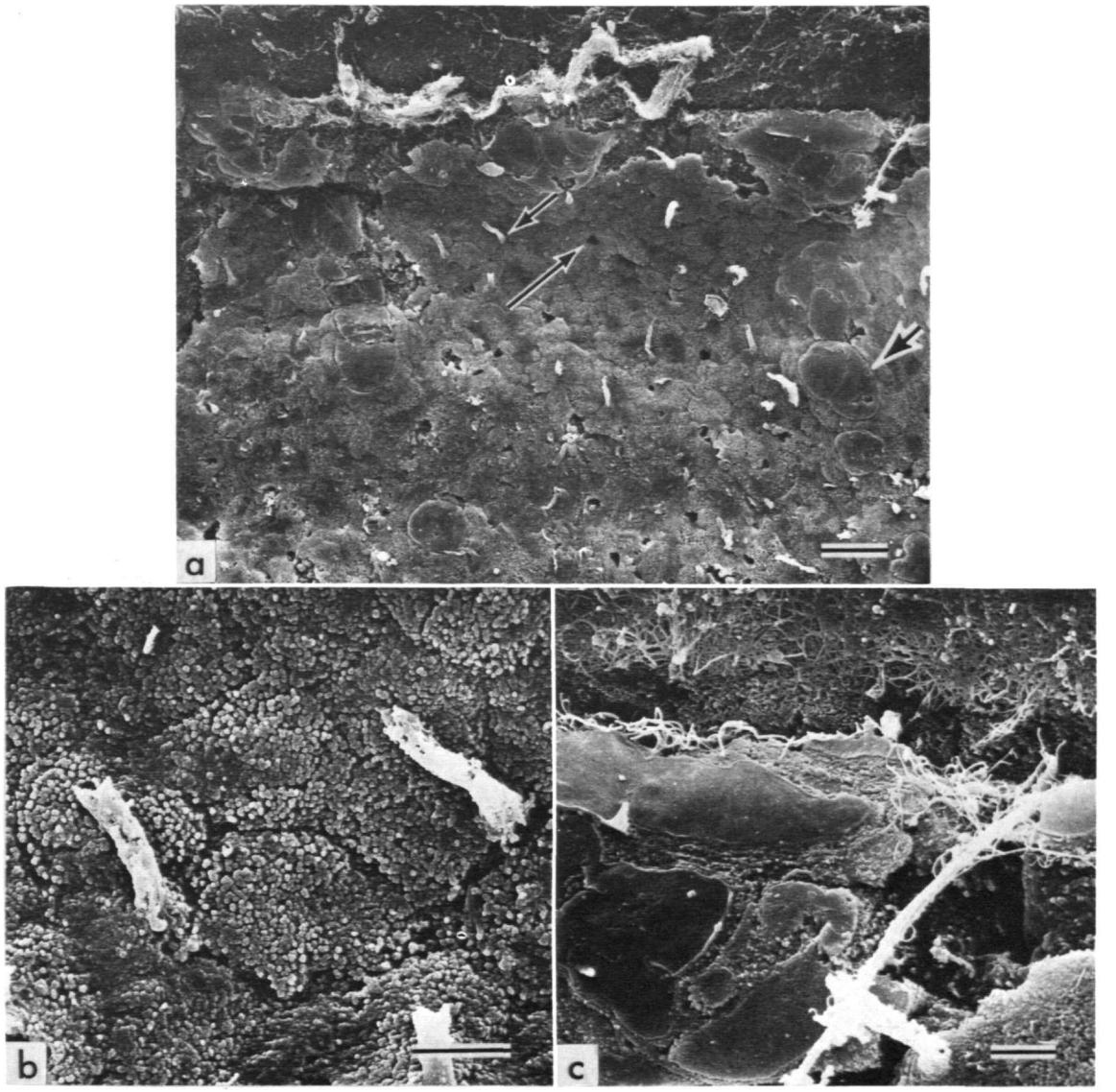

FIGURE 25.—*Arca imbricata*, USNM 794958 (planar views of outer surface of mantle inside pallial line, critical-point dried, direction of shell margin toward top): *a*, fibrous organic film adhering to outer surface of first outer fold (top) distal to crest of second outer fold; mantle epithelium showing cell boundaries, adhesive pads (thick arrow), cellular projections pulled from shell tubules (short arrow), and pores (long arrow) (× 500, bar = 20 μm); *b*, detail of *a*, mantle epithelium with projections and boundaries of microvillous cells (× 3000, bar = 5 μm); *c*, detail of *a*, crest of second outer fold, fibrous organic film at top, adhesive pads, and cellular projections (× 2000, bar = 5 μm).

radially elongate, varying in short dimension from 7 to 20 μm and in long dimension from 20 to 35 μm. In some specimens, tissue shrinkage resulting from dehydration produced wrinkling and separation of the plates (Figures 25*c*, 28*a*). Plate thickness estimated from these specimens is on the order of 0.2 μm.

Three structures are visible on the surface of the regular epithelium: microvilli, finger-like projections, and pores (Figure 25*a*,*b*). Microvilli are present on all regular epithelial cell surfaces except on the finger-like projections. The state of preservation of the material examined does not permit a detailed description of the morphology of microvilli, except that they are densely distributed, at least 0.5 μm in length and 0.1 μm in diameter, and occasionally branched (Figure 29*e*).

Each finger-like projection is a tubular extension of the apical surface of a single epithelial cell (Figure 25*b*,*c*) that occupies a tubule in the shell (Figure 26). Generally the base of a projection is broadly conical, corresponding to the conical depression surrounding each tubule opening on the inner surface of the shell (Figures 1, 20). The conical base then rapidly tapers to a cylindrical, distally inclined tube 1 to 3 μm in diameter. Lengths of the projections present on mantle surfaces stripped from the shell vary greatly, but none of the projections is complete because distal ends have been torn off and remain in the shell (Figures 22, 26).

The pores present on the regular epithelial surface (Figure 25*a*) have a random distribution (like that of the finger-like projections) and diameters similar to those of the basal portions of the projections. It seems likely that these pores mark the sites of projections that have been torn off during removal of the tissue from the shell surface.

In all specimens examined, the intracellular spaces of the outer epithelium of the mantle are packed with equidimensional, polyhedral, crystal-like bodies of unknown composition ranging in diameter from 1 to 3 μm (Figures 29*d*, 32*c*). These are absent from the mantle projections, inner mantle epithelium, and connective tissue and presumably are artifacts of preservation and critical-point drying. They may result from the presence of calcium-rich intracellular substance in the outer epithelium inside the pallial line.

FIGURE 26.—*Arca zebra*, USNM 794957: commarginal fracture through midventral inner shell layer of left valve, critical-point dried, direction of inner surface of shell toward top, elongate cellular projection (short arrow) displaced from its tubule, distal portion of cellular projection remaining in tubule (long arrow) (× 650, bar = 20 μm).

A marked contrast occurs between the appearances of regular and adhesive epithelial cells in sectional views. The former (Figure 29*d*) appear to be open structures, except for the presence of the crystal-like bodies mentioned above; the latter are filled with fibers perpendicular to the basal

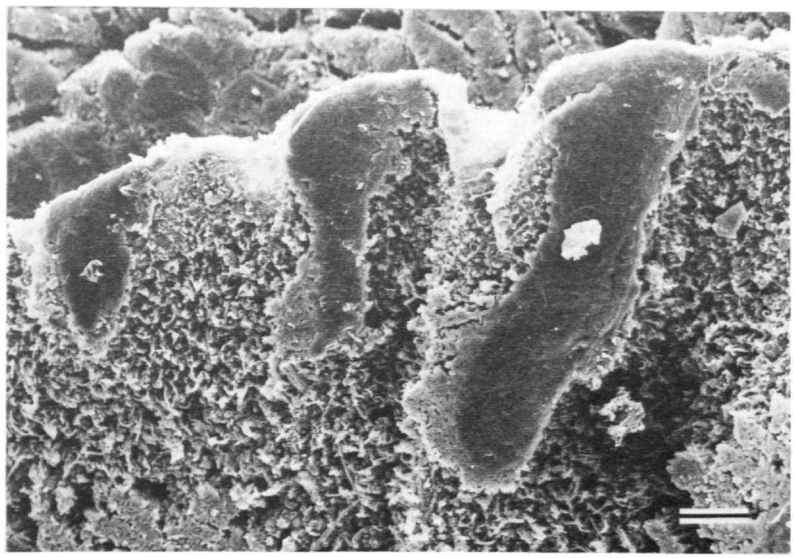

FIGURE 27.—*Barbatia cancellaria*, USNM 794959: planar view of outer surface of mantle epithelium stripped from posterior edge of left valve, three adhesive rays ending along crest of second outer fold, critical-point dried (× 200, bar = 50 μm).

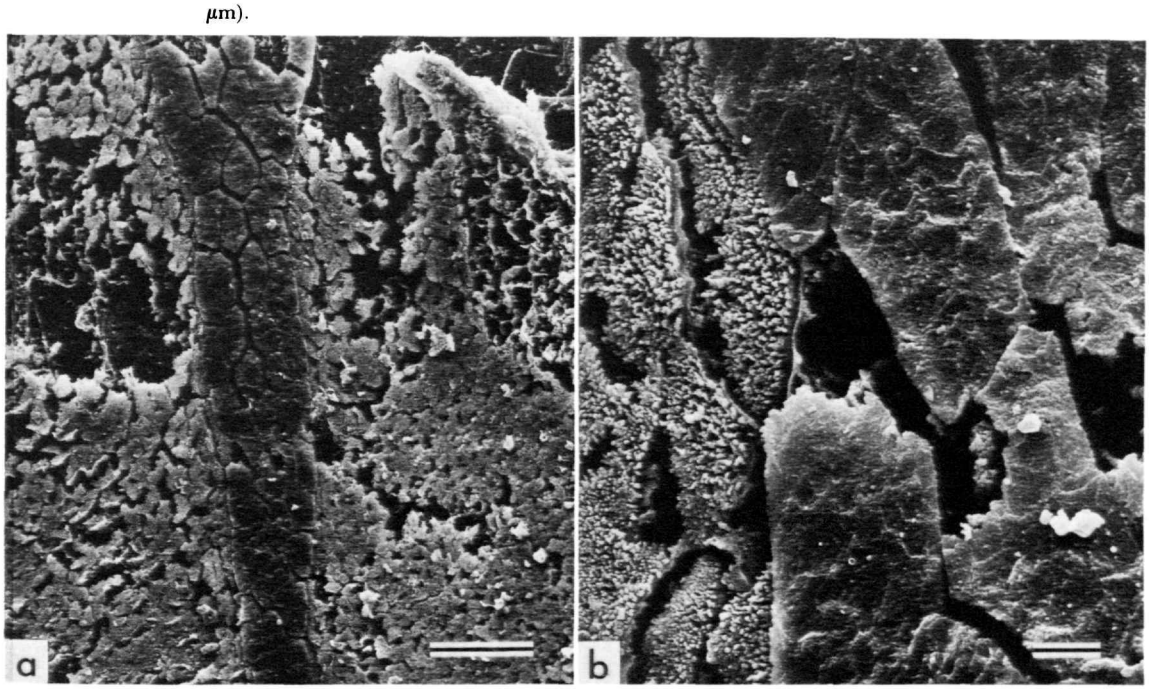

FIGURE 28.—*Glycymeris glycymeris*, USNM 794960 (planar views of mantle epithelium inside pallial line in midventral region): *a*, narrow adhesive ray and surrounding nonadhesive surface, with cells separated along boundaries by dessication (× 300, bar = 50 μm); *b*, detail of *a*, boundary between adhesive and nonadhesive surfaces, with microvillous regular epithelial cells and organic plates covering adhesive cells (× 2000, bar = 5 μm).

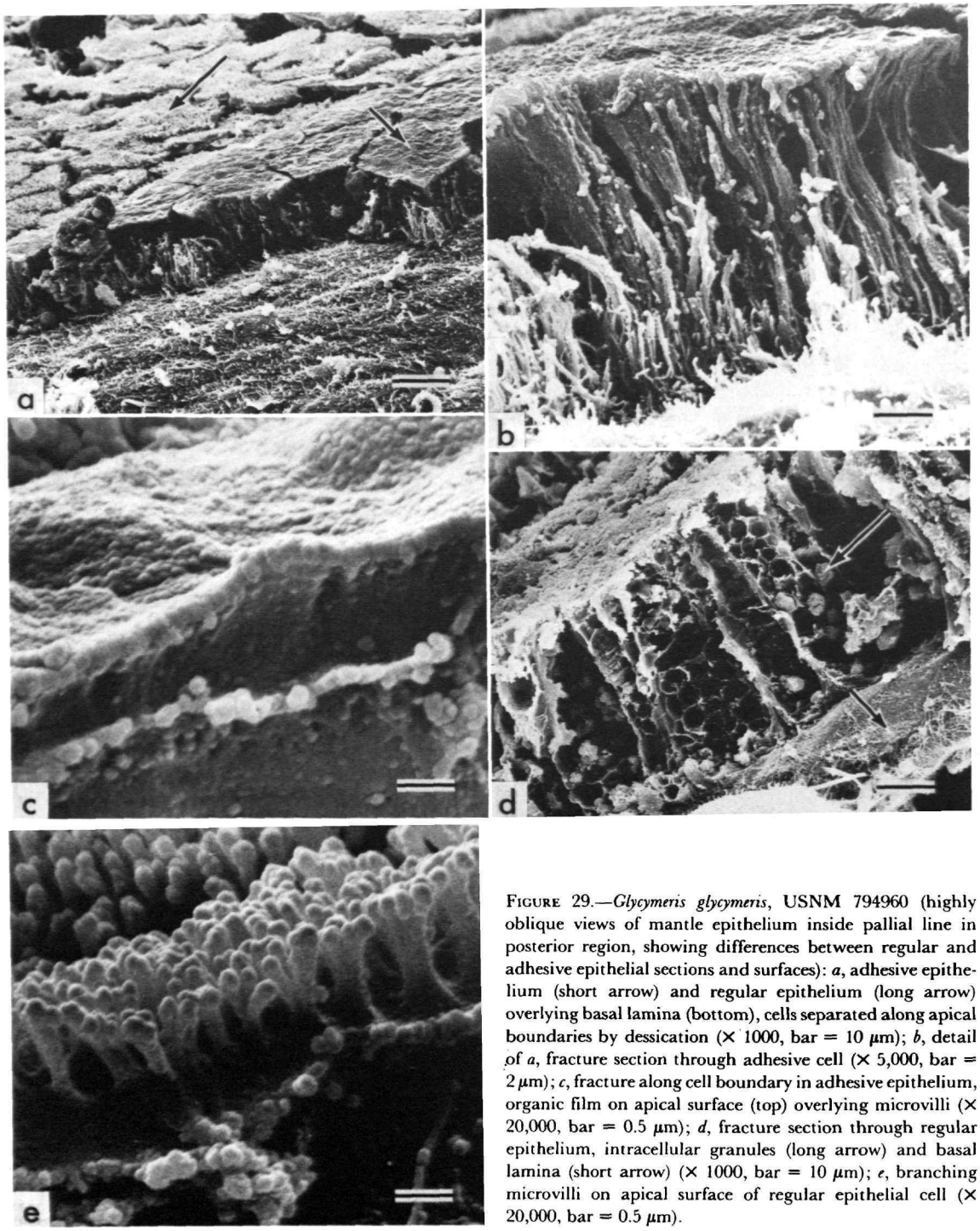

FIGURE 29.—*Glycymeris glycymeris*, USNM 794960 (highly oblique views of mantle epithelium inside pallial line in posterior region, showing differences between regular and adhesive epithelial sections and surfaces): *a*, adhesive epithelium (short arrow) and regular epithelium (long arrow) overlying basal lamina (bottom), cells separated along apical boundaries by dessication (× 1000, bar = 10 μm); *b*, detail of *a*, fracture section through adhesive cell (× 5,000, bar = 2 μm); *c*, fracture along cell boundary in adhesive epithelium, organic film on apical surface (top) overlying microvilli (× 20,000, bar = 0.5 μm); *d*, fracture section through regular epithelium, intracellular granules (long arrow) and basal lamina (short arrow) (× 1000, bar = 10 μm); *e*, branching microvilli on apical surface of regular epithelial cell (× 20,000, bar = 0.5 μm).

and apical cell surfaces (Figure 29*b*). These fibers are likely the microfilaments described by Tompa and Watabe (1976) in a study of the adhesive epithelium in gastropods by transmission electron microscopy. Cross sections across boundaries separating adhesive epithelium of pallial rays from regular epithelium show that these differences arise precisely at the boundary. In the case of adductors, the epithelium separating the adhesive surface from the muscle fibers could not be distinguished (Figure 30*b*).

Oblique views of torn adhesive epithelium show that each polygonal plate of the adhesive surface represents the outline of a single adhesive epithelial cell (Figure 31). Generally, these plates obscure the apical surfaces of the cells, but in the young specimen of *Arca imbricata*, apical surfaces can be viewed directly, where the adhesive film is partially (Figure 30*c*) or completely (Figure 30*d*) separated from cells that comprise the tiny circular patches of pallial attachment. The nature of the apical surface of adhesive cells is also revealed in a pallial adhesive ray of *Glycymeris glycymeris*, where a tear in the tissue follows cell boundaries (Figure 29*c*). In each case, adhesive cells differ from neighboring regular cells in having far more numerous microvilli.

If the microvilli of the adhesive epithelial cells are involved in secretion of the surficial plates, then the reason that the plates stop at cell boundaries is probably because microvilli are absent between cells. This also explains why the borders between the first-order polygons of the myostracal surface are not underlain by prominent organic walls, as in other prismatic shell fabrics. Here, the polygonal lines form adjacent to secretory discontinuities in the epithelium and are not active sites of secretion or aggregation of organic material.

The basal lamina of the outer epithelium inside of but near the pallial line is a dense felt of randomly arrayed extracellular connective fibers about 0.1 μm or slightly larger in diameter (Figure 32*b*). Coarser, radially oriented fibers (0.5 to 1.5 μm) are present between the dense basal lamina and the epithelial cells (Figure 32*c*). Where both the epithelium and its basal lamina have been stripped away to reveal the underlying connective tissue, numerous small, radial, flattened fibrous bundles, interpreted as muscles, are exposed (Figure 33). These are less than 3 μm in diameter and are embedded in a loosely knit mass of connective fibers. Proximal to the base of the second outer fold, these inferred muscle fibers are inclined proximally upward from the inner surface of the outer epithelium into the loose connective tissue lying between the outer and inner mantle epithelia. The ends of the muscle bundles nearest the shell surface are compact and narrow, but in the connective tissue, the other ends are lost in a mass of connective fibers. The inclination of the muscle bundles suggests that in this area contraction of the muscles pulls the inner epithelium of the mantle radially outward, possibly to exert hydrostatic pressure on the marginal mantle folds in order to extend them.

Radially aligned muscle and connective fibers are also present within the second outer fold, but because of the thinness and deformation of tissue in this exceedingly thin region of the mantle, their orientation could not be determined decisively. However, there is a suggestion in stereoscopic micrographs (not shown) that here the orientation is reversed, with the shell insertion being proximal to the insertion in connective tissue. Because adhesive pads are present on the distal edge of this fold, it is unlikely that it is retractable. Rather, this orientation of muscle fibers would suggest that the inner epithelium of the fold can be pulled downward toward the outer epithelium. What function this may serve is unknown.

The inner epithelium of the second outer fold is thin and cuboidal, not exceeding 10 μm in thickness proximally and thinning to less than 1 μm distally (Figures 34, 35*a-c*). In surface view, cells are equidimensional distally, but proximally they are commarginally elongated and radially compressed (Figure 34), possibly due to a state of contraction of the fold in the region. The epithelial surface is generally covered with secretion in the form of droplets and strands or fibers (Figure 35*c,d*), the fibers being continuous into the fibrous organic film that covers the marginal shell band.

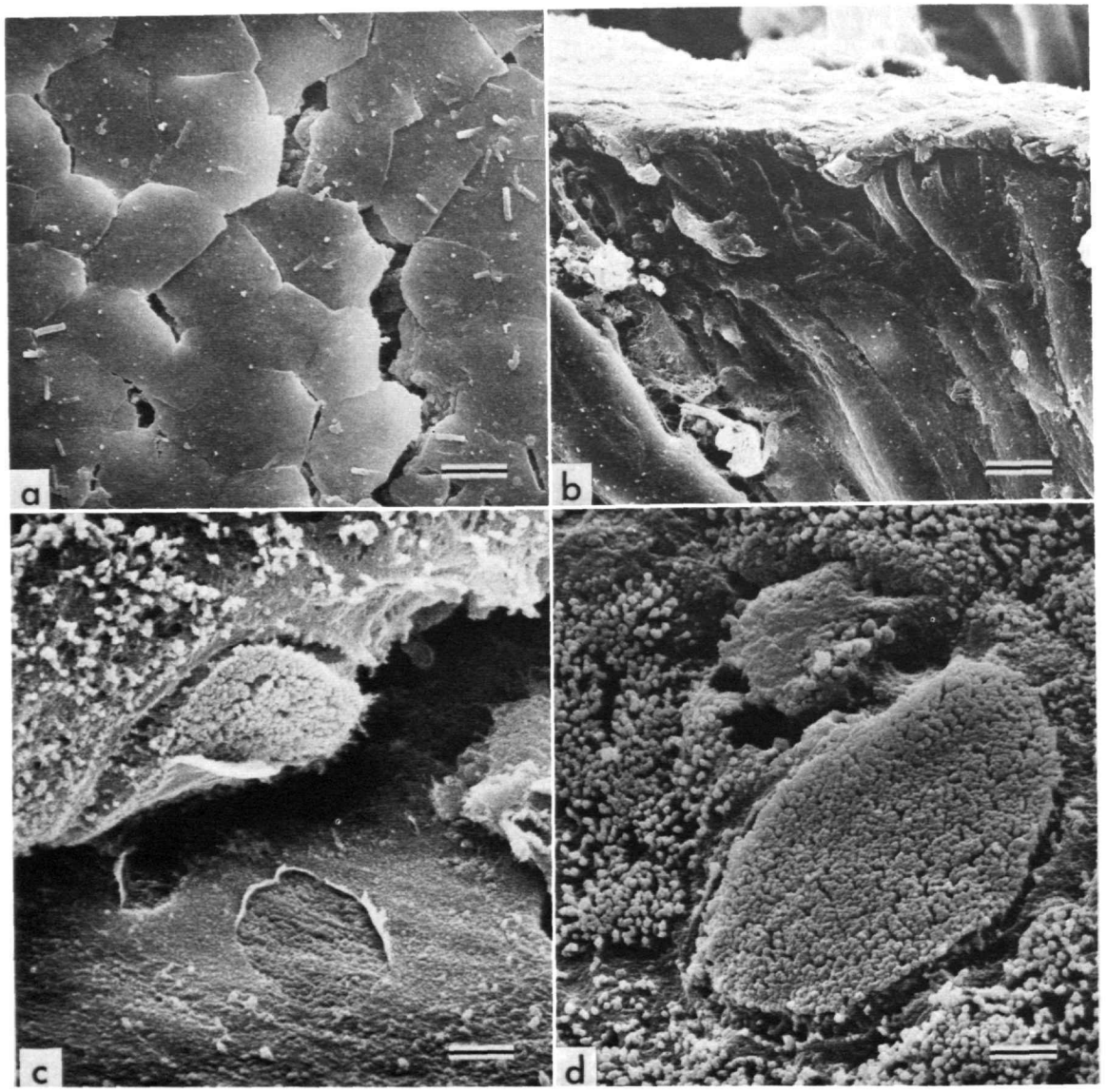

FIGURE 30.—*Arca imbricata*, USNM 794958 (critical-point dried adhesive epithelium and organic plates): *a*, planar view of surface of anterior adductor pulled from attachment to shell, adhesive plates covering apical cell surfaces (× 1000, bar = 10 μm); *b*, fracture section through anterior adductor, adhesive film at top, muscle fibers below (adhesive epithelium not distinguishable) (× 1000, bar = 10 μm); *c*, oblique view of epithelium (top) curled back from inner surface of shell (bottom) on proximal side of pallial line, adhesive cell with part of adhesive organic pad adhering to cell and remainder adhering to shell (× 5000, bar = 2 μm); *d*, planar view of apical surfaces of other adhesive cells showing greater density of microvilli compared to that on surrounding regular epithelial surface (× 5000, bar = 2 μm).

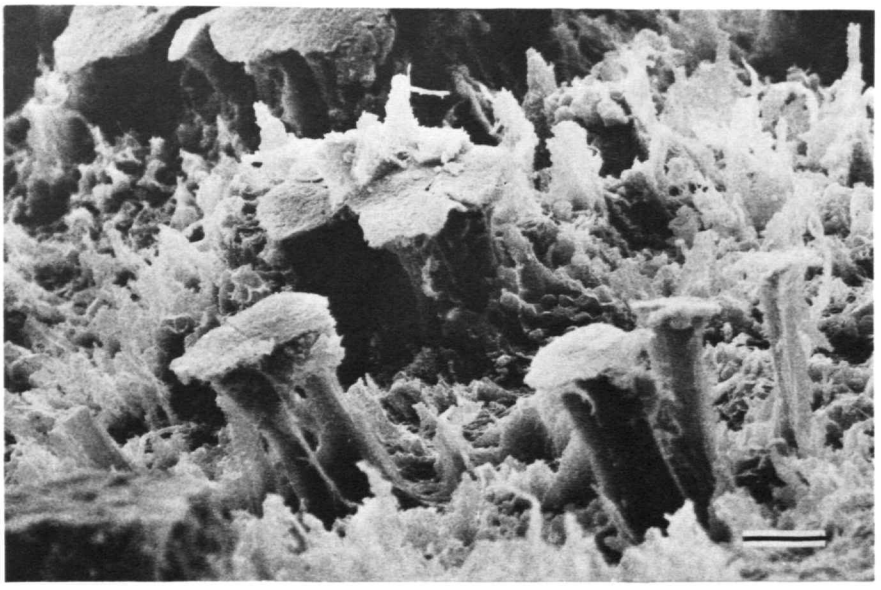

FIGURE 31.—*Arca zebra*, USNM 794957 (oblique view of torn adhesive epithelium inside but close to pallial line, critical-point dried): erect walls of columnar cells and remnants of organic plates on apical surfaces (× 1200, bar = 10 μm).

In fact, this organic film is essentially continuous from the inner surface of the marginal shell band over the inner surface of the second outer fold, but it changes in character. It is densely fibrous over the shell surface but only loosely so over the tissue surface.

The basal lamina of the inner epithelium is a randomly arrayed felt of connective fibers, similar to that beneath the outer epithelium. However, at a point midway between the proximal and distal edges of the fold in the young *Arca imbricata*, the fibers of the basal lamina are distinctly commarginal in orientation (Figure 35*c*).

The crest of the second outer fold, which lies at the base of the steplike pallial line, consists of a single row of cells bearing long, distally projecting processes (Figure 35*d*). Tubule-forming mantle projections also occur along the crest (Figure 36*a*) and produce the shell tubules that open on the pallial line (Figure 4*a*).

FIRST OUTER FOLD.—The first outer fold in each species examined by scanning electron microscopy consists of columnar epithelium enclosing a loosely organized mass of connective tissue traversed by large blood sinuses (Figure 23*a*,*b*). In all but *Barbatia cancellaria* it is by far the largest of the marginal folds. Numerous large commarginal crenulations in the epithelium (Figures 36*a*, 37*a*) attest to its contractability, but musculature was not studied in detail. The outer surface of the epithelium lacks cilia and is generally covered by dense secretion in the form of droplets and strands (Figure 36*b*). In some cases, the fibrous organic film, which generally overlies the marginal shell band and the inner surface of the second outer fold, may adhere to the outer surface of this fold (Figures 25*c*, 36*b*).

The structure of the compound eyes of arcoid bivalves has already been studied in detail (Patten 1886; Rawitz, 1890; Jacob, 1926; Nowikoff, 1926; Schulz, 1932; Levi and Levi, 1971). Briefly, two types of cells are present. High, narrow, pigmented support cells form the walls between facets, with each facet consisting of a single photoreceptive cell. As shown by Levi and Levi (1971), the entire compound eye is covered by dense microvilli, which previous authors referred to as "cuticle." They also found that the apical

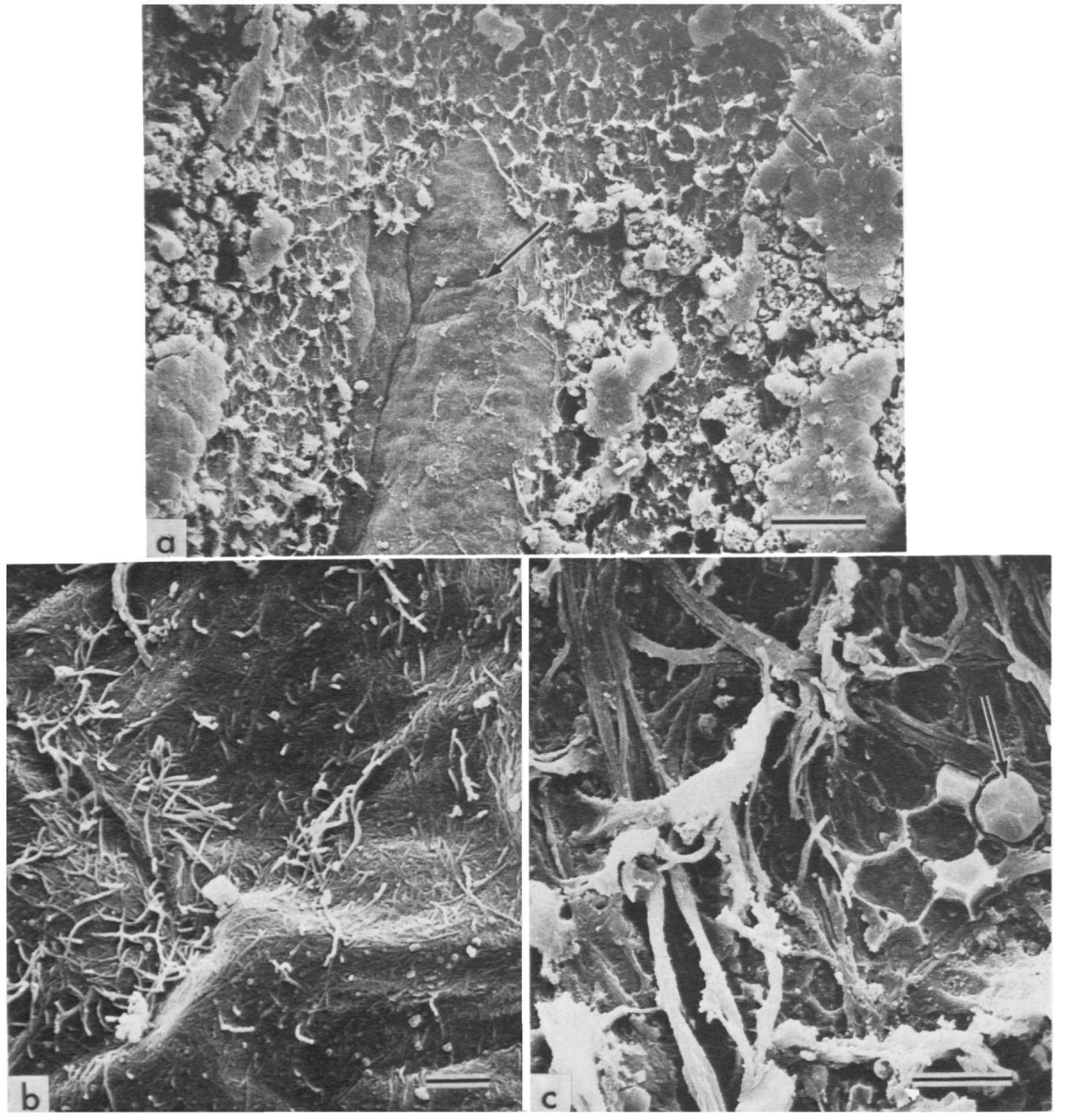

FIGURE 32.—*Arca zebra*, USNM 794957 (planar views of critical-point dried outer mantle epithelium stripped from ventral region of shell inside of pallial line; direction of shell margin toward top): *a*, basal lamina of outer epithelium (long arrow) surrounded by film-covered adhesive cells (short arrow) and fractured regular cells (× 300, bar = 50 μm); *b*, detail of basal lamina (× 5000, bar = 2 μm); *c*, detail of *a*, coarse fibers between basal lamina and epithelial cells, and polyhedral granule (arrow) within remnant of a cell (× 3000 bar = 5 μm).

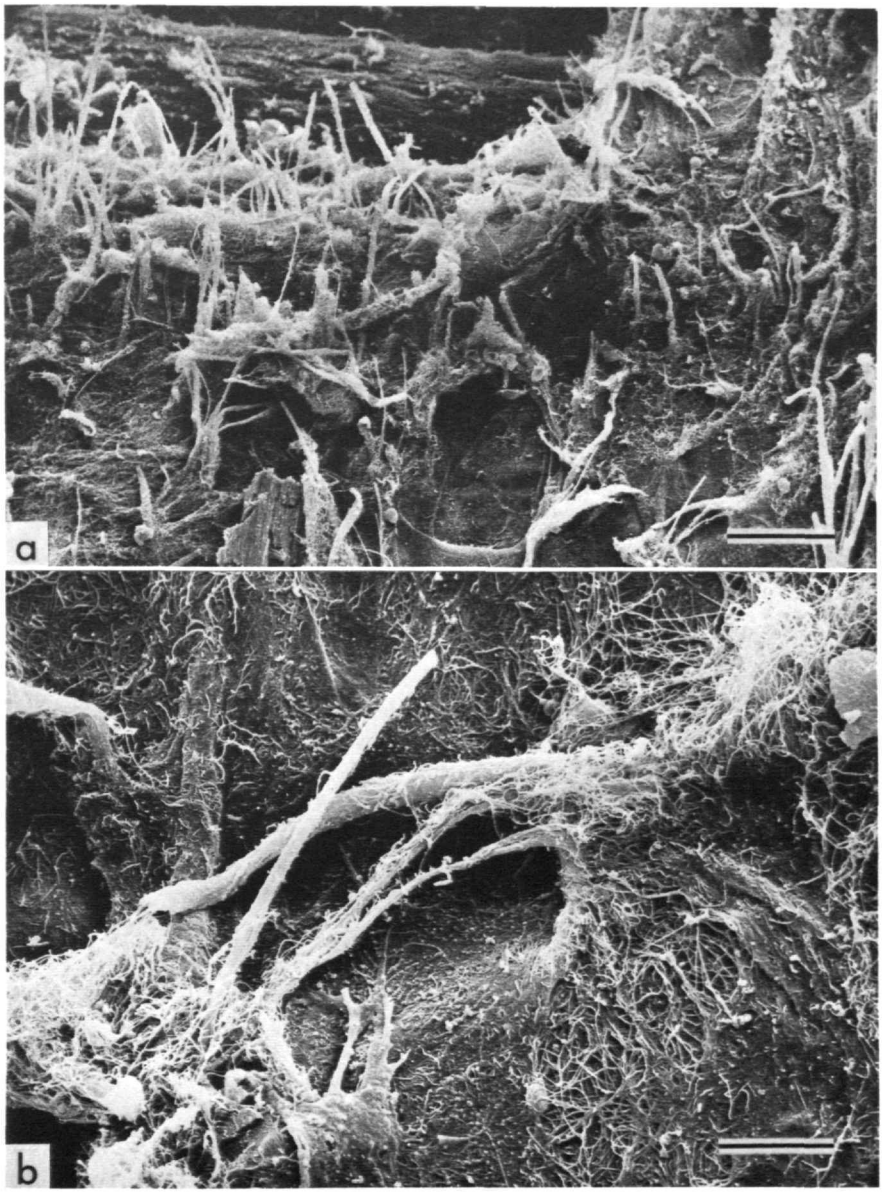

FIGURE 33.—*Arca zebra*, USNM 794957 (planar views of critical-point dried second outer fold from which outer epithelium has been stripped, viewed from outer side, direction of shell margin toward top): *a*, possible muscle fibers and felt of extracellular connective fibers (× 320, bar = 50 μm); *b*, detail of *a* (× 1700, bar = 10 μm).

FIGURE 34.—*Arca zebra*, USNM 794957: planar view of inner surface of second outer fold curled back from outer surface of first outer fold along top, cells separated along boundaries by dessication and stripped from basal lamina in area marked by arrow, connective tissue at bottom (× 300, bar = 50 μm).

ends of the support cells flare out and completely cover the depressed facets, which are the apical ends of the photoreceptive cells, so that all microvilli visible in surface views belong to only one type of cell. Lastly, they determined that the photoreceptor cells are of the ciliary-based type rather than the rhabdomeric type (Eakin, 1963, 1965, 1968; see also Salvini-Plawen and Mayr, 1977, and Rosen, Stasek, and Hermans, 1978).

The structure of the compound eyes prepared by critical-point drying and viewed with the scanning electron microscope is best shown in a specimen of *Arca zebra* that had been in preservative for no more than two months before being critical-point dried (Figure 37). The eyes are ellipsoidal, the long diameters being commarginal and ranging from 40 to 140 μm. An eye with diameters of 82 and 67 μm bears at least 45 facets, each facet being nearly circular or slightly polygonal and varying in diameter from to 6.5 to 11 μm. The surfaces of the facets are flat or very gently convex, in contrast to the walls separating them, which are strongly convex. These thick walls vary from 2 to 5 μm in thickness at their narrowest points. Dense microvilli between 0.1 and 0.2 μm in diameter are present on both walls and facets but on the latter assume a close-packed geometric arrangement so that each microvillus tends to have a polygonal form in planar view (Figure 37*d*). The compound photoreceptors in the other species examined have a similar structure.

The simple photoreceptors widely spaced on the surface of the first outer fold lateral to the compound eyes are nearly circular and range from 8 to 30 μm in diameter (Figure 37*a*,*b*). From the material on hand, little could be learned about their surficial structure other than that they have a raised rim surrounding a concave center.

PERIOSTRACAL GROOVE AND PERIOSTRACUM.—In each species, the periostracal groove is shallow, densely ciliated on its inner surface (the proximal outer surface of the first inner fold), and flanked by columnar epithelium (Figures 38*a*, 39). The newly generated periostracum is a solid sheet sculptured in radial patterns distinctive for each species (Figures 39*c*, 40*c*, 42*c*). In the case of *Barbatia cancellaria*, radial crenulations in the periostracum correspond to radial undulations on the densely ciliated inner surface of the groove (Figure 39*c*,*d*). No sharp, commarginal sculptural features are present in the new periostracum in any of the species examined.

As the periostracum passes by the first outer fold of the mantle and joins the outer surface of the shell, its character changes. Numerous commarginal pleats occur at the edge of the shell (Figure 7*a*) as the first outer fold extends and retracts, dragging the periostracal sheet with it. These pleats give the periostracum a thick, multilayered structure at the edge of the shell (Figures 41, 43*c*), and some of the broader pleats are preserved on the shell exterior as commarginal growth lines (Figures 42, 43*b*). Once the periostracum is "frozen" on the shell exterior numerous radial splits occur, giving the appearance of a

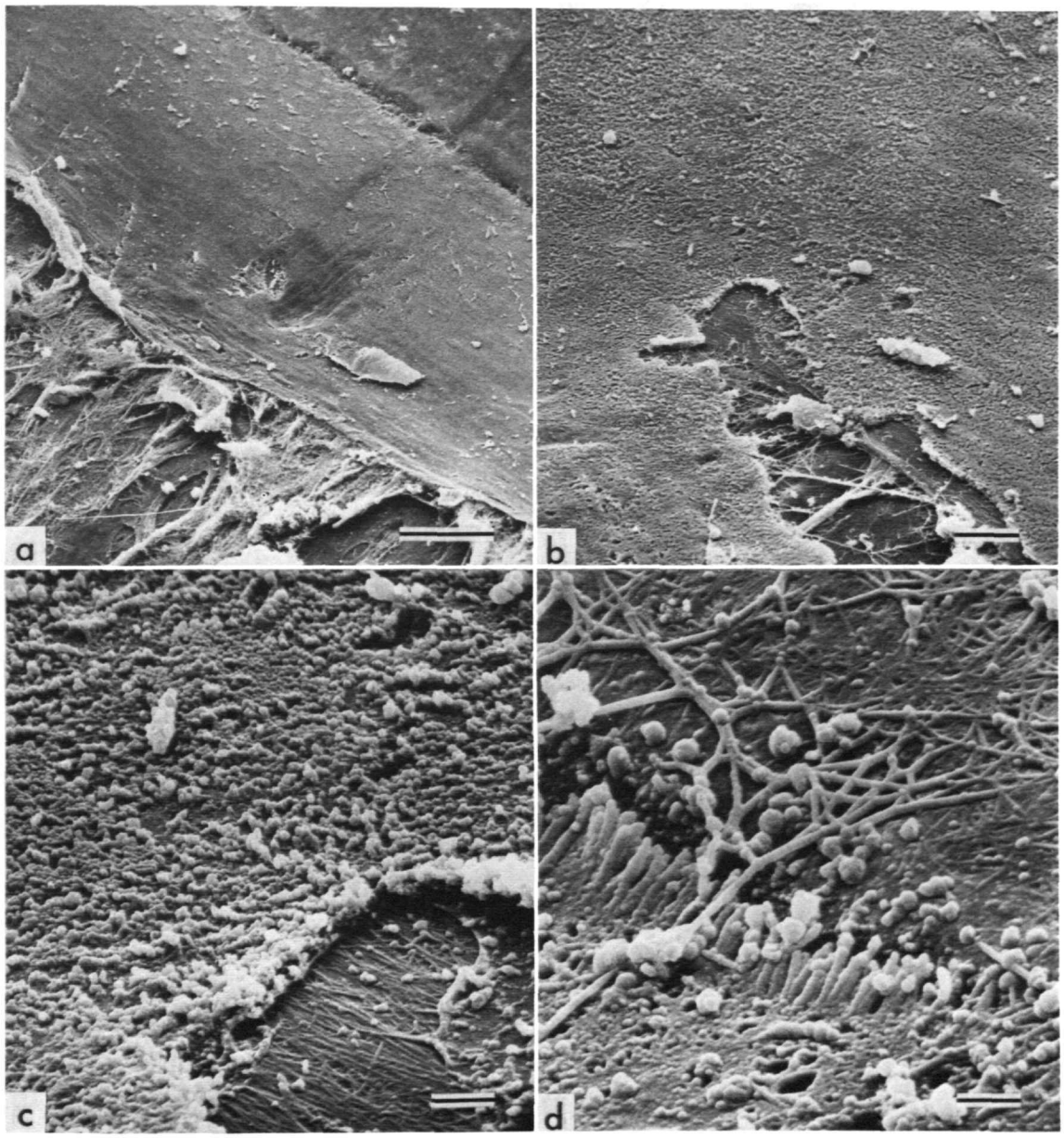

FIGURE 35.—*Arca imbricata*, USNM 794958 (oblique views of inner surface of second outer fold, critical-point dried, direction of shell margin toward upper right): *a*, second outer fold abutting pallial line (across upper right corner), with epithelium stripped off to reveal underlying connective tissue (lower left) (× 300, bar = 50 μm); *b*, detail of epithelium, with its thinness and underlying connective tissue revealed where torn (× 1000, bar = 10 μm); *c*, detail of *b*, microvillous surface of epithelium and commarginal arrangement of fibrils in basal lamina (× 5000, bar = 2 μm); *d*, detail of crest of second outer fold, with cell processes of crest lying along pallial line and secretion droplets and fibers extending from fold into fibrous organic film covering marginal shell band (× 10,000, bar = 1 μm).

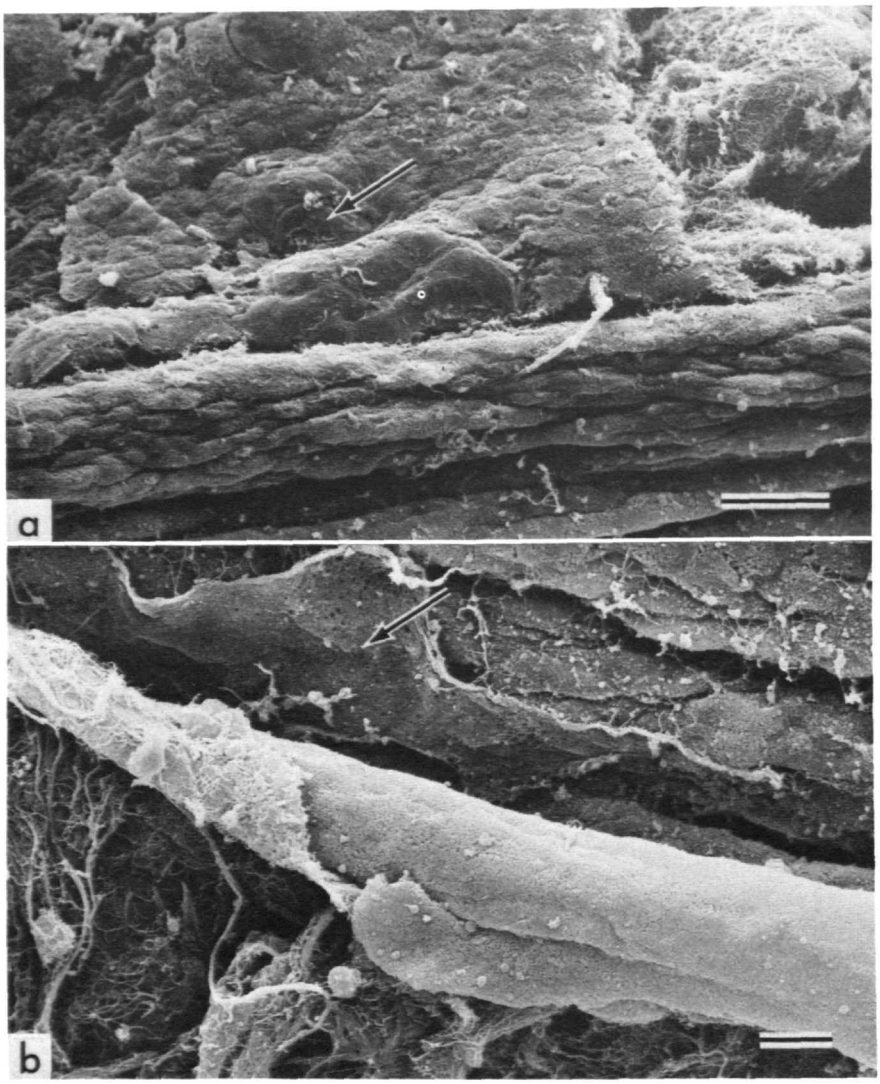

FIGURE 36.—*Arca imbricata*, USNM 794958 (edge of mantle in midventral region, critical-point dried): *a*, outer surface of second outer fold with adhesive ray (arrow) and a cellular projection near its crest, and crest of first outer fold (bottom), viewed obliquely from ventral side (× 780, bar = 20 μm); *b*, planar view of inner surface of second outer fold (diagonally across center) rolled back from outer surface of first outer fold (upper right); fibrous organic film adhering to first outer fold (arrow); connective tissue in lower left (× 1030, bar = 10 μm).

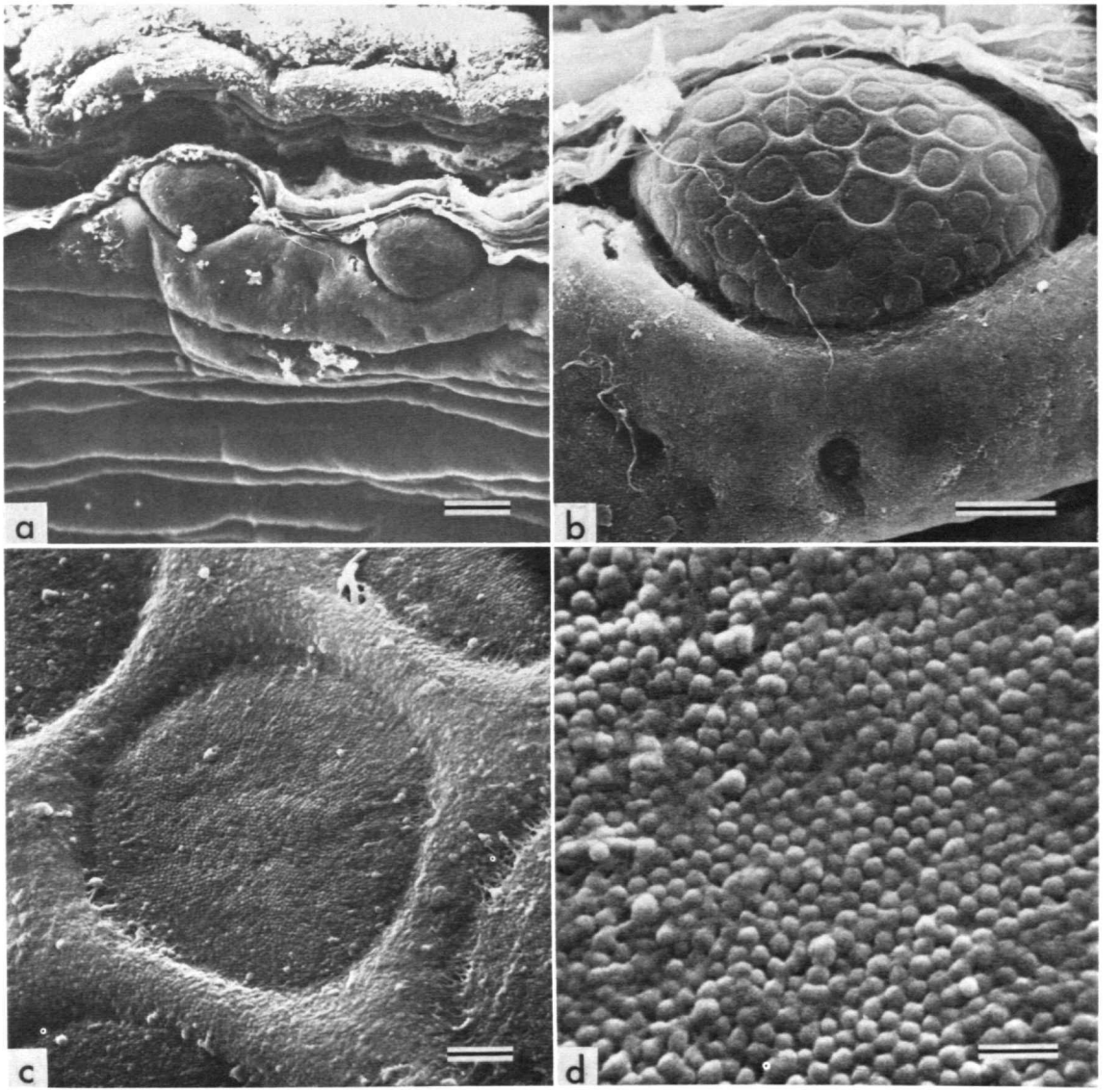

FIGURE 37.—*Arca zebra*, USNM 794957 (compound eyes on posterior mantle edge, periostracum mechanically removed, critical-point dried): *a*, two compound eyes beneath remnant of periostracum, outer surface of first outer fold at bottom, ciliated inner surface of inner fold at top (× 200, bar = 50 μm); *b*, detail of compound eye within *a*, simple eye at bottom center (× 750, bar = 20 μm); *c*, detail of a facet within *b* (× 5000, bar = 2 μm); *d*, close-packed microvilli in a facet (× 25,000, bar = 0.5 μm).

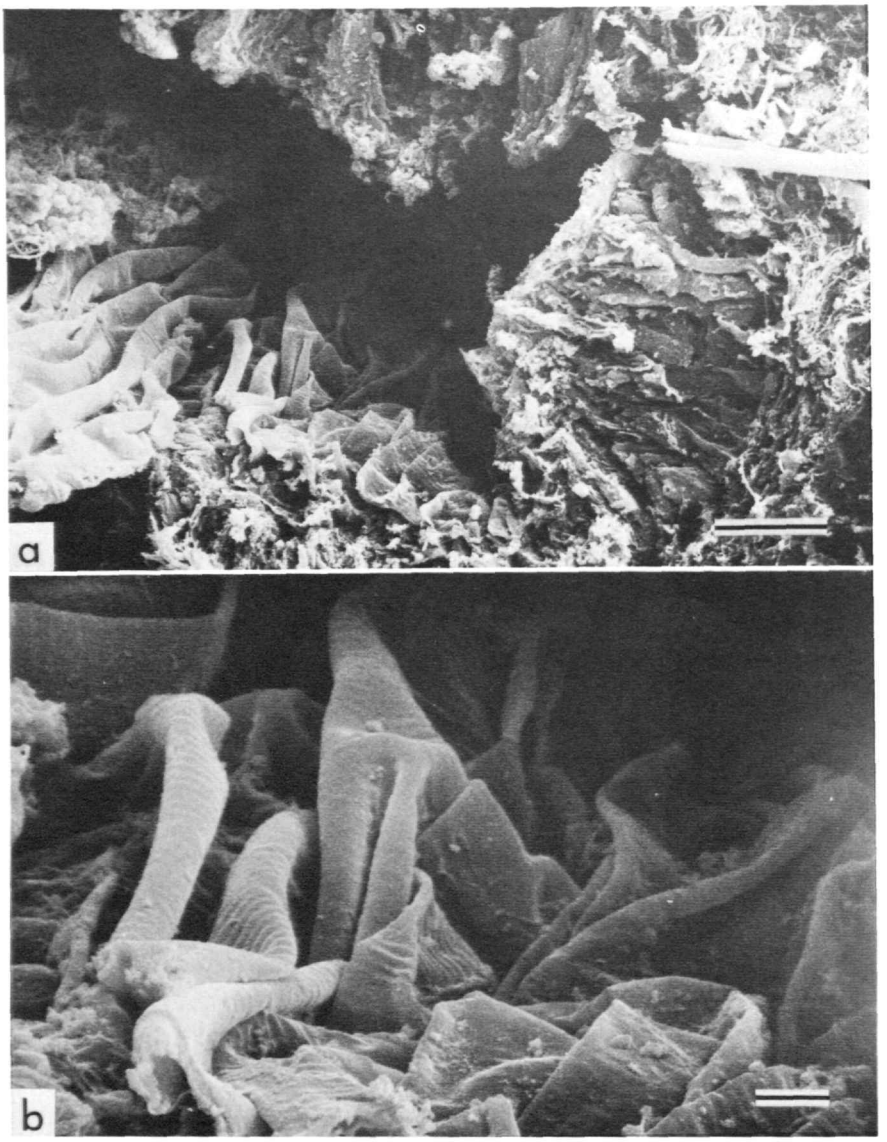

FIGURE 38.—*Arca zebra*, USNM 794957: *a*, radial section through periostracal groove, which opens toward upper left, showing epithelium at base of groove and convoluted periostracum lying along its outer side (lower left), critical-point dried (× 1580, bar = 10 μm); *b*, detail of *a*, convoluted periostracum with radially ridged outer surface (× 5260, bar = 2 μm).

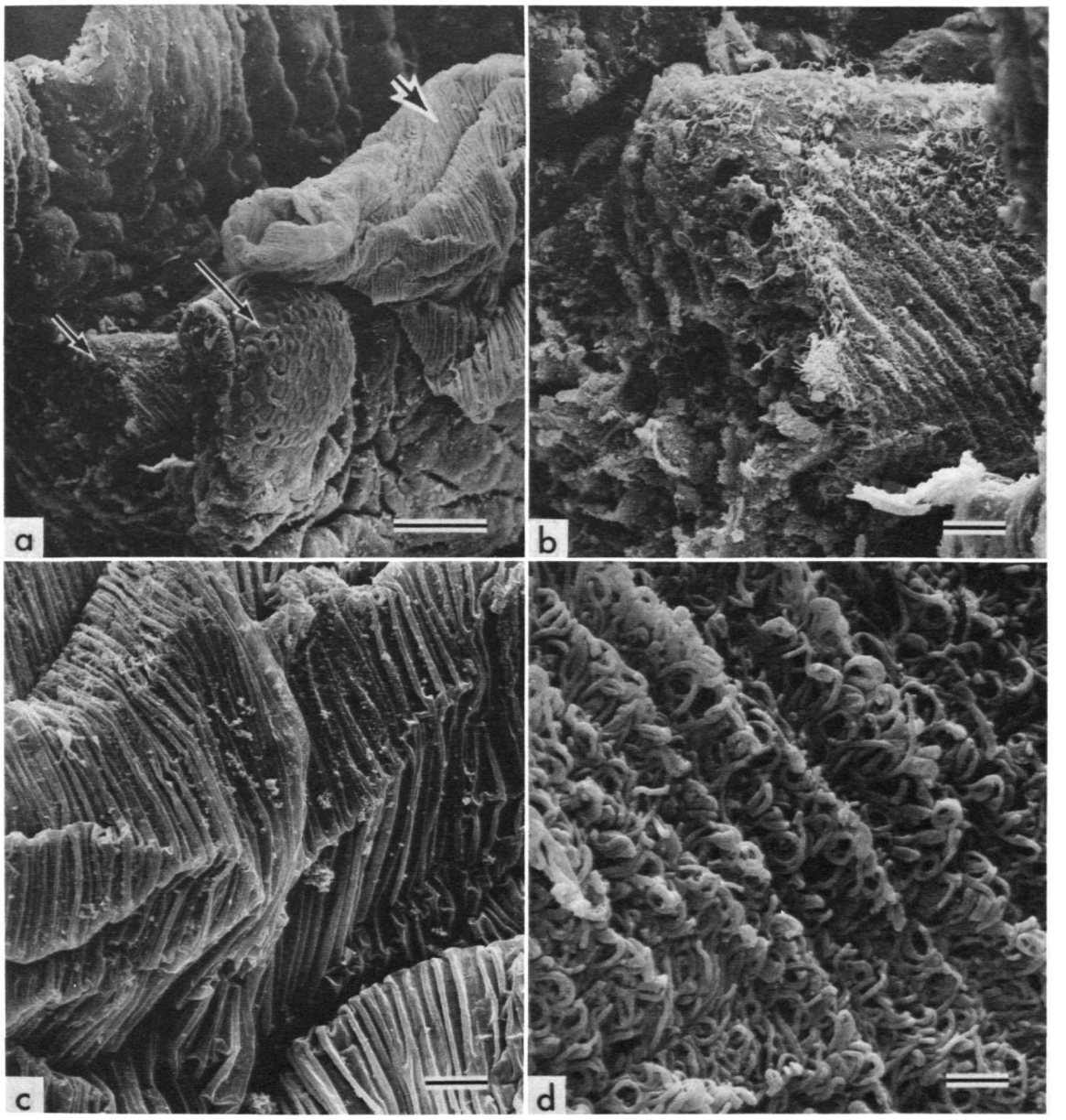

FIGURE 39.—*Barbatia cancellaria*, USNM 794959 (posterior mantle edge viewed obliquely from outer side, critical-point dried): *a*, second inner fold (top and left), first inner fold (short arrow), compound eye on first outer fold (long arrow), and adhering convoluted periostracum (thick arrow) (× 300, bar = 50 μm); *b*, detail of *a*, densely ciliated outer surface of first inner fold in periostracal groove (× 1000, bar = 10 μm); *c*, detail of *a*, radially ridged outer surface of periostracum (× 1000, bar = 10 μm), *d*, detail of *b*, ciliated outer surface of first inner fold (× 5000, bar = 2 μm).

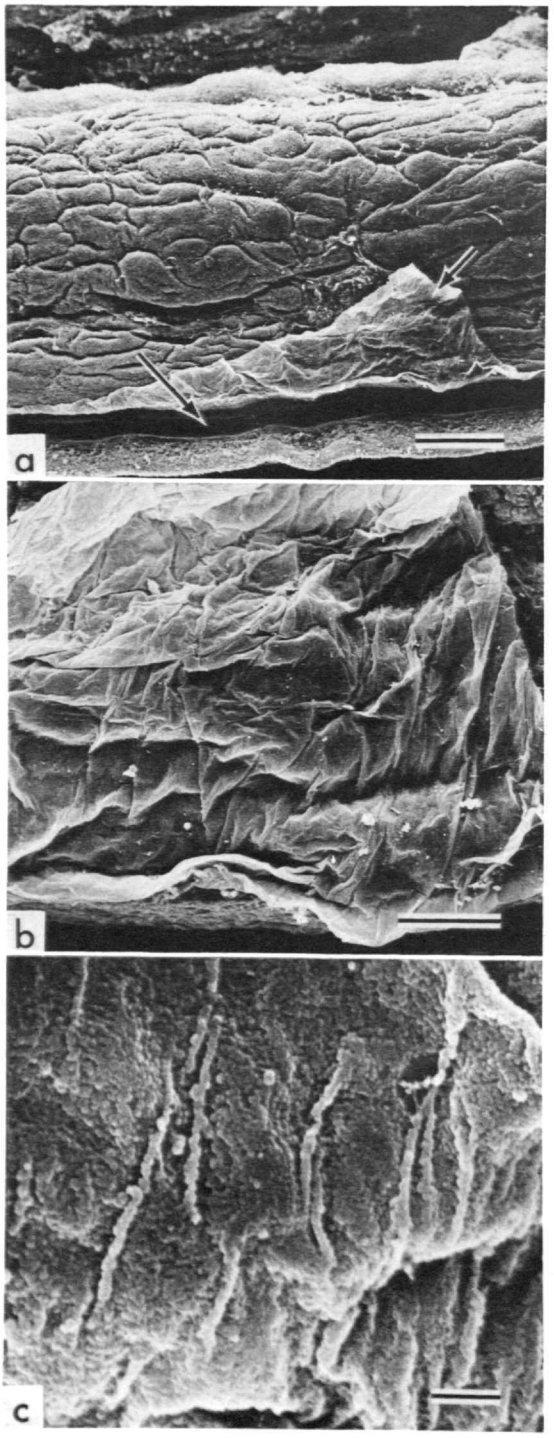

FIGURE 40.—*Glycymeria glycymeris*, USNM 794960 (posterior mantle edge and periostracal groove viewed from distal side, outer side upward, critical-point dried): *a*, periostracal groove (long arrow) above narrow first inner fold and beneath massive first outer fold with piece of adhering periostracum (short arrow) (× 65, bar = 200 μm); *b*, detail of *a*, periostracum (× 300, bar = 50 μm); *c*, detail of *b*, outer surface of periostracum (× 1000, bar = 10 μm).

shaggy, hairy, or even spiked surface (Figures 42*a*, 43*a*). That these features are secondary is indicated by the fact that they transect commarginal pleats. However, the locations of the radial breaks may be related to primary radially distributed differences in composition not visible by scanning electron microscopy. Furthermore, there is some indication that calcification occurs on the inner surface of the periostracum beyond the edge of the shell and that this calcification may also be distributed along radial lines. In *Barbatia cancellaria* it is concentrated on the inner surface of the periostracal fringe along crests of radial crenulations and is absent in troughs (Figure 44).

FIRST AND SECOND INNER FOLDS.—In each of the four species studied in detail, the first inner fold is very small, seeming to serve little purpose

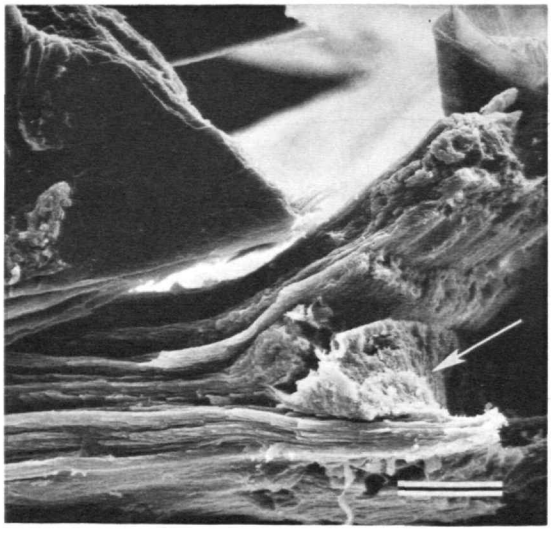

FIGURE 41.—*Arca zebra*, USNM 794957: radial fracture through distal edge of shell (arrow) with surrounding periostracal fringe, air dried, direction of shell margin to left, inner side toward top (× 300, bar = 50 μm).

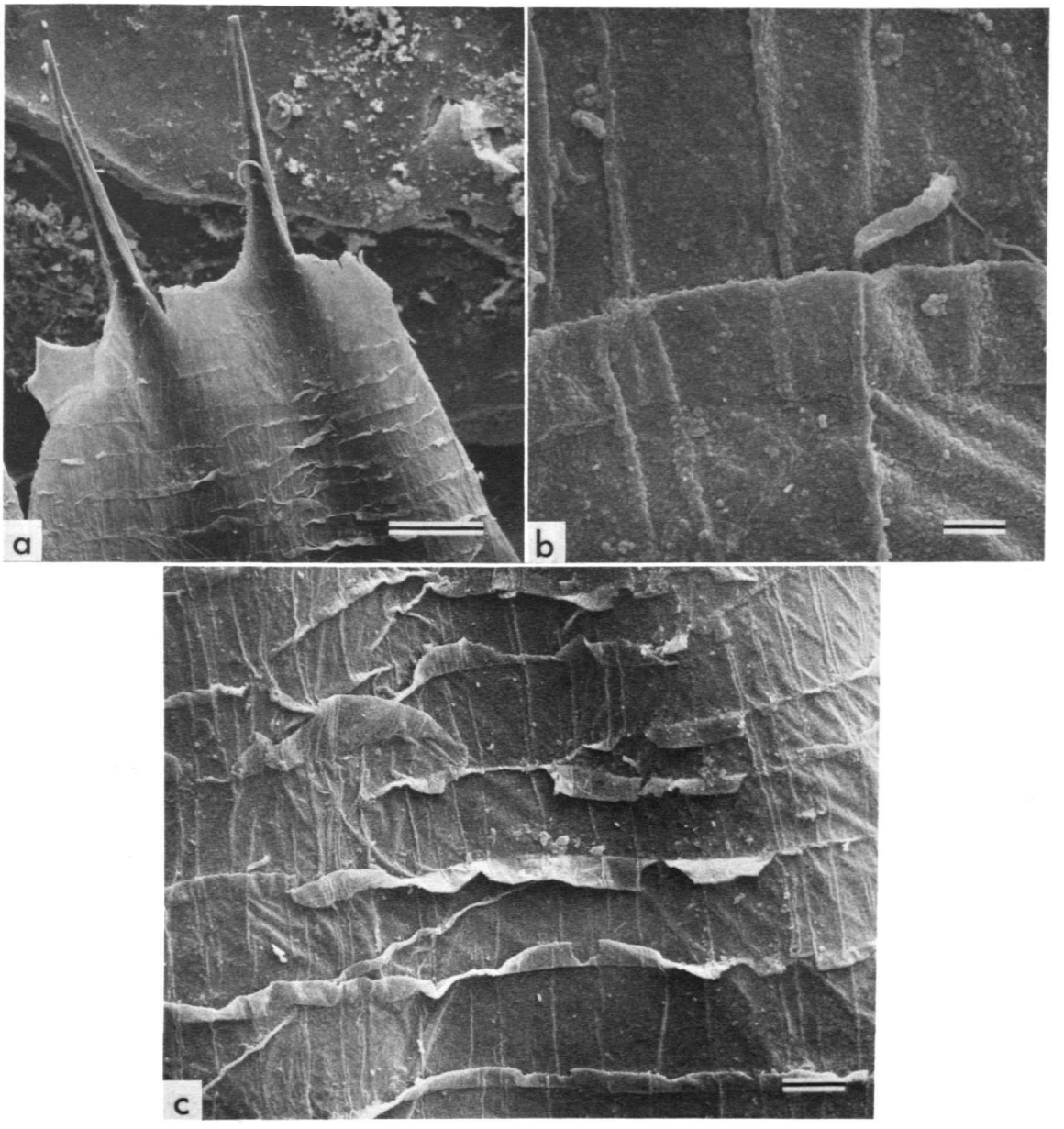

FIGURE 42.—*Arca imbricata*, USNM 794958 (planar views of outer surface of periostracum, critical-point dried): *a*, two spikes at distal edge and commarginal pleats on outer surface (× 300, bar = 50 μm); *b*, detail of *c*, outer surface with one commarginal pleat and several radial ridges (× 5000, bar = 2 μm); *c*, detail of *a*, outer surface (× 1000, bar = 10 μm).

other than to buttress the inner side of the periostracal groove. The proximal outer surface of the fold, which comprises the inner side of the periostracal groove, bears dense cilia that assist in propelling the periostracum from the groove, where it is generated (Figure 39). (The periostracum is also pulled from the groove by the extension of the first outer fold.) In both *Arca* and *Glycymeris*, cilia are present on the crest of the first inner fold and over its inner surface, which is continuous with the inner surface of the mantle. Cilia on the inner mantle surface of *Glycymeris glycymeris* are much more densely distributed than those on the inner mantle surface of *Arca zebra*, presumably because the former is a shallow burrower and must expel a greater amount of sediment from its mantle cavity. In *Barbatia cancellaria* there is a drastic reduction in the number of cilia on the first inner fold outside of the densely ciliated zone of the periostracal groove. In all species examined in detail, the epithelium on both sides of the first inner fold is columnar, and crenulations suggest that this fold is slightly extendible.

The second inner fold of *Barbatia cancellaria* is similar to the first outer fold in size in the posterior and posteroventral regions. It is ciliated on both sides; its epithelium is columnar; and cross sections demonstrate the presence of numerous cross partitions and blood sinuses in the connective tissue (Figure 23*b*). Its surfaces have only very sparsely distributed tufts of cilia (Figure 45). The opaque white tumescent papillae observed in living and preserved specimens with the binocular microscope (described above) have surfaces that do not differ from surrounding epithelium (Figure 46), except that the cells of the papillae appear to be larger. The function of the papillae is unknown.

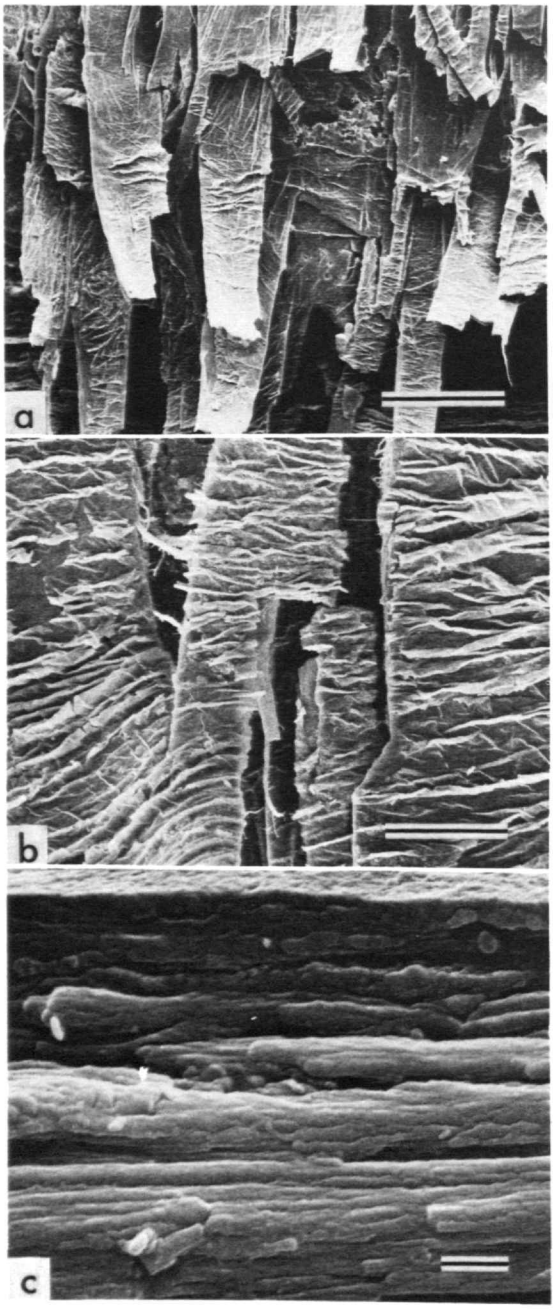

FIGURE 43.—*Glycymeris glycymeris*, USNM 794960 (periostracum with primary commarginal pleats and secondary radial fractures, air dried): *a*, hairy appearance of outer surface produced by radial fracturing, direction of shell margin toward bottom (× 90, bar = 200 μm); *b*, detail of *a*, radial fractures transecting commarginal pleats (× 360, bar = 50 μm); *c*, radial fracture through periostracal fringe, edge view, direction of shell margin toward left (× 10,000, bar = 1 μm).

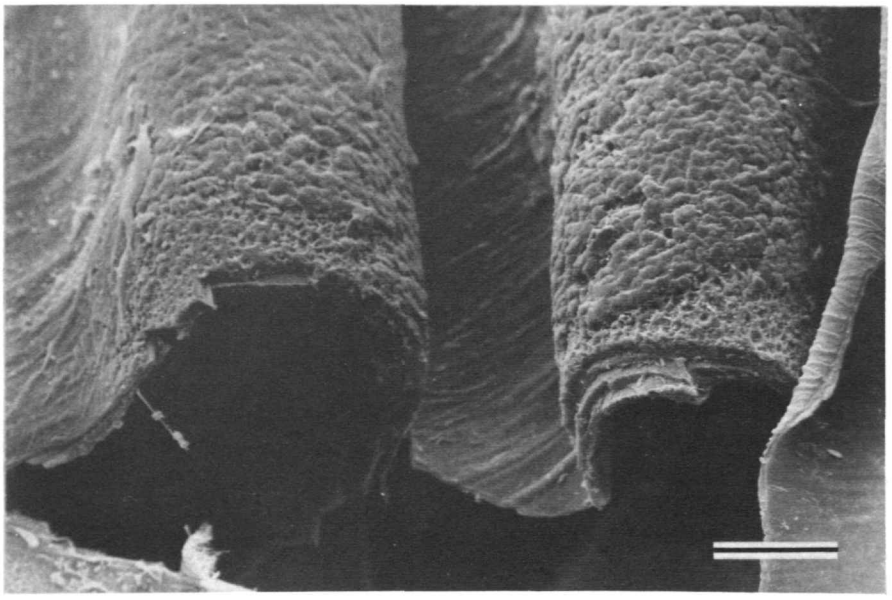

FIGURE 44.—*Barbatia cancellaria*, USNM 794959: oblique view of inner surface of distal edge of radially undulating periostracal fringe, probable calcification on crests of undulations, critical-point dried (× 360, bar = 50 μm).

Mantle Edges in Other Arcoid Species

Specimens of other species of arcoid bivalves present in preservatives in the collections of the National Museum of Natural History were examined with a binocular microscope in order to determine whether the configuration of mantle folds and the position of photoreceptors is like that in the species described above. The results of this brief survey are given in Table 1. Length measurements in some cases are based on preserved soft parts, not shells, and hence are only a general reference for specimen size. The states of preservation of specimens vary widely, and "absence" of compound eyes means only that none could be detected in the specimens on hand at magnifications up to × 50. Specimens of Philobryidae and Limopsidae were too small and transparent to permit determining by this method whether a second outer fold is present.

The results demonstrate the persistence of a second outer fold and the restriction of the position of compound photoreceptors to the first outer fold in a variety of taxa. It is evident, therefore, that these are conservative features in the order Arcoida.

Discussion

The observations on mantle and shell invite integration and discussion in four areas: (1) the mode of formation and function of shell tubules and the epithelial projections that form them; (2) the relationships between mantle and shell and their bearing on shell calcification; (3) the nature of cell generation leading to growth of the mantle; and (4) the functional and evolutionary significance of the configuration of marginal mantle folds and eyes in the Arcoida.

TUBULES

The basic structure of shell tubules and the epithelial projections that form them are the same in each of the species examined and are also like the structures present in specimens of the unrelated family Sphaeriidae (= Pisidiidae) described

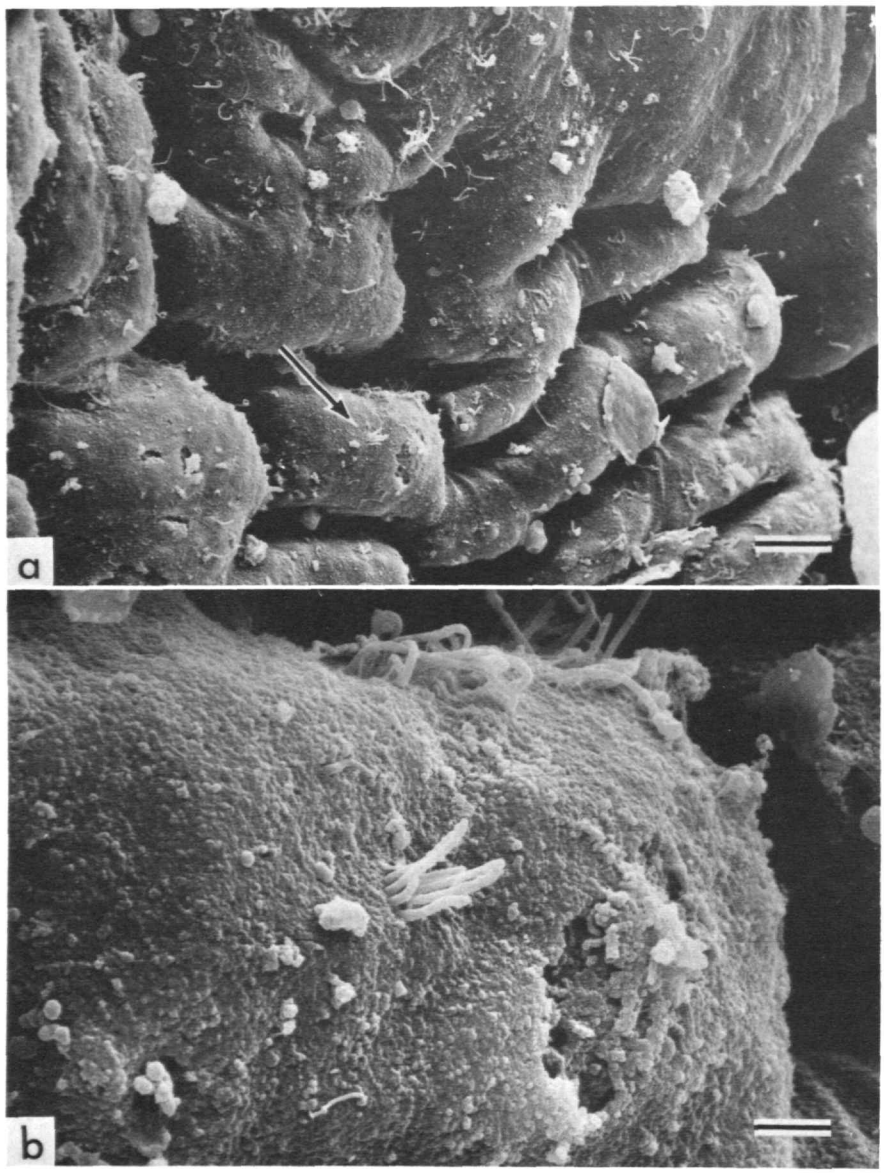

FIGURE 45.—*Barbatia cancellaria*, USNM 794959: *a*, detail of Figure 39*a*, oblique view of outer surface of second inner fold, arrow pointing to one of many ciliary tufts, critical-point dried (× 1100, bar = 10 μm); *b*, detail of *a*, tuft of cilia (× 5500, bar = 2 μm).

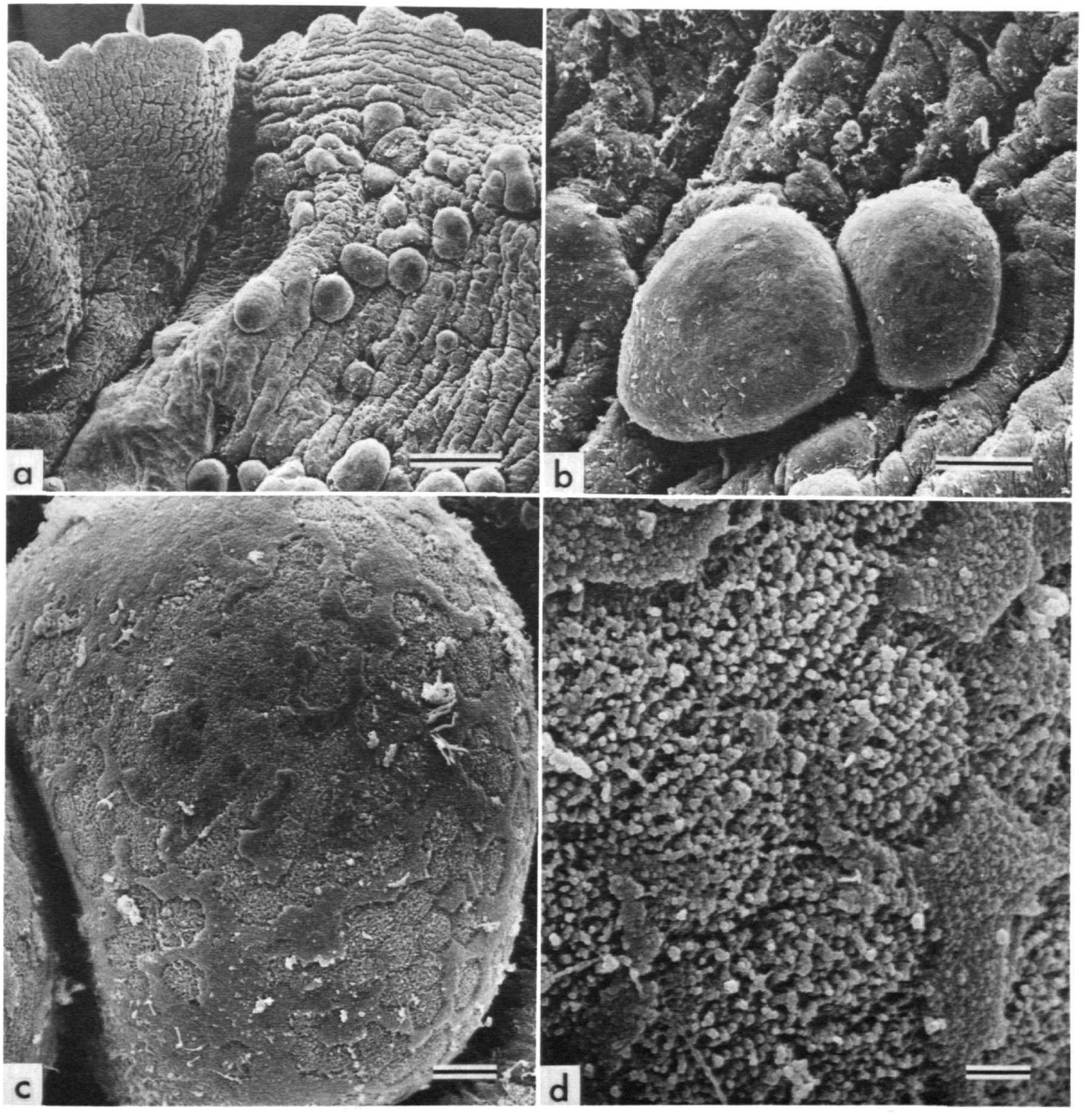

FIGURE 46.—*Barbatia cancellaria*, USNM 794959 (inner surface of second inner fold in posterior region, critical-point dried): *a*, convoluted epithelium and tumescent papillae (× 70, bar = 200 μm); *b*, detail of a pair of papillae (× 300, bar = 50 μm); *c*, detail of *b*, surface of papilla with one ciliary tuft and outlines of cells (× 1000, bar = 10 μm); *d*, detail of *c*, surface of papilla with microvilli and secretion (× 5000, bar = 2 μm).

TABLE 1.—Mantle-edge features in specimens of the order Arcoida (arranged by families) preserved in alcohol in collections of the National Museum of Natural History, Smithsonian Institution

Family	Species	Catalog number	Locality	Length (mm)	Second outer fold	Second inner fold	Position of compound photoreceptors
Arcidae	Arca noae Linné	754401	Adriatic Sea (Yugoslavia)	60	present	absent	first outer fold
	Arca navicularis Bruguière	719114	Indian Ocean (Madagascar)	24	present	absent	first outer fold
	Litharca lithodomus (Sowerby)	635321	Pacific Ocean (Ecuador)	65	present	absent	first outer fold
	Senilia senilis (Linné)	674005	Atlantic Ocean (Liberia)	53	present	present	absent
	Anadara notabilis (Röding)	703328	Caribbean Sea (Jamaica)	50	present	present	absent
	Anadara planicostata (Philippi)	621314	Pacific Ocean (Caroline Ids.)	45	present	present	absent
	Barbatia sp.	761855	Indian Ocean (Diego Garcia Ids.)	38	present	present	absent?
Cucullaeidae	Cucullaea labiata (Solander)	747257	Pacific Ocean (Moluccas Ids.)	25	present	absent	first outer fold
Limopsidae	Lissarca notorcadensis Melvill and Standen	638840	Antarctic Ocean	4	?	absent	?
Philobryidae	Philobrya sublaevis Pelseneer	638836	Antarctic Ocean	9	?	absent	absent
Glycymerididae	Glycymeris americana (DeFrance)	662862	Atlantic Ocean (Florida, USA)	57	present	absent	first outer fold
	Glycymeris subossoleta (Carpenter)	619153	Pacific Ocean (Washington, USA)	32	present	absent	first outer fold

long ago by Schröder (1907). Each tubule appears to be formed by a single, specialized epithelial cell, the apical surface of which becomes greatly extended to form a tubular projection. Although the distal tips of these cellular protuberances have not been observed nor histochemical tests made, the effects and distribution of their chemical activity are apparent.

The fact that tubules are cylindrical and do not flare except at their terminations beneath the periostracum indicates that only the distal tip of a cellular projection must be capable of dissolving the calcium carbonate and organic matrix of the shell. If the walls of the cellular projection were also able to dissolve shell, one would expect that tubules would be distally tapering along their entire length rather than cylindrical. Not only is this effect absent, but deposition of inner shell layer around the projection is evidence that calcification can resume adjacent to its base.

When the shell-dissolving tip of a cellular projection finally makes its way completely through the shell to the undersurface of the periostracum, its etching effect continues, as evidenced by the flared distal extremity of the tubule and by the partial dissolution of the inner surface of the adjacent periostracum. The tip of the cellular projection seems to be unable to penetrate through the periostracum, indicating that the outer portion of the periostracum may be more resistant to the chemical activity of the cellular projection than is the inner portion, which is indeed etched. An alternative explanation—that the etching of the inner surface of the periostracum merely indicates that the cellular projection has had insufficient time to penetrate com-

pletely through to the exterior—is unlikely, because there is no evidence for complete penetration of the periostracum in more proximal locations.

Two possible functions that are commonly advanced for shell tubulation are photoreception, as demonstrated for the aesthete canals of chitons (Boyle, 1976), and chemical secretion, most likely as a deterrent to boring organisms as suggested for the puncta-forming caeca of Brachiopoda (Owen and Williams, 1969).

The former functional interpretation was recently advanced for arcoid tubules by Omori, Kobayashi, Shibata, Mano, and Kamiya (1976). Impressed by the presence of numerous simple and compound photoreceptors on the mantle edge, they reasoned that other photoreceptors may be present inside of the pallial line on the ends of mantle protuberances that penetrate the shell. However, it seems unlikely that additional photoreceptors would be present beneath the shell when those on the mantle margin can provide nearly 360° reception to slight changes in light intensity (Braun, 1954). Even the possibility that the cellular projections may contribute to a dermal light sense not mediated by distinct photoreceptors seems unlikely. Although dermal photosensitivity is widespread in invertebrates including bivalves, it is usually accompanied by the presence of photosensitive pigments (Millott, 1968), and no such pigment in arcoid tubules has yet been detected.

The second functional interpretation of tubules—that they are involved in chemical secretion for the purpose of deterring boring organisms—is much more plausible. As already indicated, the tubular epithelial projections must be chemically active in order to perforate the shell and must remain so after reaching the inner surface of the periostracum. The structures form immediately adjacent to the leading edge of the second outer fold, which marks the beginning of strong adhesion of the mantle to the shell. Distal to this, the mantle edge is highly mobile and constantly shifting relative to the shell surface, so that it would be impossible for fine epithelial extensions into the shell to form or to be maintained. However, the orientation of the tubules, slanting distally toward the outer surface from their bases inside of the pallial line, assures complete distribution over the entire shell except for the growing edge, where secretion is actively extending the shell margin.

There is no doubt that microborers are a serious problem, because epifaunal arcoid shells are generally riddled with microborings in their outer and oldest portions. Few if any of these penetrate to the shell interior, and it appears that the greatest concentration of tubules is just medial to the greater density of borings. There is thus circumstantial evidence that tubules may be involved in deterring the progress of borers. This functional interpretation is strengthened by the taxonomic distribution of tubules. They are common in epifaunal bivalves in many unrelated groups (Oberling, 1964) but are uncommon in infaunal taxa.

Two additional functional possibilities must be mentioned. One is that tubulation serves to anchor the mantle to the shell in the region proximal to the pallial line. The second is that tubulation increases the surface area of the mantle and thus facilitates respiration and the buffering of metabolic products that may result from anaerobic metabolism when the valves are closed (Lutz and Rhoads, 1977).

Although the cellular projections that form tubules must clearly increase the adherence of mantle to shell, it seems unlikely that this is an important function, because it is already performed by adhesive epithelium. Furthermore, this interpretation would not explain the correlation of the presence of tubules with epifaunal habit. In fact, it would seem that burrowing bivalves would have an even greater need for a mantle-anchoring system because of the participation of the mantle in the hydrostatic mechanism of burrowing. In addition, if anchoring the mantle were an important function, it would seem that a different structural plan might have evolved—one entailing branching or circuitous tubules rather than straight ones parallel to the direction of mantle retraction. Lastly, if anchoring were an important function, one would expect connective

tissue, known for its mechanical strength, to extend into the tubules. This is not the case, however.

The observations on the morphology of epithelial surfaces reported above should be ample demonstration that tubules do not function solely to increase surface area for respiration or anaerobic buffering because this must already be accomplished by the dense covering of microvilli on the same epithelial surface. Although it is possible that tubules may function as conduits to the exterior and may aid respiration when the shell is closed, this is still unproven. Shibata (1971) could find no difference between survivorship of specimens of *Anadara* with their shell exteriors artificially covered and those with shell exteriors undisturbed. His later conclusion (1971:109–112) that some components of the extrapallial fluid can penetrate through tubules to the outside of the shell is unwarranted in that he did not establish that microborings through the periostracum were absent.

Mantle-Shell Relationships and Calcification

Each of the four species examined in detail by scanning electron microscopy presents three types of mantle-shell association, each resulting in a distinct calcified fabric or range of fabrics: (1) closely apposed regular (i.e., nonadhesive) epithelium and shell inside of the pallial line, associated with complex crossed lamellar fabric of the inner shell layer; (2) adhesive junctions between mantle and shell, associated with irregular prismatic shell fabric; and (3) distantly or intermittently apposed mantle and shell outside of the pallial line, associated with commarginal crossed-lamellar fabric and, in the case of some species, proximal and distal radial fabrics.

The region of the shell inside of the pallial line is in most cases distinctly depressed in relation to the marginal band and seems to represent a region of less rapid net calcification. In fact, the apposing regular epithelial surface, which is highly microvillous and presumably capable of intensive absorption as well as secretion, is consistent with a concept of great calcium mobility in this region.

The complex crossed-lamellar fabric of the inner shell layer is unrelated to the surface configuration of the regular epithelium of the apposing mantle (except in tubules), and the observations of the present study yield no clues as to how crystal orientation is achieved. No cohesive organic film comparable to that found outside of the pallial line has been observed, although such a film has been detected by transmission electron microscopy inside the pallial line of *Merceneria merceneria* (Neff, 1972b).

In contrast to regular epithelium proximal to the pallial line, adhesive epithelium is directly adherent to the shell. The ultrastructure of the components involved in this adhesion was first investigated in freshwater limpets by Hubendick (1958) and more recently in the bivalve, *Pinctada radiata*, by Nakahara and Bevelander (1970) and in gastropods by Tompa and Watabe (1976). In both gastropods and bivalves, the mode of muscle attachment is basically the same. Muscle fibers are not in direct contact with the adhesive epithelium, but rather are separated by randomly arrayed collagenous fibers like those filling the space between mantle epithelia in other regions. Nor is the adhesive epithelium in direct contact with the shell, because the apical surface of each cell secretes an organic film (the "tendon sheath" of Tompa and Watabe, 1976), referred to by Hubendick (1958) as colloidal and in the present study as nonfibrous or granular. As shown by these studies and the present report, apical microvilli of the adhesive epithelium do not insert directly into the shell but rather lie beneath this adhesive film; calcification at the growth surface of the shell occurs on and within the opposite side of the film.

As noted by Tompa and Watabe (1976), muscle fibers vary greatly in orientation with respect to the epithelial surface, ranging from perpendicular to nearly parallel. The area of the adhesive epithelium adjacent to a muscle does not necessarily reflect the cross-sectional size or shape of the muscle. Adhesive epithelial cells may form in advance of attachment of muscles to the under-

lying connective tissue.

The results of the present study indicate that the relationship between mantle and shell in areas of myostracal growth is less direct than previously thought and that it may not be possible to infer characteristics of some muscles from the configuration of their scars on the inner shell surface. There is a close relationship between large muscles (such as adductor) and their scars but a poor relationship between small muscles (such as those in the mantle folds) and their scars. No relationship was found between muscle-fiber diameter and the width of small adhesive patches adjacent to the pallial line, and it is possible that regular epithelium may be modified for adhesion in the absence of muscles in underlying connective tissue.

The structural elements in myostracal fabric are also poorly correlated with the distribution of muscle fibers. The first-order polygonal pattern on myostracal surfaces is basically a reflection of the tendency for the adhesive film to be composed of polygonal plates, each of which corresponds to the apical surface of an adhesive epithelial cell. Secretion of myostracum occurs on or in each polygonal plate, not between plates, so that boundaries between plates leave grooves on the myostracal surface. However, because these grooves are ultimately filled by the growth of crystals on either side and are not sites for the accumulation of organic material, they have little if any expression in cross-sectional views of myostracum. The second-order patches of uniformly oriented needles present on the myostracal surface and the irregular prisms present in cross sections seem to represent some sort of discontinuity in the mineralization process at a scale finer than that of single cells. What relationship they have to the intracellular structure of adhesive epithelial cells is unknown.

The relationship between mantle and shell in the region distal to the pallial line is substantially different from that discussed above. The crest of the second outer fold of the mantle margin abuts the pallial line and marks the distal end of close apposition between mantle and shell. The first outer fold is highly mobile and can bend to a position nearly perpendicular to the shell surface, so that contact between mantle and shell in this region is intermittent. During these contortions of the first outer fold, however, the periostracum remains intact, so that a uniform microenvironment for calcification is maintained in the space bounded by mantle, periostracum, and marginal shell band.

The ultrastructural complexity of the shell fabric of the marginal band, such as the three commarginal fabric zones in *Arca zebra*, cannot be related to cellular differentiation of the outer mantle fold, because corresponding differentiation has not been observed. Furthermore, it has been demonstrated above that a dense but exceedingly thin, fibrous organic film intervenes between the epithelium and the growth surface of the shell in this region. It is likely that this film is secreted by both the outer surface of the first outer fold and the inner surface of the second outer fold, because the presence of secretion droplets, some of which seem to merge into the fibers that comprise the film, can be observed directly.

What seems to be occurring, then, is that organic products secreted by the epithelium of the outer mantle folds beneath the periostracum polymerize into fibers, which finally anastomose and coalesce into a dense mat adjacent to the growth surface of the marginal shell band. Although the composition of the film is unknown, this maturation process invites comparison to a similar process occurring during the deposition of collagen (Humphreys and Porter, 1976), in which the earliest detectable fibrils also occur outside of cells. The high degree of ordering of fibrils, as in the orthogonal grid in mature annelid cuticle, seems to be achieved extracellularly, but the principles that produce the ordering are unknown.

The presence of a uniform organic film over the entire surface of the marginal shell band provides no explanation for the presence of three shell-fabric zones in the same band, as in *Arca zebra*. However, it is possible that crystal orientation in these zones may result from other influences. First, in the case of the distal radial zone, which in *Arca zebra* represents the advancing front of calcification, there may possibly be a dual

influence on crystal formation caused by the presence of the organic film on one side and the periostracum on the other. As the distal radial zone grows, its thickness increases to a point at which the periostracum no longer has any effect on the overlying calcified structure. Secondly, the proximal radial zone lies adjacent to the radially directed cell processes on the crest of the second outer fold. These processes lie between the organic film and the growth surface of the shell, and it is possible that they contribute to reorientation of sites of calcification in the region bordering the pallial line.

If the organic film is also being deposited on the inner surface of the periostracum, it is not immediately clear why calcification does not extend over the entire periostracal surface. Because the periostracum closest to the periostracal groove is the youngest, however, it may be that polymerization has not proceeded far enough to produce a combination of organic structures of sufficient maturity for calcification. Additionally, the constant tight pleating of the periostracum in the periostracal fringe effectively seals off the pleated surfaces from extrapallial fluid, except perhaps along radial folds. As shown above, in *Barbatia cancellaria* incipient calcification may extend outward along these rays.

As for the mechanism of calcification (see Towe, 1972, for a concise review of prevalent theories), the observations described above give no indication of the existence of organic compartments but provide a demonstration that an opportunity for epitaxy exists and a suggestion that there may be a relationship between the maturation of an organic film and the nature of the mineralized fabric. Future research on the stereochemistry of organic components would do well to concentrate on these films, which are known to exist outside of the pallial line in other bivalves as well (Mutvei, 1972; in *Mytilus edulis*).

Mantle Growth

Two alternative concepts currently exist to explain the manner in which the mantle grows. The usual assumption is that there is a single zone of cell proliferation in the region of the periostracal groove (Dunachie, 1963; Mutvei, 1964; Beedham and Truemen, 1967; Taylor, Kennedy, and Hall, 1969). This concept assumes that the newly generated cells pass outward from the generative zone and migrate around the mantle edge, changing their functions and successively secreting periostracum, outer shell layer, inner shell layer, and, where their paths cross those of muscles, myostracal layers as well. Williams (1968, 1977) has referred to this progression, which he applied to mantle growth in brachiopods, as a "conveyor-belt system." The alternative concept (Saleuddin, 1974; Williams, 1977; and especially Kniprath, 1975, 1978) is that there is no generative zone and no conveyor-belt progression of cells. Rather, cell division is widespread, and specialized cells maintain their functions during growth of the mantle.

The conveyor-belt concept has been developed on the basis of indirect evidence rather than on actual observation and mapping of sites of cell division. Mutvei (1964), for example, noted that "it is possible to establish fairly definitely the position of the generative territory of the shell-secreting epithelium" on the basis of the distribution of shell tubules, which are present not only in the Arcoida, but in other bivalve groups. Given Schröder's (1907) demonstration that in the Sphaeriidae these tubules are occupied by projections of single epithelial cells, Mutvei concluded that at least these cells must become fixed with respect to the shell surface. Intervening cells must also be fixed in position, because, if they were not, cell division would produce folding of the epithelium between tubules, which has never been observed. Mutvei then concluded that in tubulate bivalves "the shell-secreting epithelium . . . must grow solely in the periostracal groove where it has not yet secreted the calcareous shell layers."

In contrast, widespread cell division has been demonstrated by direct observation in both gastropods (Saleuddin, 1974; Kniprath, 1975) and bivalves (Kniprath, 1978). By using a marker that

is incorporated into mitotic cell nuclei, Kniprath (1978) showed that in *Mytilus* cell division actually does occur over broad areas of both inner and outer epithelium and suggested that it may even occur inside of the pallial line, where it has been commonly assumed that epithelial cells remain in a fixed position with respect to the shell surface.

In arcoid bivalves there are no constraints on cell division on any of the epithelial surfaces that are not attached to the shell. The conveyor-belt concept is not required, because, as demonstrated above, there is no direct connection between the secretory epithelium of the first outer fold and the commarginal zones of the distinctive shell fabric that lie outside of the pallial line. It seems likely that cell division in these epithelia is widespread and that specialized cells, such as those on the first outer fold concerned with photoreception and those in the base of the periostracal groove concerned with secretion of periostracum, maintain their relative positions and functions during increase in size of the mantle and shell.

Whether or not it is still necessary to accept the conveyor-belt hypothesis for the outer epithelium inside of the pallial line is controversial. For the reasons outlined by Mutvei (1964), widespread cell division in this region seems unlikely, although the cells that send projections into tubules may not be as fixed with regard to other epithelium cells as previously thought (Kniprath, 1978). In areas of muscle attachment, it is generally assumed that epithelial cells change from a nonadhesive to an adhesive mode and back again as muscles migrate past them during ontogeny, but even here the conveyor-belt hypothesis is an inference. As noted by Tompa and Watabe (1976), the actual sequence of steps involved in the formation of new areas of adhesive epithelium has not yet been revealed.

Evolutionary Implications

Four features of the Arcoida are possibly unique to this order among the Bivalvia: (1) compound eyes; (2) the position of eyes on the first outer fold, beneath the periostracum; (3) the dominant size of the first outer fold relative to other folds of the mantle and the tendency for this fold to function as a mantle curtain; and (4) a second outer fold. Given the primitive nature of the Arcoida (Waller, 1978), the question arises whether these features are primitive in the Bivalvia as a whole or whether they represent evolutionary specializations first attained by an ancestral arcoid and retained and shared by arcoid descendants.

The mere fact that these features have not yet been observed in other bivalve groups is a strong indication that the second alternative—that these are shared derived features—is the more likely. Their presence in both the superfamilies Arcacea and Limopsacea, which diverged from a common ancestor by late Paleozoic time (Waller, 1978), also indicates that their appearance was early in the evolution of the order.

Land (1968) showed that rhabdomeric eyes (those derived from microvilli) are associated with the "on" response to increases in light intensity, which is generally associated with orientation and habitat selection but does not require image formation. In contrast, ciliary-based receptors are associated with the "off" response to decreases in light intensity, as with moving shadows, and are involved in movement detection and defense against predation. Land reasoned that the latter response requires good image formation and suggested that the mirror-formed eye of *Pecten* and the compound eye of *Arca* both provide this capability, but in structurally very different ways. The eye of *Pecten* contains both rhabodomeric and ciliary organelles (Land, 1968), whereas the eye of *Arca* is ciliary based (Levi and Levi, 1971). It seems likely, therefore, that these eyes, although similar in function, evolved independently of one another.

Both the large size of the first outer fold in the Arcoida and its ability to function as a mantle curtain suggest another type of independent evolutionary development. If the primitive bivalve mantle margin were twofold, as in the mantle margin of veliger larvae (Waller, 1978), two evo-

lutionary pathways would be open for further development of the mantle edge: either new folds could develop in order to perform new functions, or one of the two existing folds could develop and diversify its functional capability. In the case of arcoids, the latter path has been taken. The first outer fold has not only diversified from its primary secretory role by becoming enlarged and muscular in order to serve as a mantle curtain, but it has also sustained the development of photoreceptors.

It may be that evolutionary development of the second outer fold followed as a consequence of the functional diversification of the first fold. If inferences regarding muscle orientation in the second outer fold are correct, then this fold may contribute to the functioning of the first outer fold by adding to the control of hydrostatic pressure involved in extending that fold.

The development of a second inner fold in some arcoids would seem to be yet a further evolutionary development limited to *Barbatia* and related genera. This fold appears to extend the capability for controlling the flow of water through the mantle cavity already present in the first outer fold.

Conclusions

1. The mantle edge in the order Arcoida is not in accord with the three-fold, three-function concept generally ascribed to bivalve mantle edges. In the Arcoida there are two outer folds, one being secretory in function, the other functioning in secretion, photoreception, and control of water flow. One or two inner folds are present. When only one is present, it is a minor fold, serving only to buttress one side of the periostracal groove; when a second inner fold is present, it serves as a mantle curtain, assisting the first outer fold in the control of water flow into and out of the mantle cavity.

2. Tubules in the shells of the Arcoida are formed by single cells having greatly extended apical surfaces. Only the tip of the apical projection dissolves the shell and its organic matrix. Upon reaching the inner surface of the periostracum, shell-dissolving secretion continues but penetration of the periostracum does not occur. The most likely function of the cellular projection is chemical deterrence to boring organisms.

3. Mantle-shell relationships in the Arcoida are diverse and are in part reflected by the diversity of calcified fabrics in the shell. The nonadhesive epithelium inside of the pallial line and the corresponding inner shell surface both indicate high calcium mobility and intensive reorganization of the calcified fabric. The arrangement of structural elements in complex crossed lamellar fabric bears no special relationship to epithelial cellular surfaces. In contrast, adhesive epithelium is in intimate contact with the growth of irregular prismatic fabric via an organic film secreted by the apical surface of each cell. Cell boundaries leave a polygonal imprint on the growth surface of the fabric, but this is not reflected in cross sections. Finer orders of structure in the fabric, including the irregular prisms, are of a subcellular scale, but their relationship to intracellular components, such as the tendon fibers of Tompa and Watabe (1976), is unknown.

No close relationship between epithelium and the growth surface of the shell occurs outside of the pallial line. Rather, calcification occurs beneath a fibrous organic film secreted by the adjacent epithelium. This film very likely exerts a far greater influence on the final form of the calcified fabric than does the periostracum. Ultimately, calcification may be related to a maturation process of this film.

4. The consistent presence of a second outer fold as well as the presence of photoreceptors on the first outer fold beneath the periostracum suggest that growth of the mantle outside of the pallial line does not involve cell generation in a single, concentrated zone, as in the base of the periostracal groove. Nor does it seem likely that there is a simple conveyor-belt movement of cells outward from such a zone with each cell undergoing an orderly progression of functions. Rather, cell division in the epithelia of the mantle margin is probably widespread, with cells tending to

maintain their functional integrity. The presence of tubule-forming cells inside of the pallial line indicates that these cells remain fixed in position with respect to the shell surface and also maintain their functions. Whether the conveyor-belt concept should be applied to epithelium in areas of muscle attachment to the shell is controversial and cannot be resolved until more is learned about epithelial cell morphology beneath migrating muscle insertions.

5. The unique compound photoreceptors of the Arcoida, the position of these and simple photoreceptors on an outer fold beneath the periostracum, the tendency for the outer fold to function as a mantle curtain, and the presence of a second outer fold all seem to be secondarily derived features that arose early in the evolution of the group from primitive bivalves.

Addendum

B. S. Morton (1978, *Journal of Zoology*, 185(2): 173–196) described the biology and functional morphology of *Philobrya munita* Finlay, 1930. Like other members of the order Arcoida described herein, representatives of this species have a second outer fold ("secondary outer mantle fold" of Morton), pigmented eye spots (but not compound eyes) on an outer fold beneath the periostracum, and two inner mantle folds. As in the present study, these and other features of the Arcoida provided a basis for questioning established theories regarding functional morphology and phylogeny of the Bivalvia.

Literature Cited

Anderson, T. F.

1951. Techniques for the Preservation of Three-dimensional Structures in Preparing Specimens for the Electron Microscope. *Transactions of the New York Academy of Science*, series 2, 13(3):130–133.

1956. Electron Microscopy of Micro-organisms. *In* G. Oster and A. Pollistor, editors, *Physical Techniques in Biological Research*, 3(5):177–240, 22 figures, 1 table. New York: Academic Press.

Becker, R. P., and O. Johari

1978. *Scanning Electron Microscopy—1978.* Volume 2, 1134 pages. AMF O'Hare, Illinois: Scanning Electron Microscopy, Inc. [Post Office Box 66507].

Beedham, G. E.

1958. Observations on the Mantle of the Lamellibranchia. *Quarterly Journal of Microscopical Science*, 99(2): 181–197, 4 figures.

Beedham, G. E., and E. R. Trueman

1967. The Relationship of the Mantle and Shell of the Polyplacophora in Comparison with That of Other Mollusca. *Journal of Zoology* (London), 151(2):215–231, 6 figures, 1 table.

Bevelander, G., and H. Nakahara

1967. An Electron Microscope Study of the Formation of the Periostracum of *Macrocallista maculata*. *Calcified Tissue Research*, 1(1):55–67, 6 figures.

Boyde, A.

1978. Pros and Cons of Critical Point Drying and Freeze Drying for SEM. *In* R. P. Becker and O. Johari, editors, *Scanning Electron Microscopy—1978*, 2:303–314. AMF O'Hare, Illinois: Scanning Electron Microscopy, Inc. [Post Office Box 66507].

Boyle, P. R.

1976. The Aesthetes of Chitons, III: Shell Surface Observations. *Cell and Tissue Research*, 172:379–388, 4 figures.

Braun, R.

1954. Zum Lichtsinn facettenaugentragender Muscheln (Arcacea). *Zoologische Jahrbucher Abteilung für Allgemeine Zoologie und Physiologie der Tiere*, 65(1):91–125, 4 figures.

Bubel, A.

1973a. An Electron-Microscope Study of Periostracum Formation in Some Marine Bivalves, I: The Origin of the Periostracum. *Marine Biology*, 20(3):213–221, 9 figures.

1973b. An Electron-Microscope Study of Periostracum Formation in Some Marine Bivalves, II: The Cells Lining the Periostracal Groove. *Marine Biology*, 20(3):222–234, 2 figures.

Charles, G. H.

1966. Sense Organs (less Cephalopods). *In* K. M. Wilbur and C. M. Yonge, editors, *Physiology of Mollusca*, 2: 455–521, 10 figures. New York and London: Academic Press.

Dunachie, J. F.

1963. The Periostracum of "*Mytilus edulis.*" *Transactions of the Royal Society of Edinburgh*, 65(15):383–411, 12 figures, 1 plate.

Eakin, R. M.

1963. Lines of Evolution of Photoreceptors. *In* D. Mazia and A. Taylor, editors, *General Physiology of Cell Specialization*, chapter 21:393–425, 38 figures. New York: McGraw-Hill.

1965. Evolution of Photoreceptors. In *Cold Spring Harbor Symposia on Quantitative Biology*, 30:363–370, 2 figures. Cold Spring Harbor, Long Island, New York: Cold Spring Harbor Laboratory of Quantitative Biology.

1968. Evolution of Photoreceptors. *In* T. Dobzhansky, M. K. Hecht, and W. Steere, editors, *Evolutionary Biology*, 2(5):194–242, 24 figures. New York: Appleton-Century-Crofts.

Hubendick, B.

1958. On the Molluscan Adhesive Epithelium. *Arkiv für Zoologi utgivet av Kungliga Svenska Vetenskapsakademien* (Stockholm), second series, 11:31–36, 1 figure, 3 plates.

Humphreys, S., and K. R. Porter

1976. Collagenous and Other Organizations in Mature Annelid Cuticle and Epidermis. *Journal of Morphology*, 149(1):33–51, 16 figures.

Jacob, W.

1926. Über die Komplexaugen von *Arca* und *Pectunculus*. *Zoologischer Anzeiger*, 67:162–171, 6 figures.

Kniprath, E.

1975. Das Wachstum des Mantels von *Lymnaea stagnalis* (Gastropoda). *Cytobiologie*, 10(2):260–267, 6 figures.

1978. Growth of the Shell-Field in *Mytilus* (Bivalvia). *Zoologica Scripta*, 7(2):119–120, 3 figures.

Kobayashi, I.

1964. Microscopical Observations on the Shell Structure of Bivalvia, I: *Barbatia obtusoides* (Nyst.). *Science Reports of the Tokyo Kyoiku Daigaku*, section C (Geology, Mineralogy, and Geography), 8(82):295–301, 4 figures, 3 plates.

1976. Internal Structure of the Outer Shell Layer of *Anadara broughtonii* (Schrenck). *Venus, the Japanese Journal of Malacology*, 35(2):63–72, 3 figures, 2 plates.

Land, M. F.
1968. Functional Aspects of the Optical and Retinal Organization of the Mollusc Eye. *In* J. D. Carthy and G. E. Newell, editors, *Invertebrate Receptors: Symposia of the Zoological Society of London*, 23:75–96, 5 figures. London and New York: Academic Press.

Levi, P., and C. Levi
1971. Ultrastructure des Yeux Palleaux d'*Arca noe* (L.). *Journal de Microscopie*, 11(3):425–432, 1 figure, 4 plates.

Lutz, R. A., and D. C. Rhoads
1977. Anaerobiosis and a Theory of Growth Line Formation. *Science*, 198:1222–1227, 2 figures.

Millott, N.
1968. The Dermal Light Sense. *In* J. D. Carthy and G. E. Newell, editors, *Invertebrate Receptors: Symposia of the Zoological Society of London*, 23:1–36, 17 figures. London and New York: Academic Press.

Mutvei, H.
1964. On the Shells of *Nautilus* and *Spirula* with Notes on the Shell Secretion in Non-cephalopod Molluscs. *Arkiv för Zoologi utgivet av Kungliga Svenska Vetenskapsakademien*, second series, 16:221–278, 30 figures, 22 plates.
1972. Formation of Nacreous and Prismatic Layers in *Mytilus edulis* L. (Lamellibranchiata). *Biomineralization Research Reports*, 6:96–100, 2 plates.
1978. Ultrastructural Characteristics of the Nacre in Some Gastropods. *Zoologica Scripta*, 7(4):287–296, 43 figures.

Nakahara, H., and G. Bevelander
1970. An Electron Microscope Study of the Muscle Attachment in the Mollusc *Pinctada radiata*. *Texas Reports of Biology and Medicine*, 28(3):279–286, 5 figures.
1971. The Formation and Growth of the Prismatic Layer of *Pinctada radiata*. *Calcified Tissue Research*, 7(1):31–45, 16 figures.

Neff, J. M.
1972a. Ultrastructural Studies of Periostracum Formation in the Hard-shelled Clam *Mercenaria mercenaria* (L.). *Tissue and Cell*, 4(2):311–326, 18 figures.
1972b. Ultrastructure of the Outer Epithelium of the Mantle in the Clam *Mercenaria mercenaria* in Relation to Calcification of the Shell. *Tissue and Cell*, 4(4):591–600, 10 figures.

Newell, N. D.
1969. Order Arcoida Stoliczka, 1871. *In* R. C. Moore, editor, *Treatise on Invertebrate Paleontology*, 1(N):248–269. Lawrence, Kansas: Geological Society of America and University of Kansas Press.

Nowikoff, M.
1926. Über die Komplexaugen der Gattung *Arca*. *Zoologischer Anzeiger*, 67(11–12):277–289, 8 figures.

Oberling, J. J.
1964. Observations on Some Structural Features of the Pelecypod Shell. *Mitteilungen der Naturforschenden Gesellschaft in Bern*, new series, 20: 60 pages, 3 figures, 6 plates.

Omori, M., and I. Kobayashi
1963. On the Micro-canal Structures Found in the Shell of *Arca navicularis* Bruguiére and *Spondylus barbatus* Reeve. *Venus, the Japanese Journal of Malacology*, 22(3):274–280, 1 figure, plates 19, 20. [In Japanese with English summary.]

Omori, M., I. Kobayashi, and M. Shibata
1962. Preliminary Report on the Shell Structure of *Glycymeris vestita* (Dunker). *Science Reports of the Tokyo Kyoiku Daigaku*, section C (Geology, Mineralogy, and Geography), 8(77):197–202, 3 figures, 3 plates.

Omori, M., I. Kobayashi, M. Shibata, K. Mano, and H. Kamiya
1976. On Some Problems Concerning Calcification and Fossilization of Taxodontid Bivalves. *In* N. Watabe and K. M. Wilbur, editors, *The Mechanisms of Mineralization in the Invertebrates and Plants*, pages 403–426, 12 figures, 2 tables. Columbia, South Carolina: University of South Carolina Press.

Owen, G., and A. Williams
1969. The Caecum of Articulate Brachiopoda. *Proceedings of the Royal Society of London*, series B, 172:187–201, 26 figures.

Patten, W.
1886. Eyes of Molluscs and Arthropodes. *Mittheilungen aus der Zoologischen Station zu Neapel*, 6:542–756, plates 28–32.

Petit, H., W. L. Davis, and R. G. Jones
1978. Morphological Studies on the Mantle of the Fresh-Water Mussel *Amblema* (Unionidae): Scanning Electron Microscopy. *Tissue and Cell*, 10(4):619–627, 12 figures.

Pojeta, J., Jr.
1971. Review of Ordovician Pelecypoda. *United States Geological Survey Professional Paper*, 695:1–46, 9 figures, 20 plates.

Rawitz, B.
1890. Der Mantelrand der Acephalen, II: Arcacea, Mytilacea, Unionacea. *Jenaischen Zeitschrift für Naturwissenschaft*, new series, 24:1–83, 3 figures, 4 plates.

Rosen, M. D., C. R. Stasek, and C. O. Hermans
1978. The Ultrastructure and Evolutionary Significance of the Cerebral Ocelli of *Mytilus edulis*, the Bay Mussel. *The Veliger*, 21(1):10–18, 4 figures, 4 plates.

Saleuddin, A. S. M.
1974. An Electron Microscopic Study of the Formation and Structure of the Periostracum in *Astarte* (Biv-

alvia). *Canadian Journal of Zoology*, 52(12):1463–1470, 22 figures.

Salvini-Plawen, L. v., and E. Mayr

1977. On the Evolution of Photoreceptors and Eyes. *In* M. K. Hecht, W. C. Steere, and B. Wallace, editors, *Evolutionary Biology*, 10:207–263, 12 figures, 1 table. New York and London: Plenum Press.

Schröder, O.

1907. Beiträge zur Histologie des Mantels von *Calyculina* (*Cyclas*) *lacustris* Müller. *Zoologischer Anzeiger*, 31(15–16):506–510, 2 figures.

Schulz, E.

1932. Uber den Bau der Komplexaugen von *Arca Noae* L. *Zoologischer Anzeiger*, 99(5–6):163–165, 1 figure.

Shibata, M.

1971. The Experimental Researches on the Function of the Canals Found on the Shell of *Anadara* (*Scapharca*) *subcrenata* (Lischke). *Research Institute for Natural Resources* (*Shigen Kagaku Kankyuio*), *Miscellaneous Report*, 75: part 1, pages 103–108, 3 figures, 1 table; part 2, pages 109–112, 1 figure, 1 table. [In Japanese with English summary.]

Stanley, S. M.

1970. Relation of Shell Form to Life Habits of the Bivalvia (Mollusca). *Geological Society of America*, *Memoir*, 125: 292 pages, 47 figures, 40 plates.

Taylor, J. D., W. J. Kennedy, and A. Hall

1969. The Shell Structure and Mineralogy of the Bivalvia, Introduction: Nuculacea—Trigonacea. *Bulletin of the British Museum* (*Natural History*), *Zoology*, supplement 3: 125 pages, 77 figures, 29 plates.

Tompa, A., and N. Watabe

1976. Ultrastructural Investigation of the Mechanism of Muscle Attachment to the Gastropod Shell. *Journal of Morphology*, 149(3):339–351, 1 figure, 3 plates.

Towe, K. M.

1972. Invertebrate Shell Structure and the Organic Matrix Concept. *Biomineralization Research Reports*, 4:1–14, 2 figures, 7 plates.

Tsujii, T.

1976. An Electron Microscopic Study of the Mantle Epithelial Cells of *Anodonta* sp. during Shell Regeneration. *In* N. Watabe and K. M. Wilbur, editors, *The Mechanisms of Mineralization in the Invertebrates and Plants*, pages 339–353, 21 figures. Columbia, South Carolina: University of South Carolina Press.

Wada, K.

1968. Electron Microscopic Observations on the Formation of the Periostracum of *Pinctada fucata*. *Bulletin of the National Pearl Research Laboratory*, 13: 1540–1560.

Waller, T. R.

1973. The Habits and Habitats of Some Bermudian Marine Mollusks. *The Nautilus*, 87(2):31–52, 33 figures.

1978. Morphology, Morphoclines, and a New Classification of the Pteriomorphia (Mollusca: Bivalvia). *Philosophical Transactions of the Royal Society of London*, *B*, 284(1001):345–365, 2 figures, 2 tables.

Williams, A.

1968. Evolution of the Shell Structure of Articulate Brachiopods. *Special Papers in Palaeontology*, 2: vi + 55 pages, 27 figures, 24 plates, 1 table. London: The Palaeontological Association.

1977. Differentiation and Growth of the Brachiopod Mantle. *American Zoologist*, 17:107–120, 14 figures.

Wise, S. W., Jr.

1971. Shell Ultrastructure of the Taxodont Pelecypod *Anadara notabilis* (Röding). *Ecologae Geologicae Helvetiae*, 64(1): 12 pages 3 figures, 9 plates.

Yonge, C. M.

1953. The Monomyarian Condition in the Lamellibranchia. *Transactions of the Royal Society of Edinburgh*, 62(2):443–478, 13 figures.

1957. Mantle Fusion in the Lamellibranchia. *Pubblicazioni della Stazione Zoologica di Napoli*, 29:151–171, 11 figures.

REQUIREMENTS FOR SMITHSONIAN SERIES PUBLICATION

Manuscripts intended for series publication receive substantive review within their originating Smithsonian museums or offices and are submitted to the Smithsonian Institution Press with approval of the appropriate museum authority on Form SI–36. Requests for special treatment—use of color, foldouts, casebound covers, etc.—require, on the same form, the added approval of designated committees or museum directors.

Review of manuscripts and art by the Press for requirements of series format and style, completeness and clarity of copy, and arrangement of all material, as outlined below, will govern, within the judgment of the Press, acceptance or rejection of the manuscripts and art.

Copy must be typewritten, double-spaced, on one side of standard white bond paper, with 1¼" margins, submitted as ribbon copy (not carbon or xerox), in loose sheets (not stapled or bound), and accompanied by original art. Minimum acceptable length is 30 pages.

Front matter (preceding the text) should include: **title page** with only title and author and no other information, **abstract page** with author/title/series/etc., following the established format, **table of contents** with indents reflecting the heads and structure of the paper.

First page of text should carry the title and author at the top of the page and an unnumbered footnote at the bottom consisting of author's name and professional mailing address.

Center heads of whatever level should be typed with initial caps of major words, with extra space above and below the head, but with no other preparation (such as all caps or underline). Run-in paragraph heads should use period/dashes or colons as necessary.

Tabulations within text (lists of data, often in parallel columns) can be typed on the text page where they occur, but they should not contain rules or formal, numbered table heads.

Formal tables (numbered, with table heads, boxheads, stubs, rules) should be submitted as camera copy, but the author must contact the series section of the Press for editorial attention and preparation assistance before final typing of this matter.

Taxonomic keys in natural history papers should use the alined-couplet form in the zoology and paleobiology series and the multi-level indent form in the botany series. If cross-referencing is required between key and text, do not include page references within the key, but number the keyed-out taxa with their corresponding heads in the text.

Synonymy in the zoology and paleobiology series must use the short form (taxon, author, year:page), with a full reference at the end of the paper under "Literature Cited." For the botany series, the long form (taxon, author, abbreviated journal or book title, volume, page, year, with no reference in the "Literature Cited") is optional.

Footnotes, when few in number, whether annotative or bibliographic, should be typed at the bottom of the text page on which the reference occurs. Extensive notes must appear at the end of the text in a notes section. If bibliographic footnotes are required, use the short form (author/brief title/page) with the full reference in the bibliography.

Text-reference system (author/year/page within the text, with the full reference in a "Literature Cited" at the end of the text) must be used in place of bibliographic footnotes in all scientific series and is strongly recommended in the history and technology series: "(Jones, 1910:122)" or ". . . Jones (1910:122)."

Bibliography, depending upon use, is termed "References," "Selected References," or "Literature Cited." Spell out book, journal, and article titles, using initial caps in all major words. For capitalization of titles in foreign languages, follow the national practice of each language. Underline (for italics) book and journal titles. Use the colon-parentheses system for volume/number/page citations: "10(2):5–9." For alinement and arrangement of elements, follow the format of the series for which the manuscript is intended.

Legends for illustrations must not be attached to the art nor included within the text but must be submitted at the end of the manuscript—with as many legends typed, double-spaced, to a page as convenient.

Illustrations must not be included within the manuscript but must be submitted separately as original art (not copies). All illustrations (photographs, line drawings, maps, etc.) can be intermixed throughout the printed text. They should be termed **Figures** and should be numbered consecutively. If several "figures" are treated as components of a single larger figure, they should be designated by lowercase italic letters (underlined in copy) on the illustration, in the legend, and in text references: "Figure 9b." If illustrations are intended to be printed separately on coated stock following the text, they should be termed **Plates** and any components should be lettered as in figures: "Plate 9b." Keys to any symbols within an illustration should appear on the art and not in the legend.

A few points of style: (1) Do not use periods after such abbreviations as "mm, ft, yds, USNM, NNE, AM, BC." (2) Use hyphens in spelled-out fractions: "two-thirds." (3) Spell out numbers "one" through "nine" in expository text, but use numerals in all other cases if possible. (4) Use the metric system of measurement, where possible, instead of the English system. (5) Use the decimal system, where possible, in place of fractions. (6) Use day/month/year sequence for dates: "9 April 1976." (7) For months in tabular listings or data sections, use three-letter abbreviations with no periods: "Jan, Mar, Jun," etc.

Arrange and paginate sequentially EVERY sheet of manuscript—including ALL front matter and ALL legends, etc., at the back of the text—in the following order: (1) title page, (2) abstract, (3) table of contents, (4) foreword and/or preface, (5) text, (6) appendixes, (7) notes, (8) glossary, (9) bibliography, (10) index, (11) legends.